

# **Application of Rock Mass Classification and Blastability Index for the improvement of wall control at Phoenix Mine**

**Gomotsegang Seth Kealeboga Segaletsho**

A research report submitted to the Faculty of Engineering and the Built Environment, University of the Witwatersrand, Johannesburg, in partial fulfilment of the requirements for the degree of Master of Science in Engineering.

Johannesburg, 2017

**DECLARATION**

I declare that this Research Report is my own unaided work. It is being submitted to the Degree of Master of Science in Engineering at the University of the Witwatersrand, Johannesburg. It has not been submitted before for any degree or examination to any other University.

.....

*(Signature of Candidate)*

..... day of ....., .....

## **ABSTRACT**

The study sought to establish the applicability of rock mass classification as a primary input to wall control blasting. Conventional rules of thumb are used to develop blast designs based on parametric ratios with insufficient consideration of the rock mass factors that influence the achievability of final wall designs. Control of the western highwall of the Phoenix pit had proven to be challenging in that the designed catchment berms and wall competence were perpetually unachievable from the pit crest to the current mining levels. This exposed the mining operation to safety hazards such as local wall rock failure from damaged crests, frozen toes and rolling rock falls from higher mining levels. There was also an effect of increased standoff distances from the concerned highwall which reduce the available manoeuvring area on the pit floor and subsequently the factor of extraction that is safely achievable. The study investigated the application of rock mass classification and the Blastability Index (BI) as a means to improve wall control. This was achieved by establishing zones according to rock type forming the western highwall rock mass wherein distinguishing rock mass classification factors were used to establish the suitable wall control designs through a Design Input Tool (DIT). The DIT consolidated rock mass classification methodologies such as the Geological Strength Index (GSI) and the Rock Mass Rating (RMR) and related them to the BI and discontinuities of the rock mass to produce a tool that can be used to develop objective wall control designs. The designs driven by the tool inherently take into account the rock mass characteristic factors at the centre of rock mass classification methods and significantly reduce the dependence on rule of thumb. It was found that this approach yields designs with powder factors that are consistent with the rock breaking effort and the behaviour of discontinuities while remaining biased towards preservation of perimeter wall rock.

## **ACKNOWLEDGEMENTS**

I would first like to thank my research advisor Mr Tawanda Zvarivadza of the School of Mining Engineering at University of the Witwatersrand. He availed himself whenever I had questions about my research or writing. He consistently allowed this work to be my own, while patiently steering me in the right direction.

I would also like to thank the Mr Nathaniel Mokwele (Section Manager – Geotech) and Agnes Ramere (Section Manager – Planning) for their assistance with the study from the beginning to the end. Further appreciation is extended to Tati Nickel Mining Company and its management for allowing me to use data from Phoenix Mine for furtherance of the research.

A final special note of appreciation goes to my family and loved ones for seeing me through the various stages and challenges of this research.

## TABLE OF CONTENTS

<b>DECLARATION.....</b>	<b>i</b>
<b>ABSTRACT.....</b>	<b>ii</b>
<b>ACKNOWLEDGEMENTS .....</b>	<b>iii</b>
<b>TABLE OF CONTENTS .....</b>	<b>iv</b>
<b>LIST OF FIGURES .....</b>	<b>vii</b>
<b>LIST OF TABLES .....</b>	<b>ix</b>
<b>LIST OF ABBREVIATIONS .....</b>	<b>x</b>
<b>CHAPTER 1: INTRODUCTION .....</b>	<b>1</b>
<b>1.1 Mine Background and General Information.....</b>	<b>1</b>
<b>1.2 Purpose of the Study .....</b>	<b>3</b>
<b>1.3 Project Background .....</b>	<b>4</b>
<b>1.4 Problem Statement.....</b>	<b>8</b>
<b>1.5 Key Questions to be Addressed.....</b>	<b>9</b>
<b>1.6 Research Objectives .....</b>	<b>9</b>
<b>1.7 Research Assumptions .....</b>	<b>9</b>
<b>1.8 Contents of the Research Report .....</b>	<b>9</b>
<b>CHAPTER 2: LITERATURE REVIEW .....</b>	<b>11</b>
<b>2.1 Rock Breaking Mechanism .....</b>	<b>11</b>
<b>2.2 Effect of Simultaneous Detonation of Adjacent Holes.....</b>	<b>13</b>
<b>2.3 Blasting Design Principles .....</b>	<b>15</b>
2.3.1 Energy Distribution.....	16
2.3.2 Energy Confinement .....	17
2.3.3 Energy Level.....	17
2.3.4 Relief.....	17

2.3.5	Explosives Ratio .....	17
<b>2.4</b>	<b>Effect of Rock Properties on Blasting .....</b>	<b>19</b>
2.4.1	Variability .....	19
2.4.2	Mechanical Properties.....	19
<b>2.5</b>	<b>Rock Mass Classification .....</b>	<b>20</b>
2.5.1	GSI - Geological Strength Index.....	21
2.5.2	RMR – Rock Mass Rating .....	22
<b>2.6</b>	<b>Influence of Geology on Wall Control.....</b>	<b>24</b>
<b>2.7</b>	<b>Blastability Index (BI).....</b>	<b>28</b>
2.7.1	Components of the Blastability Index.....	29
<b>2.8</b>	<b>Blasting Quality System (BQS) .....</b>	<b>31</b>
<b>2.9</b>	<b>Geotechnical Model and Geotechnical Database Approaches .....</b>	<b>31</b>
<b>2.10</b>	<b>Controlled Blasting Techniques.....</b>	<b>31</b>
<b>2.11</b>	<b>Literature Discussion .....</b>	<b>33</b>
<b>CHAPTER 3:</b>	<b>RESEARCH METHODOLOGY .....</b>	<b>35</b>
<b>3.1</b>	<b>Introduction .....</b>	<b>35</b>
<b>3.2</b>	<b>Literature Review.....</b>	<b>35</b>
<b>3.3</b>	<b>Data Collection .....</b>	<b>35</b>
<b>3.4</b>	<b>Results and Analysis of Results.....</b>	<b>35</b>
<b>3.5</b>	<b>Conclusion.....</b>	<b>36</b>
<b>CHAPTER 4:</b>	<b>RESULTS AND ANALYSIS OF RESULTS .....</b>	<b>37</b>
<b>4.1</b>	<b>Description and Audit of drilling and blasting at Phoenix Mine .....</b>	<b>37</b>
4.1.1	Blast Planning .....	37
4.1.2	Bench Blasting .....	39
4.1.3	Perimeter Blasting.....	42
4.1.4	Timing Design .....	45
<b>4.2</b>	<b>Rock Mass Data.....</b>	<b>48</b>

4.2.1	Stereographic Data.....	48
4.2.2	Mechanical Properties.....	52
<b>4.3</b>	<b>Field data.....</b>	<b>54</b>
4.3.1	Method of Data Collection.....	55
4.3.2	Joint Spacing.....	55
4.3.3	Rock Mass Rating.....	56
4.3.4	Geological Strength Index .....	58
4.3.5	Blastability Index (BI) .....	58
4.3.6	Slope Mass Rating (SMR) .....	60
<b>4.4</b>	<b>Design Input Tool (DIT) .....</b>	<b>63</b>
<b>4.5</b>	<b>Application of the DIT .....</b>	<b>67</b>
<b>4.6</b>	<b>RMC and BI Informed Blast Design – A Case Study of DIT Application.....</b>	<b>69</b>
<b>4.7</b>	<b>Discussion of Results and Analysis .....</b>	<b>74</b>
<b>CHAPTER 5:</b>	<b>CONCLUSIONS AND RECOMMENDATIONS .....</b>	<b>76</b>
5.1	Conclusions .....	76
5.2	Recommendations .....	78
<b>REFERENCES.....</b>		<b>79</b>
<b>Appendix A – BQS Chart.....</b>		<b>83</b>
<b>APPENDIX B – FIELD DATA.....</b>		<b>84</b>
<b>Appendix C – RQD Data.....</b>		<b>87</b>
<b>Appendix D - BI Calculation Data .....</b>		<b>88</b>
<b>Appendix E – RMR Calculation Data.....</b>		<b>91</b>
<b>Appendix F – SMR Calculation Data.....</b>		<b>94</b>

## LIST OF FIGURES

Figure 1.1: Location of Tati Nickel Mine (Google Earth, 2016).....	1
Figure 1.2: Phoenix Regional Geology (Hornsby and Jermy, 2011).....	2
Figure 1.3: Structural Geology Map of Phoenix (Hornsby and Jermy, 2011).....	3
Figure 1.4: Phoenix pit cutback sequence (Hornsby and Jermy, 2011).....	4
Figure 1.5: Plan view of a 3-D model of the Phoenix Pit.....	5
Figure 1.6: East - West section through the Phoenix Cut 8 Pit.....	6
Figure 1.7: Western highwall showing crest damage and highwall damage .....	7
Figure 1.8: Back damage and frozen toe material, Kekana (2015) .....	8
Figure 2.1: Zone of Crushing (Adapted from Cruise, 2011) .....	12
Figure 2.2: Zone of Radial Cracking (Cruise, 2011) .....	12
Figure 2.3: Crack Extension Zone (Cruise, 2011) .....	13
Figure 2.4: Intersection of radial waves from adjacent holes detonating simultaneously (Cruise, 2011) .....	14
Figure 2.5: Effect of detonation wave superimposition (Adapted from Google, 2016) .....	14
Figure 2.6: Split propagation and secondary mechanisms (de Graaf, 2011) .....	15
Figure 2.7: Blast performance factors (ISEE, 2011).....	16
Figure 2.8: Blast Layout (de Graaf, 2011).....	18
Figure 2.9: Section of blast layout (Adapted from de Graaf, 2011) .....	19
Figure 2.10: Effect of weakness planes on the final wall outcome (Rorke, 2003) .....	26
Figure 2.11: Shallow dipping structures striking parallel to the face (Workman and Calder, 1993) .....	27
Figure 2.12: Steep dipping structures striking parallel to the face (Rorke, 2003) .....	28
Figure 4.1: Schematic of misaligned pattern .....	38
Figure 4.2: Reversal of burden and spacing; spacing is larger than designed burden .....	38
Figure 4.3: Transverse section through a typical bench .....	40
Figure 4.4: Transverse section through bench adjacent to the final wall.....	42
Figure 4.5: Post-split design (Meta-Gabbro) .....	43
Figure 4.6: Rock hung-up against highwall.....	45
Figure 4.7: Typical timing design schematic .....	46
Figure 4.8: Timing contours for previous design.....	47



Figure 4.9: Timing contours for change implemented.....	48
Figure 4.10: Weighted joint data stereonet (Bosman, 2008) .....	49
Figure 4.11: Stereonet of joint set plane orientations and the western highwall .....	50
Figure 4.12: 3-D projection of J3 to J5 and the western highwall .....	51
Figure 4.13: Data distribution per rock type .....	55
Figure 4.14: Joint spacing data distribution .....	56
Figure 4.15: RQD % as a function of joint spacing (Bieniawski, 1979) .....	57
Figure 4.16: J-Block view of J3, J4 and J5 .....	62
Figure 4.17: Crest block loss indicated by J-Block .....	63
Figure 4.18: Design Input Tool for Dolerite .....	64
Figure 4.19: Design Input Tool for Meta-Gabbro .....	65
Figure 4.20: Design Input Tool for Pegmatite .....	65
Figure 4.21: Design Input Tool for Tonalite.....	66
Figure 4.22: General Design Input Tool .....	67
Figure 4.23: Information flow for Design Input Tool.....	68
Figure 4.24: DIT application on Meta-Gabbro .....	69
Figure 4.25: Pre-split design .....	71
Figure 4.26: Powder factor extrapolation .....	72
Figure 4.27: Trim Design.....	73
Figure A.1: BQS System Chart (Chatziangelou and Christaras, 2015) .....	83

## LIST OF TABLES

Table 2.1: GSI system chart (Hoek et al, 2005).....	22
Table 2.2: RMR parameter ratings (Bieniawski, 1989).....	24
Table 4.1: Phoenix Mine bench blasting parameters .....	39
Table 4.2: Buffer row parameters .....	41
Table 4.3: Post-split design parameters .....	43
Table 4.4: Initiation accessories.....	46
Table 4.5: Stereonet data.....	50
Table 4.6: Phoenix mine core sample data (TNMC, 2012) .....	53
Table 4.7: SMR metrics (Hudson, 2013).....	60
Table 4.8: SMR Classes (Hudson, 2013).....	61
Table 4.9: RMC informed Pre-split design using DIT inputs.....	71
Table B.1: Dolerite field data.....	84
Table B.2: Meta-Gabbro field data .....	85
Table B.3: Pegmatite field data.....	86
Table B.4: Tonalite field data .....	86
Table C.1: RQD percentage values.....	87
Table D.1: Dolerite BI Data.....	88
Table D.2: Meta-Gabbro BI Data .....	89
Table D.3: Pegmatite BI Data.....	90
Table D.4: Tonalite BI Data.....	90
Table E.1: Dolerite RMR Data .....	91
Table E.2: Meta-Gabbro RMR Data.....	92
Table E.3: Pegmatite RMR Data .....	93
Table E.4: Tonalite RMR Data .....	93
Table F.1: Dolerite SMR data.....	94
Table F.2: Meta-Gabbro SMR data .....	94
Table F.3: Pegmatite SMR data.....	94
Table F.4: Tonalite SMR data.....	95

## **LIST OF ABBREVIATIONS**

ANFO	Ammonium Nitrate Fuel Oil
BCL	Bamangwato Concessions Limited
BI	Blastability Index
BME	Bulk Mining Explosives
BQS	Blasting Quality System
DIT	Design Input Tool
GDIT	General Design Input Tool
GSI	Geological Strength Index
H	Hardness Factor
HEF	High Energy Fuel
HFC	Half Cast Factor
JPO	Joint Plane Orientation
JPS	Joint Plane Spacing
NE	North East
NHI	National Highway Institute
NW	North West
MPa	Mega Pascals
SE	South East
SGI	Specific Gravity Influence
PGE	Platinum Group Elements
RBS	Relative Bulk Strength
RMC	Rock Mass Classification
RMD	Rock Mass Description
RMR	Rock Mass Rating

RQD	Rock Quality Designation
RWS	Relative Weight Strength
SMR	Slope Mass Rating
UCS	Uniaxial Compressive Strength
WHW	Western Highwall

## CHAPTER 1: INTRODUCTION

Blasting is the first step in the comminution process of a mining operation. Various coordinated inputs contribute to its success, and in turn to the efficient execution of processes that lie downstream from the blasting unit step. Primary to meeting production and operational objectives of a mine, as well as the protection of the mineral resource and human life, is the achievement of highwall design specifications and competence. To this end, this study will investigate the use of existing tools and knowledge for the achievement of highwall control goals.

### 1.1 Mine Background and General Information

Tati Nickel Mining Company is a joint venture between BCL (Bamangwato Concessions Limited at 85%) and the Botswana Government (15%). The mine achieves a total production of 18million tons at a stripping ratio of 1.28. The primary mineral produced is nickel in the form of a concentrate; secondary minerals include gold and PGE's (Platinum Group Elements).

#### Location

Tati is located approximately 35km east of the city of Francistown in the North East District of Botswana. Figure 1.1 is a map showing the location of Tati Nickel Mine - Phoenix.

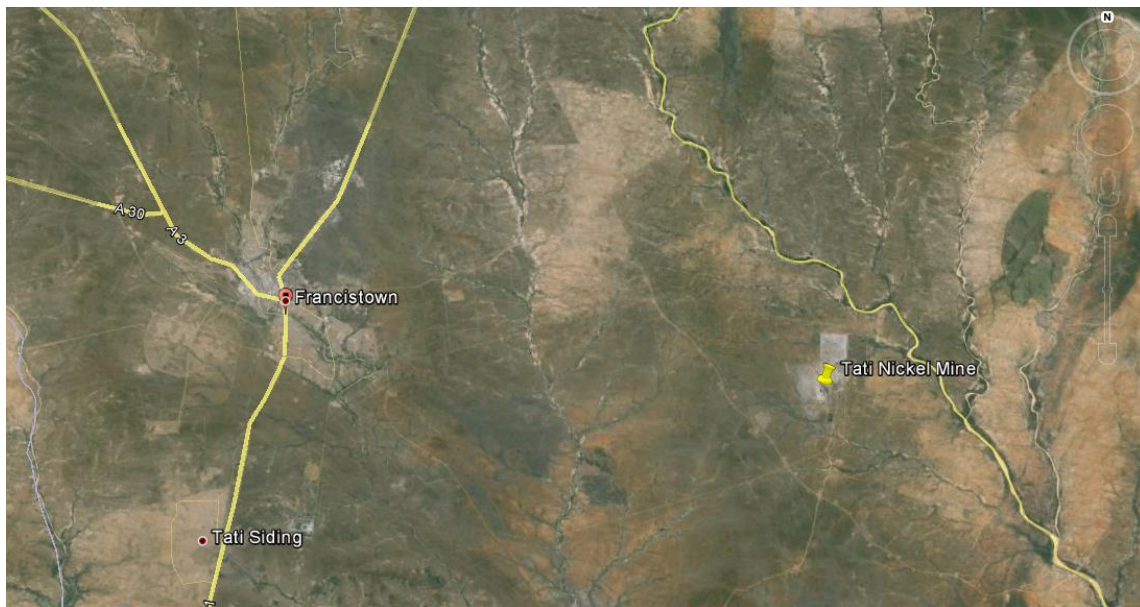
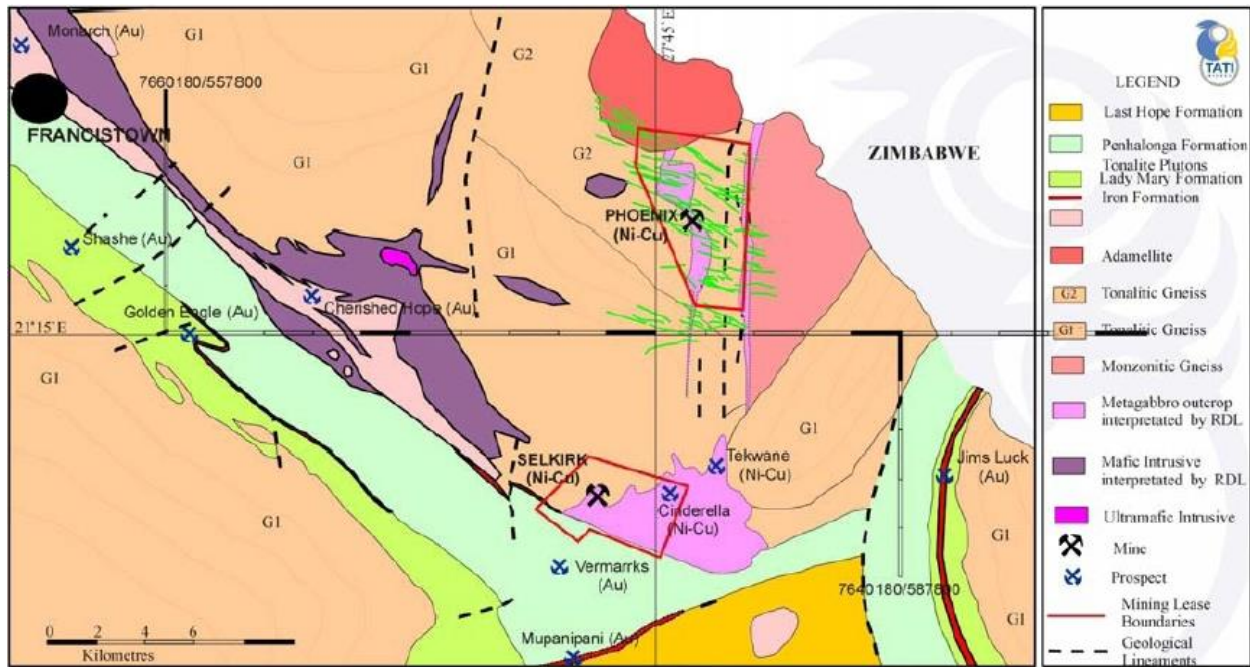


Figure 1.1: Location of Tati Nickel Mine (Google Earth, 2016)

## Geology

The regional geology hosting Tati Nickel's formations is that of the Tati Greenstone Belt. The local geology features a massive sulphide suite consisting of pentlandite, chalcopyrite, pyrite and pyrrhotite, hosted in a metagabbro envelope (Morolong, 2014). The basement rock is a granite with high silica content. A map of the regional geology of Phoenix is shown in Figure 1.2.



**Figure 1.2: Phoenix Regional Geology (Hornsby and Jermy, 2011)**

There is high variability in the structurally controlled style of mineralization that occurs at Phoenix. This is manifested in the form of domains of mineralization that have internal intrusions of granite (gangue) and vertical East-West striking dolerite dyke intrusions. Brittle to ductile shear zones occur across the pit with the large moderate to steep south and south-south-west dipping thrusts (Hornsby and Jermy, 2011). These authors further stated that smaller shears form a network between the large shears, including steeply NE dipping shears, vertical N-S trending shears and rare NE trending shears that dip either moderately to the NW or SE. Figure 1.3 shows the local structural geology at Phoenix.

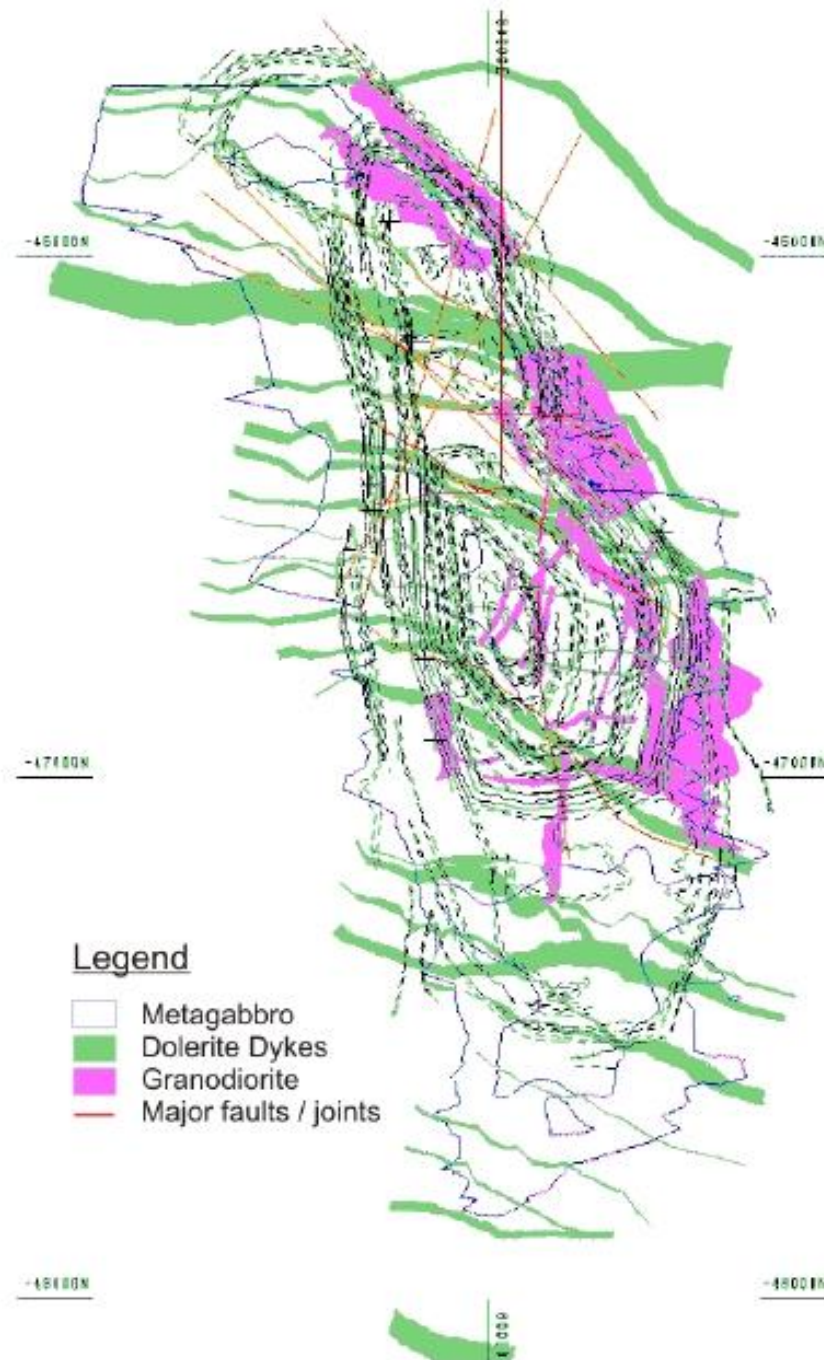


**Figure 1.3: Structural Geology Map of Phoenix (Hornsby and Jermy, 2011)**

## 1.2 Purpose of the Study

This study seeks to establish the applicability of rock mass classification as a primary input to wall control blasting. Traditionally, rules of thumb are used to develop blast designs based on



parametric ratios, without due cognizance of the rock mass factors that influence the achievability of final wall designs. In the study, it will be attempted to establish distinguished zones along a highwall forming a rock mass, wherein the zoning factors will be used to establish the suitability of the wall control designs currently applied, and their contribution to the failure in achieving the highwall design; in particular the designed catchment berm widths and berm competence.

### 1.3 Project Background

There was a growing concern over the condition of the western highwall of the Phoenix Cut 8 Pit (Figure 1.4). The trend appeared to go back as far as the previously mined cuts 6 and 7, and if not attended to, it is likely to carry on into the future Cut 9 and Cut 10 as these will be primarily mined in the western highwall.

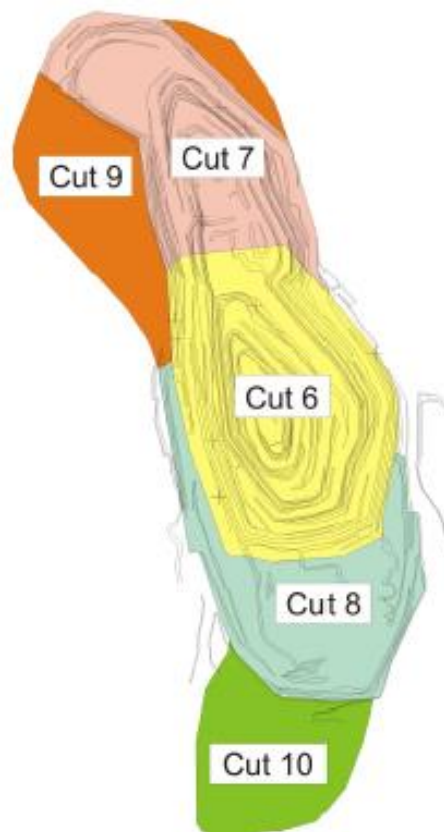


**Figure 1.4: Phoenix pit cutback sequence (Hornsby and Jermy, 2011)**

The concern was brought about by the fact that this highwall had one mildly undulated plunge from the top benches to the present mining grade levels (approximately 200m). This is to say that



the designed catchment berms in between bench stacks were not in their correct form and the stepwise bench and stack profiles were reduced to an almost single drop of highwall face.

Figure 1.5 is plan view of a 3D model of the Phoenix pit in its present state. The line AB runs through the portion of the pit that is Cut 8. The east west section through AB (Figure 1.6) plots the planned pit profile in grey against the profile actually achieved. The superimposition of the two profiles demonstrates how the designed wall profile has not been achieved, particularly along the western highgwall.

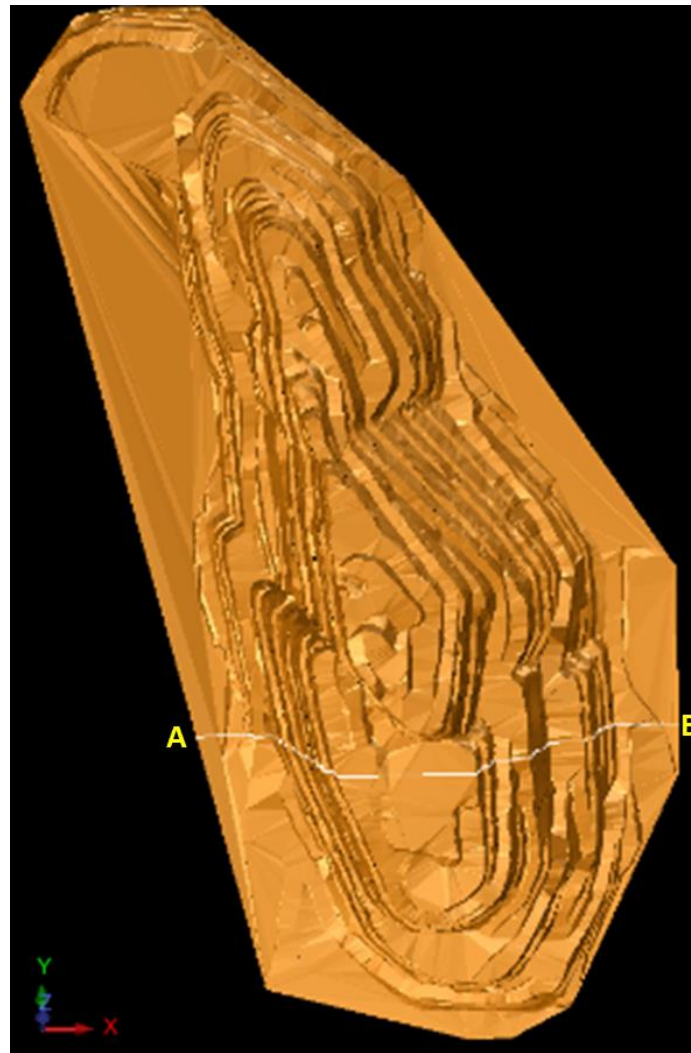


**Figure 1.5: Plan view of a 3-D model of the Phoenix Pit**

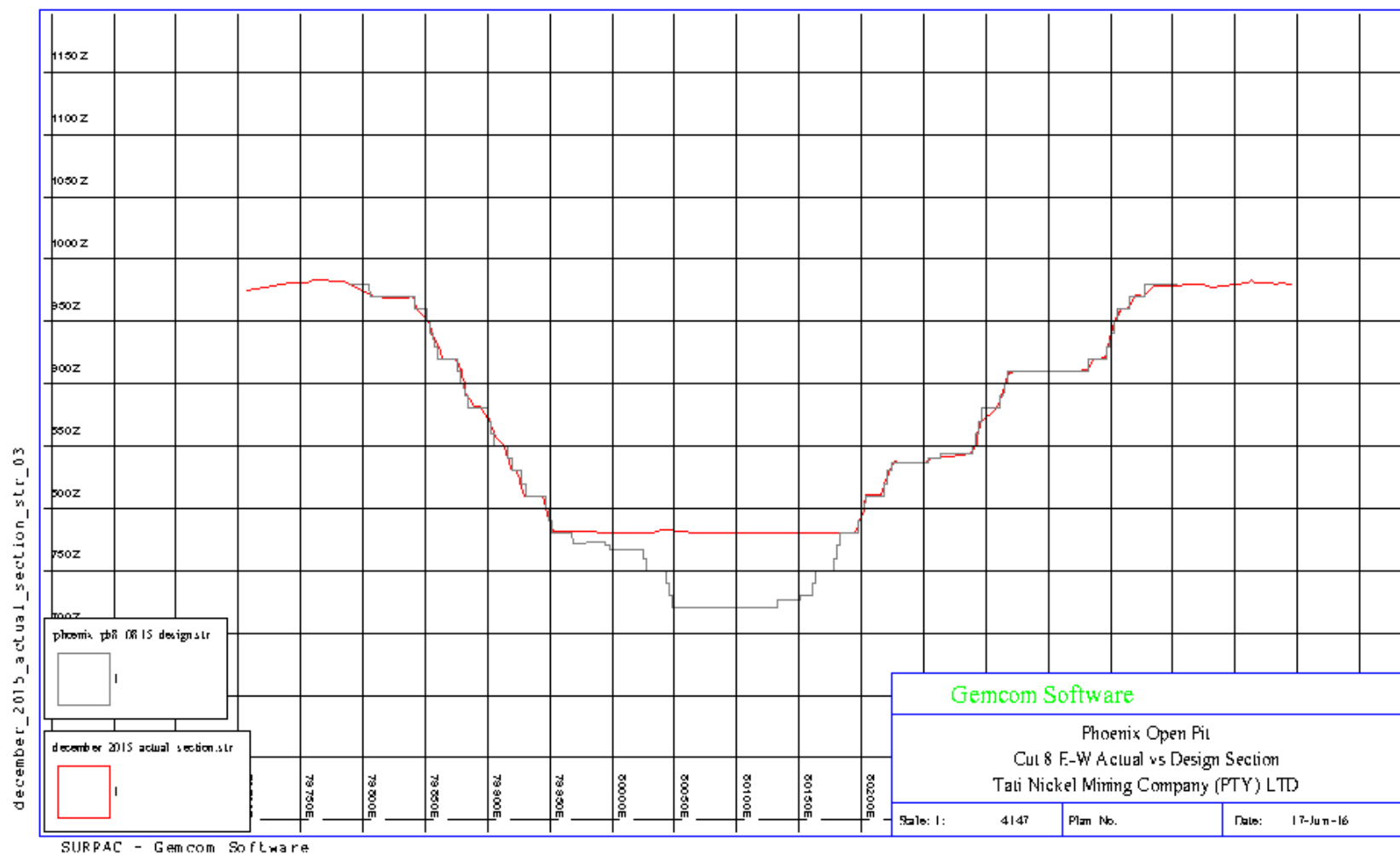


**Figure 1.6: East - West section through the Phoenix Cut 8 Pit**

Several subsequent concerns came to light following this observation, the most obvious of which being the fact that there was no catchment facility should there be any rockfalls from higher benches. This created a hazardous work environment in which both men and machines could easily fall into harm's way from the falling loose rock fragments and localized failures of the highwall.

Although various phenomena, individually and synergistically, could have brought about the undesired result, a decision was taken to look into the contribution of drilling and blasting to the problem. During an investigation into the blasting practices at the mine, it was established that there were four main rock types (of hardness ranging between 138 MPa and 313 MPa) forming the pit and its walls. It was further noted that the approach taken to wall control blasting did not pay particular attention to the geological and geotechnical characteristics of the various rock mass zones corresponding with the rock types present. Instead, a blanket design approach was followed; the result was an inconsistent yield of results featuring various areas of acceptable highwall competence, highwall material hangups, back damage, overbreak and localized failure along weakness planes (Segaetsho, 2014). Figure 1.7 presents the western highwall showing crest damage and highwall damage.

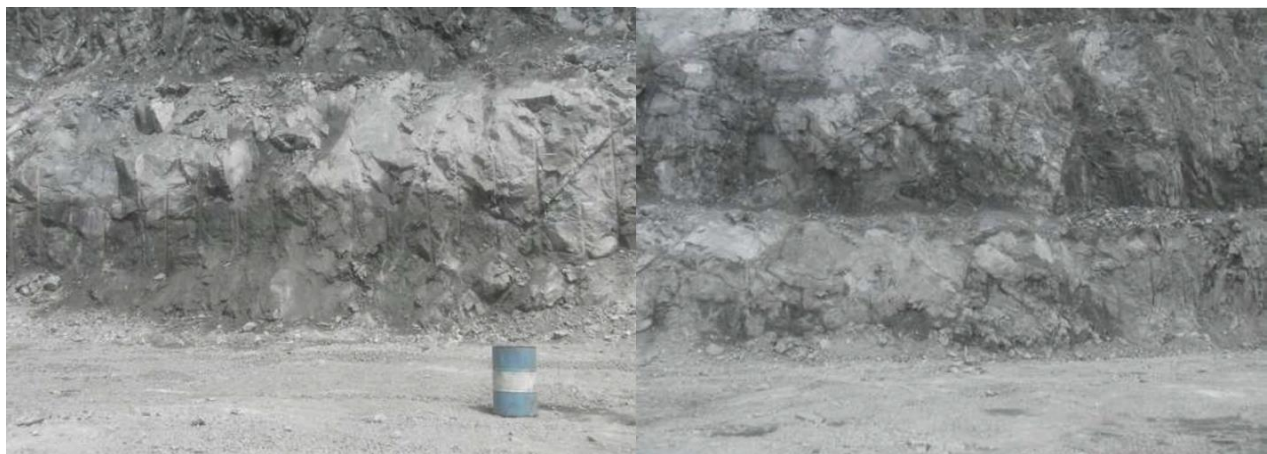


**Figure 1.7: Western highwall showing crest damage and highwall damage**

Kekana (2015) outlined bench crest failure as a contributing factor to the wall control problem observed along the western highwall of the pit. The author's investigation report (Kekana 2015) stated that the crest damage, even where berms were planned, had the effect of reducing the intended width of the berm and in turn its functional catchment capacity. It appeared at the time of the study, that preferential failure along planes of weakness could have been a major contributory factor to the failure of bench crests. Charging control near the collars of holes was also cited as a

possible cause of the persistently unsatisfactory crest competence. It was further stated that under broken material at the toes of the benches added to the reduction of berm width and increased the potential for rolling down of falling rock once mining has proceeded to lower levels. Figure 1.8 is a schematic section showing the phenomena alluded to.

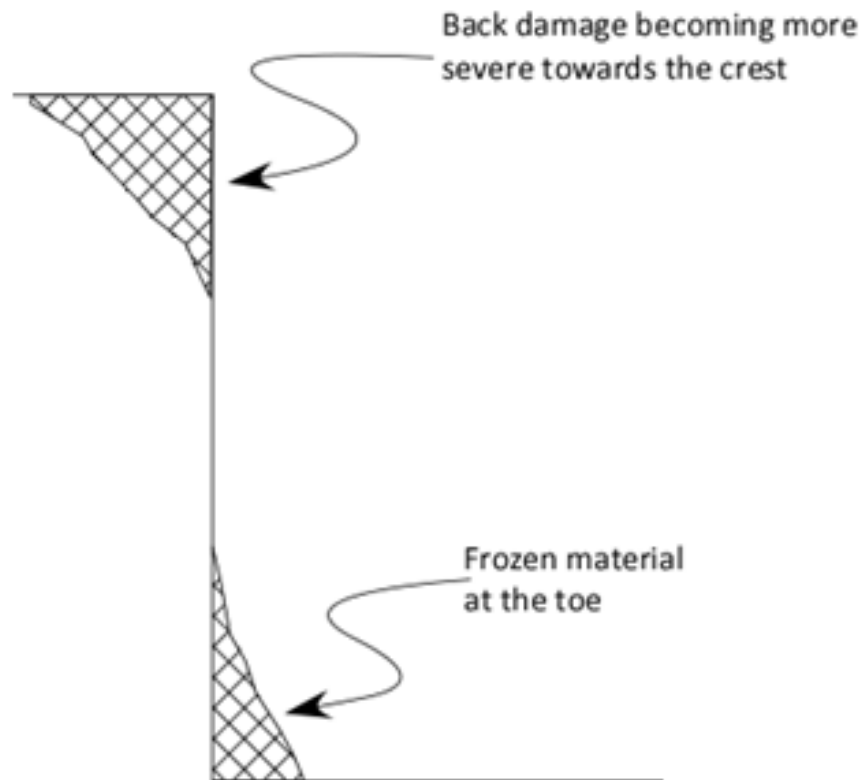


**Figure 1.8: Back damage and frozen toe material, Kekana (2015)**

#### **1.4 Problem Statement**

Control of the western highwall of the Phoenix pit has proven to be challenging in that the designed catchment berms and wall competence have been perpetually unachievable from the pit crest to the current mining levels. This exposes the mining operation to safety hazards such as local wall rock failure from damaged crests, frozen toes and rolling rock falls from higher mining levels. There are also increased standoff distances from the highwall concerned which reduce the available manoeuvring area on the pit floor, and subsequently the factor of extraction that is safely achievable. This study seeks to investigate the application of rock mass classification and the Blastability Index (BI) as a means to improve wall control. The BI was developed and applied in

the estimation of explosive energy applicable to rock masses of varying characteristics; and more contemporarily in the estimation rock mass fragmentation. In the study context, it will be used as means of zoning the area of interest according to the BI, and using its rock mass classification inputs to inform rock blast designs for wall control.

### **1.5 Key Questions to be Addressed**

The following are questions that ought to be addressed by the study:

- Can BI be used as an indicator of the achievability of wall control in rock mass and the need to pay special attention to blast design inputs?
- Can rock mass classification be incorporated into the decision making process for effective perimeter wall control?
- How do the outcomes of designs informed by rock mass classification weigh up against the economics of the design?

### **1.6 Research Objectives**

The objectives of the study are as follows:

- To establish zoning boundaries within the pit based on rock type, rock mass characteristics and Lilly's Blastability Index (BI).
- To use rock mass classification to inform perimeter blast design with the BI as an indicator of potential rock response.
- To develop a design input tool which allows for the concurrent consideration of rock mass characteristics and wall control factors.

### **1.7 Research Assumptions**

The main assumption when carrying out this study is that the correct pit and slope design discipline was observed in the design stages of the mine, as informed by the geotechnical and geomechanical elements of the local rock mass. As such, the geotechnical and rock mass data collected and utilized is assumed to be correct.

### **1.8 Contents of the Research Report**

Chapter one introduces the operation under consideration in the study and delivers an appreciation of the problem experienced. The objectives to be met through the project are also highlighted. Chapter two gives a broad understanding of the mechanisms at play during rock breaking with explosives, and looks into the rock mass characteristics that influence the outcomes observed.

Relevant rock mass classification methodology applications are also briefly discussed. Chapter three details the methodology observed in conducting the research. In Chapter four, the results and analysis of results are presented in detail. Components include the audits, field data, key findings, design tool development, a brief case study and related discussions. Chapter five presents the conclusions drawn from the study relative to the objectives outlined. Recommendations derived from the study are also presented in Chapter five.

## CHAPTER 2: LITERATURE REVIEW

Rock masses comprise of geological formations which are subjected to various stages of chemical and mechanical disintegrative processes. These conditions affect the achievability of mining process outcomes from the primary design phases through to the implementation of plans and execution of respective mining activity.

This section summarises the current state of knowledge around the use of rock mass classification methodology in the formulation of the Blastability Index (BI) as a means of determining the effort required to successfully break rock. Further to this, the literature review is geared at exploring the possibility of building on available approaches and uses of the BI towards using it to inform wall control design parameters and inputs.

### 2.1 Rock Breaking Mechanism

The detonation of a column of explosives induces two modes of stress in the surrounding rock mass. The first occurs in the form of a shock stress wave which is transmitted to the surrounding rock immediately upon detonation. The second stress induced on the surrounding rock mass is a result of gas pressure from the rapid expansion of the explosive.

The stress – strain relationship of rocks is such that they tend to be far stronger in compression than they are in tension (Cruise, 2011). The tensile strength of rocks is in the order of a tenth of their compressive strength. This being the case, the most likely failure mechanism of rock placed under stress due to blasting is tension.

Cruise (2011) describes the sequence of events after the initiation of a blast hole as follows:

- **Zone of Crushing:** due to the fact that stresses resulting from a detonating column are in the order of Giga-Pascals, the rock immediately surrounding a blast hole (with strengths in lower hundred Mega-Pascals) undergoes compressive failure. This phenomenon radiates outward from the hole until the magnitude of the stress wave is equal to or less than the compressive strength of the rock (Figure 2.1).

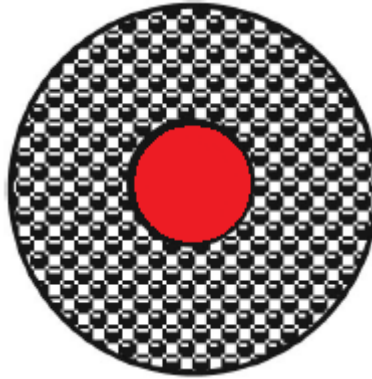


**Figure 2.1: Zone of Crushing (Adapted from Cruise, 2011)**

- **Zone of Radial Cracking:** beyond the crushed zone, the intensity of the shock wave is less in magnitude than what is required to overcome the compressive strength of the rock; however, it remains sufficient to overcome the tensile strength of the rock. There is thus a zone which lies beyond the crushed zone where the failure that results in the rock is due to tension. This is expressed in the form of radial cracks due to the outward propagation of the stress wave (Figure 2.2).

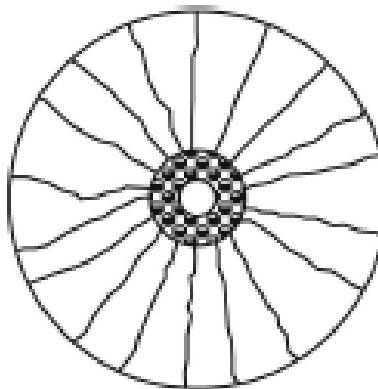


**Figure 2.2: Zone of Radial Cracking (Cruise, 2011)**

- **Zone of Crack Extension:** the second phase of the detonation process takes effect in the form of explosives gases exerting pressure on the walls of the hole. In the attempt to escape and balance the internal borehole pressure with the atmospheric pressure, the gases enter



the cracks formed thereby supporting their propagation. The dominant cracks expand at the expense of less developed cracks, and develop to their maximum potential when the gas pressure within them can no longer cause them to extend further. The zone of maximum crack extension lies within a radius of 40 hole diameters from the centre of the blast hole. It is in this zone that cracks from adjacent holes are expected to interact to produce the desired rock breaking effect. Equally, the dominant influence of geological structures in the rock mass would also take effect in this zone (Figure 2.3).

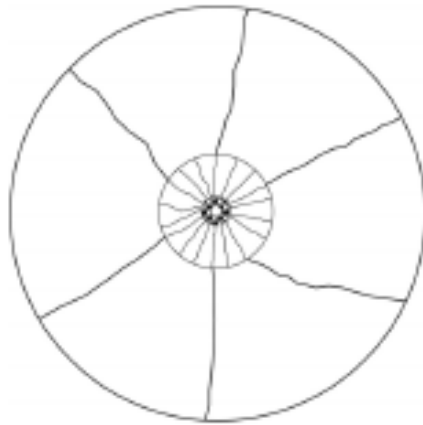


**Figure 2.3: Crack Extension Zone (Cruise, 2011)**

## **2.2 Effect of Simultaneous Detonation of Adjacent Holes**

When two adjacent holes are detonated simultaneously, the radial stress waves from the holes intersect. When this intersection occurs at the median point between the two holes (Figure 2.4), the waves are superimposed constructively and their effect on a particle at that point is equal to the sum of the two waves as shown in Figure 2.5.

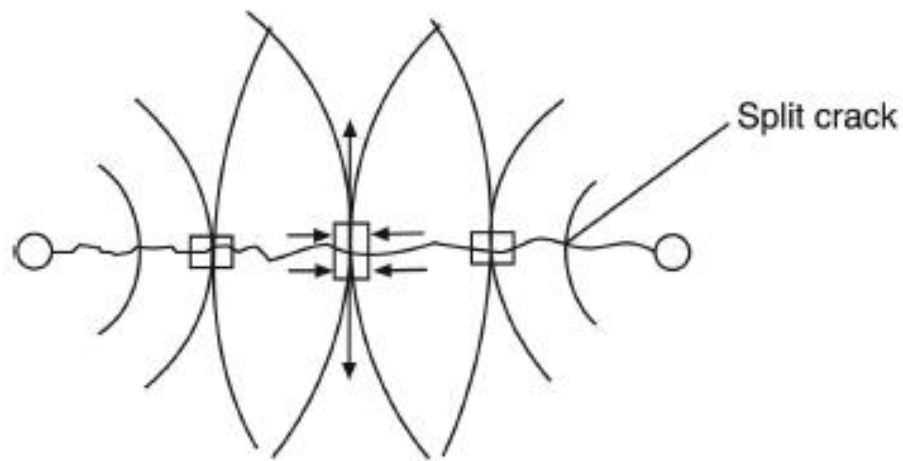


**Figure 2.4: Intersection of radial waves from adjacent holes detonating simultaneously (Cruise, 2011)**

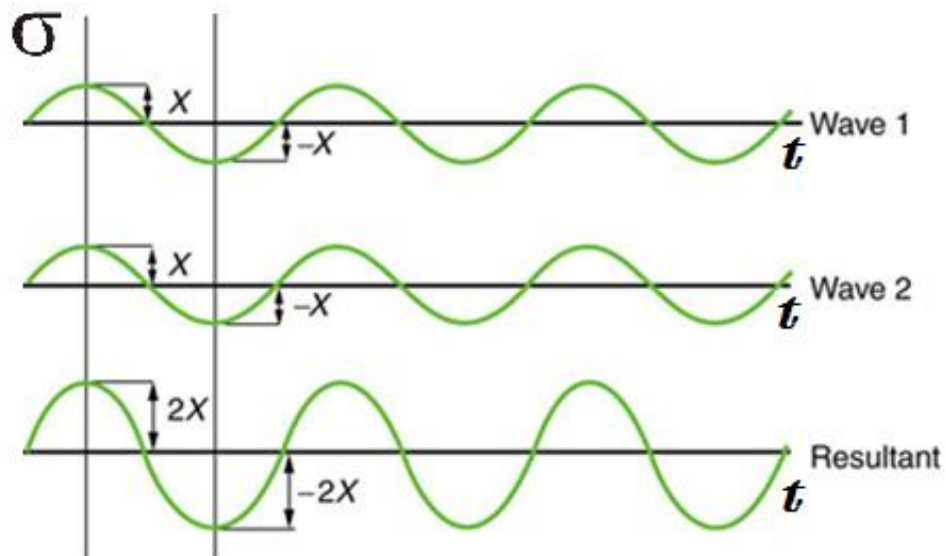


**Figure 2.5: Effect of detonation wave superimposition (Adapted from Google, 2016)**

Considering the amplitude of the waves in Figure 2.5 as the stress  $\sigma$ , the combined effect of the two waves acting at a common point is the sum of the compressive stresses of the two waves. If the waves impose the same peak stress at that point, then the magnitude of the compressive stress observed is doubled.

As denoted in Figure 2.4, the application of a directional compressive stress on a piece of rock induces a tensile stress perpendicular to the axis of the compressive stress (Cruise, 2011). In the case of two superimposed waves, the resultant tensile stress is also doubled. If that tensile stress surpasses the tensile strength of the rock, tensile failure occurs thereby initiating a crack from the median point between two holes. The propagation of the crack along a system of holes forms what is referred to as a split.

Figure 2.6 is an annotated schematic of the larger scale mechanism in effect during the development of the split. In a massive undisturbed rock mass, the extension of cracks other than those in the plane of the split is precluded by the compressive stress from the adjacent holes (De Graaf, 2011).

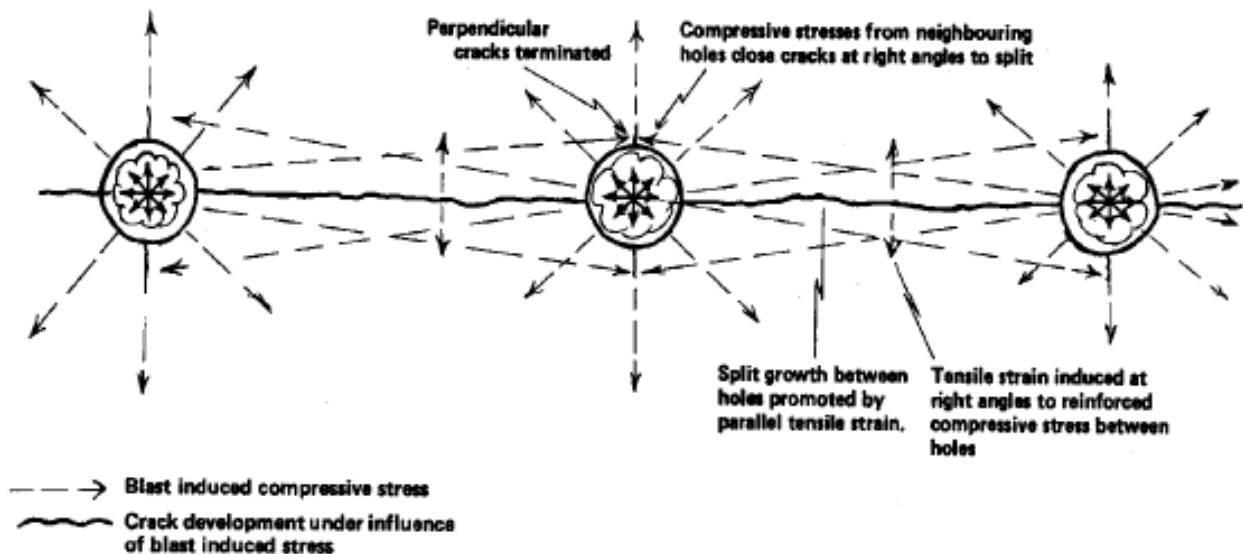
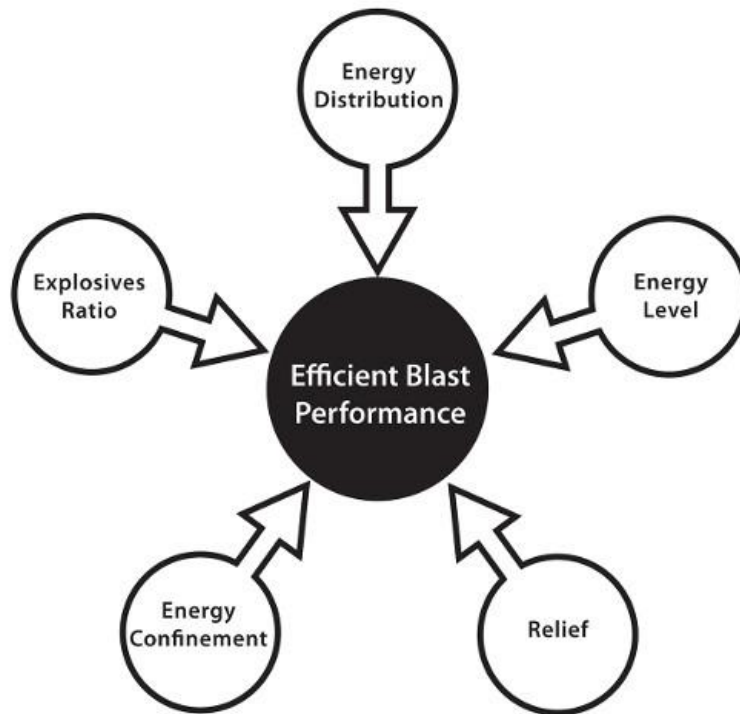


Figure 2.6: Split propagation and secondary mechanisms (de Graaf, 2011)

### 2.3 Blasting Design Principles

In order to be able to assess the outcome of a blast and its attainment of set objectives, it is important to have an understanding of the various factors that influence its performance. The most fundamental of these factors are the energy distribution, energy level, relief, confinement, and explosives ratio as shown in Figure 2.7.



**Figure 2.7: Blast performance factors (ISEE, 2011)**

### **2.3.1 Energy Distribution**

ISEE (2011) proposed that the most significant blast design parameter is the actual borehole that is drilled. This is due to the fact that it controls the amount of energy that is loaded into it by way of its fixed volume. This in turn controls the amount of energy that can be effected on the blast.

In general, smaller blast holes allow for improved uniformity of explosives distribution, as patterns involving small diameter holes are drilled with appreciably smaller spacings. Improved energy dissemination using small hole diameters is particularly advantageous when dealing with highly structured rock. Among the several advantages of improved energy distribution is the enhanced ability to control the effect of a blast on perimeter walls (Newton's Third Law of Motion). A balance is usually struck between a blast hole diameter size for optimum energy distribution and one that allows for production requirements to be met effectively.

### **2.3.2 Energy Confinement**

In order for the explosives to effectively break rock, energy from the detonation process must be contained long enough for it to do work on the rock (achieving peak pressure and extending cracks). Premature venting of energy results in insufficient crack network maturity resulting in poor fragmentation and fragment displacement (relief).

It is important to note that explosive energy always takes the path of least resistance (ISEE, 2011). Such paths are usually in low burden areas, zones of weak geology and weak stemming (either by design or selection of stemming material).

### **2.3.3 Energy Level**

This refers to total energy the explosive will avail for application to the rock mass. The available energy from explosives detonation is estimated using complex thermodynamic models and is measured in units of kilojoules per kilogram (kJ/kg) (Rorke, 2003). This complexity necessitates the use of relative measures of explosives energy in order to compare the energy of a known reference explosive (typically ANFO at a density of  $0.8\text{g/cm}^3$ ) to another explosive. The two most common measures of comparison are the Relative Weight Strength (RWS) and the Relative Bulk Strength (RBS). The former compares the energy in equal weights of explosives whereas the latter compares the energy in equal volumes of explosives.

### **2.3.4 Relief**

The term relief refers to a free surface that borders an unoccupied volume in space large enough for blasted rock to occupy (ISEE, 2011). For optimal blast performance, there must be a sufficient void volume adjacent to the rock to be blasted into which it can move and expand. The surface bordering such void space is known as the “free face”.

From a dynamic standpoint, the term relief speaks to the effect of the progressive formation of the free face as the detachment of one hole’s burden leaves the hole behind it with sufficient void volume into which its burden can move and expand. This is termed burden relief.

### **2.3.5 Explosives Ratio**

The measure of how much explosive (in kg) is used per unit of rock mass is termed the explosive ratio. The most common expression of the explosive ratio in the mining industry is the powder factor, measured in  $\text{kg/m}^3$ . This ratio is given by the equation:

$$\text{Powder Factor} = \frac{\text{Charge Mass (kg)}}{\text{Burden} \times \text{Spacing} \times \text{Bench Height}}$$

Figure 2.8 and Figure 2.9 are schematics of the typical blast layouts showing the various parameters that go into the calculation of the powder factor. Burden is the perpendicular distance between the two successive rows of blast holes, or the distance between the first row of holes and the crest. Spacing is the distance between two successive holes within a row of holes. The volume of rock considered in the calculation of the powder factor is a product of burden, spacing and the bench height. This is known as the “yield” of the hole, and it is the amount of rock fragmented by the explosive over the length of the borehole to the floor grade level.

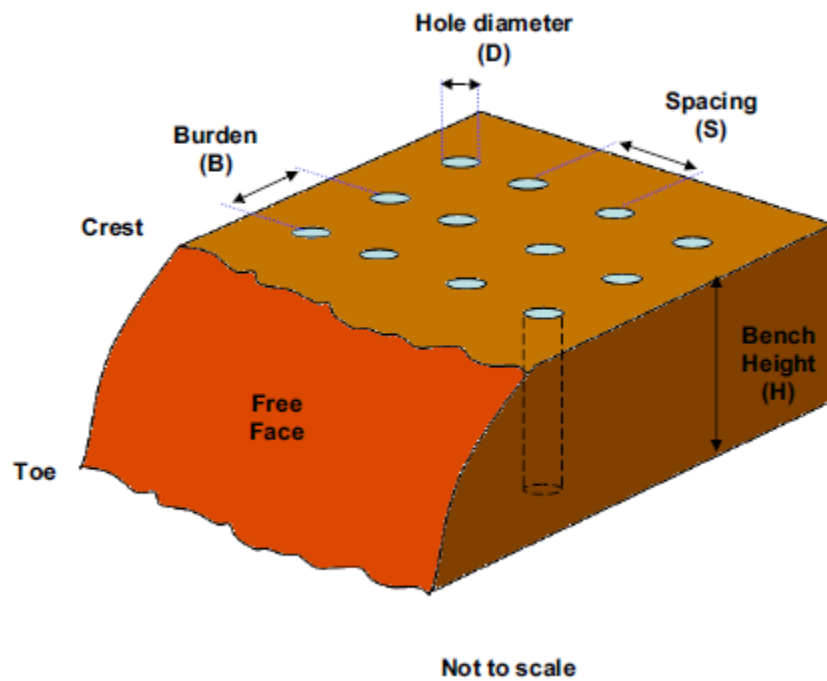


**Figure 2.8: Blast Layout (de Graaf, 2011)**

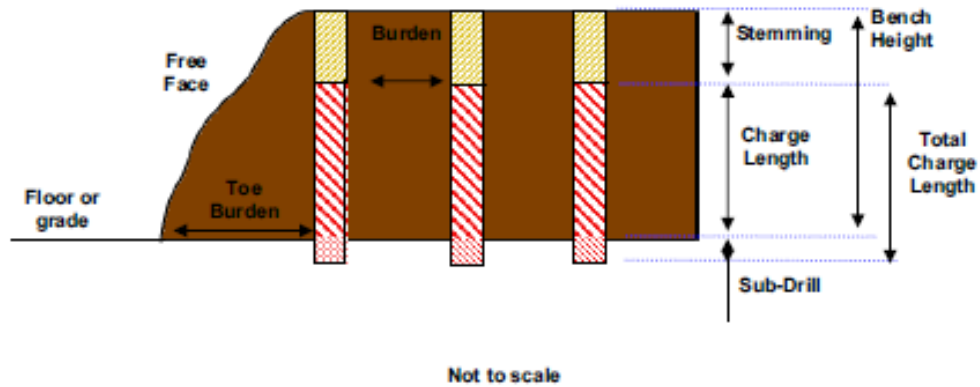


**Figure 2.9: Section of blast layout (Adapted from de Graaf, 2011)**

## **2.4 Effect of Rock Properties on Blasting**

The influence of rock properties on both production and perimeter wall blasting is unavoidable. The extent to which the inherent properties take effect on the achievability of rock breaking designs, however, is dependent on one's consideration of the properties in the design process.

### **2.4.1 Variability**

Variability of properties within a rock mass has a significant effect on the outcome of rock breaking. Variations in the rock mass can be brought about by changes in material properties, weathering, geological structures and other features of a rock mass (ICI, n.d). Insufficient consideration of variability, and the zones in which it occurs, results in missed opportunities to modify blast designs to suit the design ends aspired to.

### **2.4.2 Mechanical Properties**

Mechanical properties have a marked effect on blasting. Some of these will be discussed in this section.

#### **Dynamic Compressive Strength**

Strength of rock that is commonly referred to is the static compressive strength. It is worth noting that the dynamic compressive strength of rock is in the order of 10 times more than its static compressive strength (ICI, n.d). This being said, more explosive energy is used in the extension of cracks in rock with high dynamic strength, as crushing of the rock forming the borehole walls is minimal.

## **Dynamic Tensile strength**

In a similar manner to the dynamic compressive stress, the dynamic tensile stress of a rock is greater than the static tensile stress. The formation of radial cracks around a blast hole therefore commences when the tensile stress exceeds the dynamic tensile strength (ICI, n.d). At a point the tensile stress drops below dynamic stress threshold where new cracks are formed, but the residual tensile stress is sufficient to continue extending pre-existing cracks (ICI, n.d)..

## **Elasticity**

Rocks generally display elastic behaviour (Cruise, 2011). The elasticity of rock is typically described using Young's modulus; the ratio of stress applied to the strain resulting from the applied stress. De Graaf (2011) and ICI (n.d) agree that rocks with a low modulus of elasticity deform more before failure thereby absorbing more energy than stiffer rock which makes them less responsive (de Graaf, 2011) .

## **Density and Porosity**

Rock with high density tends to require higher explosives energy than rock with low density in order to achieve the desired rock breaking outcome. This is due to the increased inertia of the higher density rock (ICI, n.d)..

Porosity takes effect by way of reducing the gas pressure of the rock as gases are wedged into pores (ICI, n.d). The propagation of cracks as desired is also hindered by pore voids.

## **2.5 Rock Mass Classification**







The complexity of a rock mass can be such that it becomes impossible to consider each of the geological weaknesses individually. Addressing the need to understand the rock mass using the sum of mechanical properties of rock samples of appropriate sizes becomes impracticable, thus necessitating the treatment of the rock mass as a pseudo continuum (Stacey, 2015). Such rock masses are effectively assessed using acceptable rock mass classification methodology. The GSI (Geological Strength Index) and RMR (Rock Mass Rating) are relevant to this study.



### **2.5.1 GSI - Geological Strength Index**

The GSI is a quick visual method of quantifying the geological condition of a rock mass (Stacey, 2015). It makes use of a chart (Table 2.1) with a range of rock mass structures and associated sketches on the column axis and a range of surface condition descriptions on the row axis. The correlation of the descriptions from the two axes give a range of GSI values for the rock mass under consideration. As reflected by the chart, it is recommended that a range of values is selected instead of attempting to assign a finite value to a rock mass under assessment.

**Table 2.1: GSI system chart (Hoek et al, 2005)**

<p><b>GEOLOGICAL STRENGTH INDEX FOR JOINTED ROCKS (Hoek and Marinos, 2000)</b></p> <p>From the lithology, structure and surface conditions of the discontinuities, estimate the average value of GSI. Do not try to be too precise. Quoting a range from 33 to 37 is more realistic than stating that GSI = 35. Note that the table does not apply to structurally controlled failures. Where weak planar structural planes are present in an unfavourable orientation with respect to the excavation face, these will dominate the rock mass behaviour. The shear strength of surfaces in rocks that are prone to deterioration as a result of changes in moisture content will be reduced is water is present. When working with rocks in the fair to very poor categories, a shift to the right may be made for wet conditions. Water pressure is dealt with by effective stress analysis.</p>		<p><b>SURFACE CONDITIONS</b></p> <p>VERY GOOD Very rough, fresh unweathered surfaces</p> <p>GOOD Rough, slightly weathered, iron stained surfaces</p> <p>FAIR Smooth, moderately weathered and altered surfaces</p> <p>POOR Slacksided, highly weathered surfaces with compact coatings or fillings or angular fragments</p> <p>VERY POOR Slacksided, highly weathered surfaces with soft clay coatings or fillings</p>				
<p><b>STRUCTURE</b></p>		<p><b>DECREASING SURFACE QUALITY</b> →</p>				
<p><b>DECREASING INTERLOCKING OF ROCK PIECES</b></p> <p>↓</p>	 <p>INTACT OR MASSIVE - intact rock specimens or massive in situ rock with few widely spaced discontinuities</p>	90			N/A	N/A
	 <p>BLOCKY - well interlocked undisturbed rock mass consisting of cubical blocks formed by three intersecting discontinuity sets</p>	80	70			
	 <p>VERY BLOCKY- interlocked, partially disturbed mass with multi-faceted angular blocks formed by 4 or more joint sets</p>		60			
	 <p>BLOCKY/DISTURBED/SEAMY - folded with angular blocks formed by many intersecting discontinuity sets. Persistence of bedding planes or schistosity</p>		50			
	 <p>DISINTEGRATED - poorly interlocked, heavily broken rock mass with mixture of angular and rounded rock pieces</p>		40			
	 <p>LAMINATED/SHEARED - Lack of blockiness due to close spacing of weak schistosity or shear planes</p>		30			
			20			
				10		
		N/A	N/A			

## 2.5.2 RMR – Rock Mass Rating

The GSI was found to be identical to the 1976 version of Bieniawski's RMR under the conditions that the rock mass is completely dry (with a ground water rating of 10), and that it has favourable orientation of jointing with an orientation adjustment of zero. This version of the RMR:GSI

equation is only valid when an RMR value greater than 18 is obtained (Hoek et al, 2005). A revision of the RMR in 1989 saw the establishment of another correlation as follows (Hoek, 1995):

$$\text{GSI} = \text{RMR} - 5$$

The condition observed with this version is that an RMR value greater than 23 is obtained, with the ground water rating equal to 15 and the joint orientation adjustment equal to 0. If the RMR obtained with this version is equal to or below 23, then neither the 1989 nor the 1976 versions of the method may be used to estimate the GSI. The RMR is calculated by the summation of the parameter ratings in Table 2.2.

Table 2.2: RMR parameter ratings (Bieniawski, 1989)

PARAMETER			Range of values // ratings						
1	Strength of intact rock material	Point-load strength index	> 10 MPa	4 - 10 MPa	2 - 4 MPa	1 - 2 MPa	For this low range uniaxial compr. strength is preferred		
		Uniaxial compressive strength	> 250 MPa	100 - 250 MPa	50 - 100 MPa	25 - 50 MPa	5 - 25 MPa	1 - 5 MPa	< 1 MPa
	RATING		15	12	7	4	2	1	0
2	Drill core quality RQD		90 - 100%	75 - 90%	50 - 75%	25 - 50%	< 25%		
	RATING		20	17	13	8	5		
3	Spacing of discontinuities		> 2 m	0.6 - 2 m	200 - 600 mm	60 - 200 mm	< 60 mm		
	RATING		20	15	10	8	5		
4	Condition of discontinuities	Length, persistence	< 1 m	1 - 3 m	3 - 10 m	10 - 20 m	> 20 m		
		Rating	6	4	2	1	0		
		Separation	none	< 0.1 mm	0.1 - 1 mm	1 - 5 mm	> 5 mm		
		Rating	6	5	4	1	0		
		Roughness	very rough	rough	slightly rough	smooth	slickensided		
		Rating	6	5	3	1	0		
		Infilling (gouge)	none	Hard filling		Soft filling			
			-	< 5 mm	> 5 mm	< 5 mm	> 5 mm		
		Rating	6	4	2	2	0		
		Weathering	unweathered	slightly w.	moderately w.	highly w.	decomposed		
Rating	6	5	3	1	0				
5	Ground water	Inflow per 10 m tunnel length	none	< 10 litres/min	10 - 25 litres/min	25 - 125 litres/min	> 125 litres /min		
		$p_w / \sigma_1$	0	0 - 0.1	0.1 - 0.2	0.2 - 0.5	> 0.5		
		General conditions	completely dry	damp	wet	dripping	flowing		
	RATING		15	10	7	4	0		

$p_w$  = joint water pressure;  $\sigma_1$  = major principal stress

$p_w$  = joint water pressure;  $\sigma_1$  = major principal stress

#### B. RATING ADJUSTMENT FOR DISCONTINUITY ORIENTATIONS

		Very favourable	Favourable	Fair	Unfavourable	Very unfavourable
<b>RATINGS</b>	Tunnels	0	-2	-5	-10	-12
	Foundations	0	-2	-7	-15	-25
	Slopes	0	-5	-25	-50	-60

## 2.6 Influence of Geology on Wall Control

In order to achieve the desired final wall stability and functionality in conjunction with rock breaking activity, it is imperative that mining is preceded by a good understanding of the rock mass geology. Scoble et al (1996) emphasised the importance of accounting for geology in the characterisation and control of rock mass damage.

Singh (2003) pointed to the fact that the heterogeneous and anisotropic nature of in-situ rock masses is a crucial factor to consider, albeit typically ignored in the blasting process. He spoke to the negative effect of discontinuities and flaws in the rock mass on the achievability of blasting outcomes, particularly when a standard blanket approach is taken to blast designs.

Although several geological and geomechanical factors contribute to the competence of an excavated wall, planar weaknesses have a dominant influence on the outcome of the planned wall. These include joints, faults, bedding planes and geological contacts. Rorke (2003) and Chiappetta (1991) suggested that jointing is a particularly dominant factor when it comes to final wall control, and that the occurrence of more than two or three joints within a single span of blast hole spacing has an adverse effect on the achievement of wall control goals.

It is understood that blasting in a homogeneous massive rock mass yields perceptibly more desirable outcomes than in jointed rock, particularly with reference to highwall competence and control. Worsey et al (1981) found that when joint angles are less than 60 degrees to the free face, the achievability of the wall control goals diminishes considerably. NHI – National Highway Institute (1991) stated that the presence of jointing that intersects the face at an angle less than 15 degrees will not yield effective results with any wall control blasting techniques. It must be borne in mind, however, that failure to achieve cosmetically pleasing results is not necessarily an indication of highwall instability or the inability to achieve desired final wall configuration.

Figure 2.10 is an annotated schematic demonstration of the influence of geology on the final wall blast outcomes. The joints depicted are dipping perpendicularly to the face. The combination of mechanisms described in Section 2.2 and the findings of the authors cited in this section yield results much like those exemplified in the bottom picture of Figure 2.10.

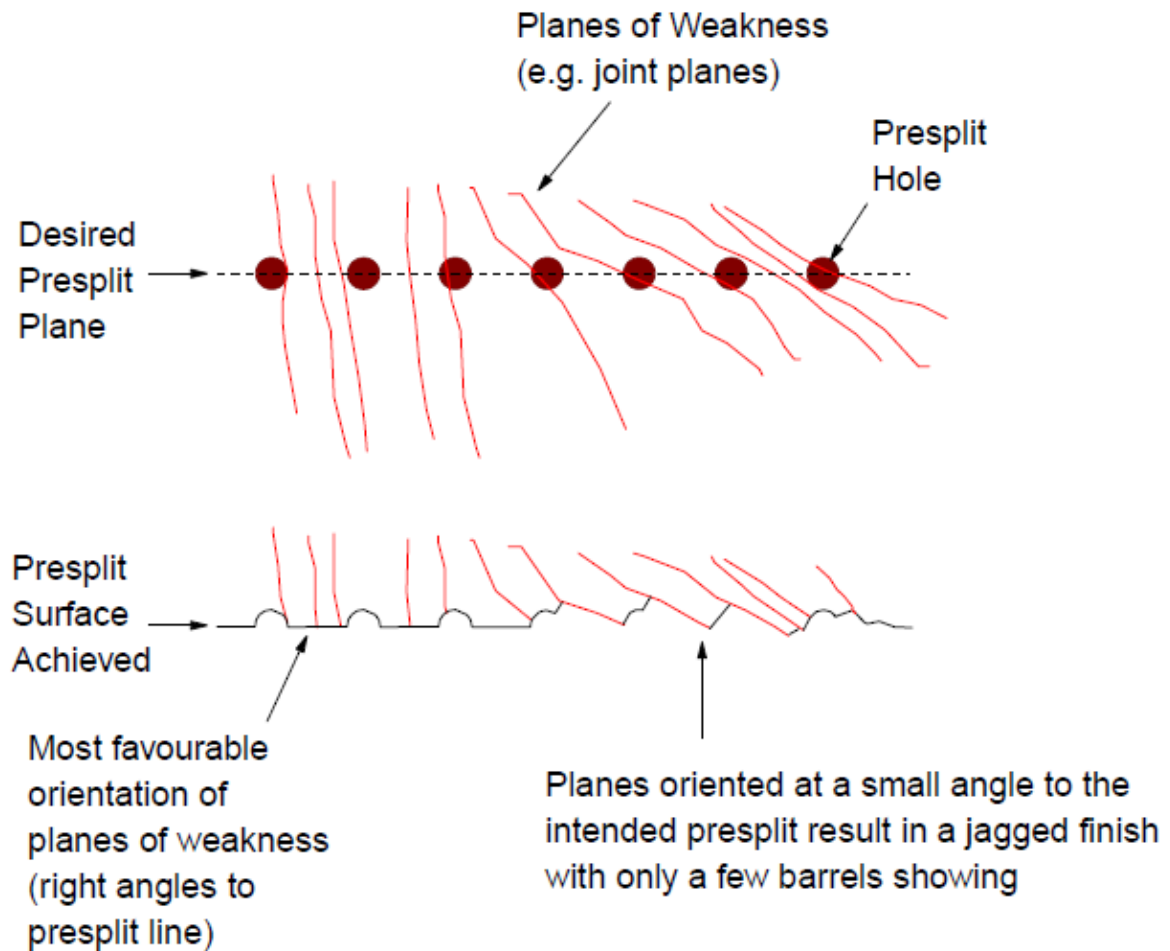


**Figure 2.10: Effect of weakness planes on the final wall outcome (Rorke, 2003)**

The effect of shallow and steep dipping discontinuities that strike in directions that are close to the orientation of the face are shown in Figure 2.11 and Figure 2.12 respectively. The figures demonstrate the way in which discontinuities may have an effect that overshadows other physical and mechanical properties of a rock mass.

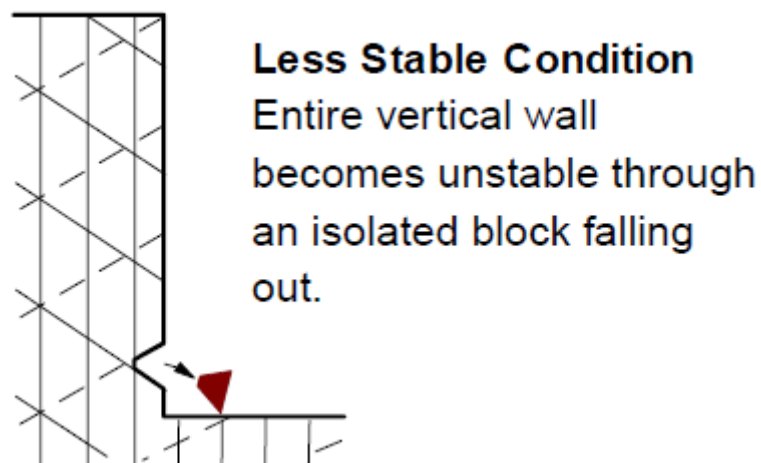
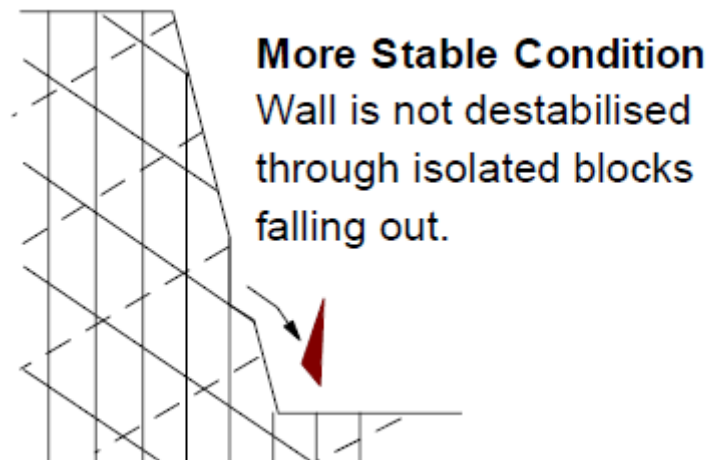
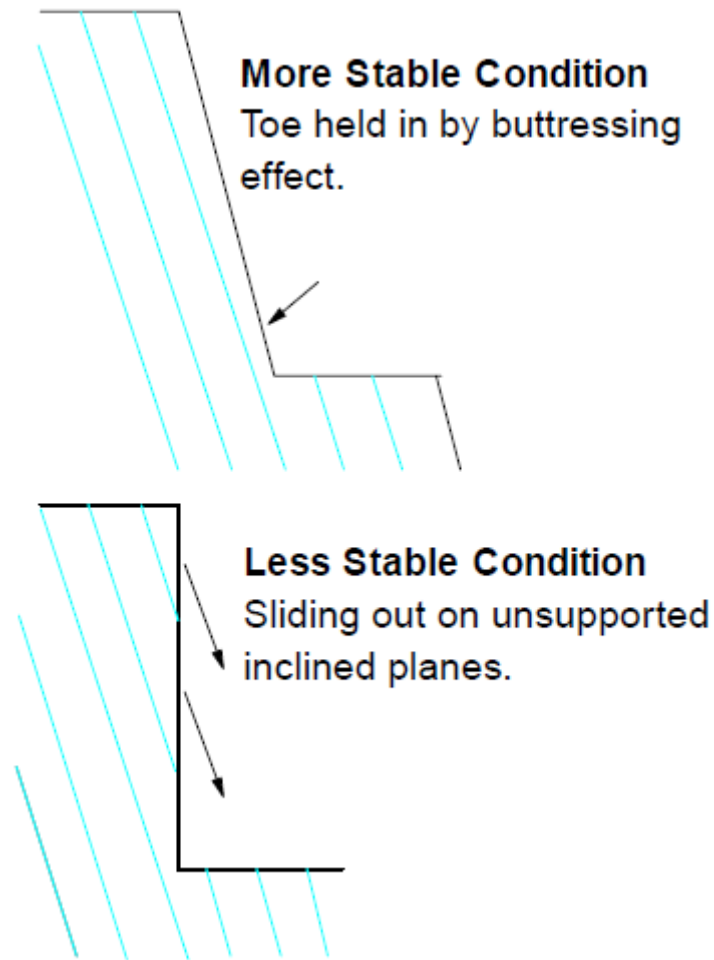


Figure 2.11: Shallow dipping structures striking parallel to the face (Workman and Calder, 1993)



**Figure 2.12: Steep dipping structures striking parallel to the face (Rorke, 2003)**

## **2.7 Blastability Index (BI)**

Lilly's (1986) Blastability Index resulted from his observation that rock breaking inputs were typically aggregates of estimates of operators and or consultants charged with executing rock breaking tasks. In contemporary times, inputs observed in the rock breaking discipline are still aggregates of experiential efforts of participants from various engineering disciplines involved. This is the case in spite of the abundant availability of current information and data collection methods.



### 2.7.1 Components of the Blastability Index

The BI system allows for the collation of geotechnical information that affords the engineer a decent estimate of the in-situ characteristics of a rock mass; and as such, the opportunity to approximate the response of the rock mass in question to explosive energy.

Lilly (1986) found that there are four main parameters that contribute significantly to blasting performance. These are the structural nature of the rock mass, the spacing and orientation of weakness planes, the specific gravity of the material in question and its hardness. The influence of the stated parameters can be summarised as follows:

- **Structural Nature (RMD):** if a rock mass has a blocky composition, that characteristic is likely to supersede the effect of explosive energy and the associated rock breaking mechanisms in the determination of the size of fragments that result from the blasting process. Conversely, in a massive rock mass, the formation of fragments is primarily brought about by the interaction of the explosive energy with the rock.
- **Joint Plane Spacing (JPS):** in the context of Lilly's (1986) work, joint planes refer to all planes of weakness observed in a rock mass : bedding planes, planes of foliation or schistosity, fault planes, and geological and mining-induced joints. This parameter has bearing on the size and shape of the fragments achievable. Rocks with closely spaced joints require relatively low levels of explosive energy to achieve the desired blasting outcome. The joint plane spacing plays a primary role in the effectiveness of wall control blasting.
- **Joint Plane Orientation (JPO):** the dip and dip direction has been found to play a large role in the ease with which rock responds to blasting. The orientations of planes of weakness also affect the profile of the rock that remains on the periphery of the block that was blasted; that is, the highwalls and floor.
- **Specific Gravity (SGI) and Hardness (H):** in general, harder, heavier rock requires more explosive energy to break and move than lighter rock. Such rock also tends to behave in a brittle fashion in response to stress.

The components of the BI have been arranged to give the following equation Lilly (1986):

$$\mathbf{BI = 0.5 (RMD + JPS + JPO + SGI + H)}$$

Where:

**BI** is

Blastability Index

**RMD (Rock mass Description)** is

10 (for Powdery/Friable rock mass),

20 (for Blocky rock mass),

50 (for a Massive rock mass)

**JPS (Joint Plane Spacing)** is

10 (for closely spaced discontinuities),

20 (for intermediate spaced discontinuities)

50 (for widely spaced discontinuities)

**JPO (Joint Plane Orientation)** is

10 (for Horizontal),

20 (for Dip out of the Face),

30 (for Strike Normal to Face),

40 (for Dip into Face)

**SGI (Specific Gravity Influence)** is

$25 \times \text{Specific Gravity of rock (t/m}^3) - 50$

**H- Hardness** is

Hardness Scale (1-10)

The outcome of the computed index is such that a low BI (say 20) is indicative of difficult blasting rock conditions. On the contrary, a rock with a high BI (approaching 100) is easy to blast. Lilly (1986) emphasized that the index is heavily biased towards the nature and orientation of weakness

planes in the rock mass. This is an indication of the importance of those elements in the success of rock breaking as derived from historic experience leading up to the development of the index.

## **2.8 Blasting Quality System (BQS)**

Chatziangelou and Christaras (2015) are in agreement with Lilly (1986) in that the BI calls upon the same parameters as that which form the basis of the Rock Mass Rating (RMR) system by Bieniawski. The authors added that the Geological Strength Index (GSI) classification system is also embodied within the BI. It can therefore be inferred that it can be used as a practical field index for data collection in the process that would eventually feed into the blast design process.

In their study, Chatziangelou and Christaras (2015) used the BI to develop a Blasting Quality System (BQS). Their system used the rock mass classification metrics of the BI to develop a chart (Figure A.1 in Appendix A) reflecting the RMR, GSI and BI of the rock mass concerned. In summary, the BQS allows the engineer to use collected field data from the exposed mining face to quickly evaluate the blastability of the rock mass taking into account the quality of the rock mass in question. The appropriate powder factor is then selected, depending on the BI output realised from the BQS chart.

## **2.9 Geotechnical Model and Geotechnical Database Approaches**

Bye (2006) introduced the application of a three dimensional parametric model for optimisation in open pit mining. His system adopted the form of a block model. Geotechnical rock mass characteristics, BI values, as well as other mining data such as mine planning parameters, were assigned to predefined mining units. This approach concentrated relevant mining data into a primary tool where could be accessed by all stakeholders in the value chain ahead of designing and executing mining functions.

Similarly, Little (2006) described the development of a database of geotechnical information from drilling core logging, face mapping, laboratory tests and field tests. The database was further linked to mine planning and modelling platforms to insure that mining plans, designs for slope stability and blasting would be directed by the latest relevant geotechnical information.

## **2.10 Controlled Blasting Techniques**

Several techniques are practised in the mining industry in order to manage the effect of blast damage on excavation walls. Williams et al (2009) summarised the most common of these as follows:

**Buffer Blasting:** involves the modification of a production blast by reducing the pattern width, modifying the delay sequence for reduced vibration and maximised burden relief as well as the reduction or elimination of the subdrill. This method is typically applied when soft material is encountered with batter angles less than 60 degrees.

The last row of holes in a buffer design are placed at a certain distance (known as the stand-off) away from the intended highwall. The author agrees with the observation by Williams et al (2009) that when blasting in hard structured rock, stand-off distances that allow for the definition of the highwall toe tend to result in damage to the subsequent crest. Larger than optimum stand-off distances, on the other hand, tend to result in frozen material at the toe of the highwall.

**Trim Blasting:** this is considered to be the most commonly used method in wall control blasting. It is applied in moderate to hard rock where batter angles range between 60 to 75 degrees. However, geological features in hard rock tend to dominate the achievability wall control. Trims are drilled, charged and fired into a free-face after a production blast has been loaded out.

Modifications to the bench blast design include the reduction of the bench width, elimination of the subdrill (particularly above and adjacent to a catchment berm), reduction in the burden and spacing, and reduction in the charge mass of the two holes closest to the highwall – achieved using appropriately placed air decks to allow for adequate fragmentation on the top part of the bench and to reduce highwall damage caused by over confinement of energy.

**Pre-Splitting:** a row of closely spaced holes is drilled along the perimeter of an excavation. The holes are primed with decoupled charges and fired simultaneously in order to create a free plane at the perimeter of the new block or highwall. Split holes are not stemmed as the role of the explosive is to provide sufficient borehole pressure to create a tension crack as opposed to inducing compressive damage. This method is best when applied to massive rock masses with tight joints that have an angle that is more than 30 degrees relative to the strike of the free face plane.

**Post-Split:** the technique is executed in the same way as the pre-split, however the line of holes is fired after the production holes have gone. This method is best applied in environments where highly fragmented rock masses are encountered.

**Line Drilling:** this method is characterised by a line of closely drilled holes along the perimeter of the excavation. When placed under stress the webs between the holes collapse into the plane of

strike thereby guiding the formation of a competent highwall. Line Drilling is typically applied in weekly cemented overburden material.

## **2.11 Literature Discussion**

In line with the findings of Dey and Sen (2003) in their review of the concept of blastability across its various versions and applications, it is evident that rock mass properties play a pivotal role in blast performance. On the other hand, the same rock mass characteristics play an equally important role in the control of blast damage, particularly where perimeter walls are concerned. Lilly (1986) is no exception to this observation.

Consideration has been given, in the past, to the relationship between the BI and the powder factor ( $\text{kg/m}^3$ ). This relationship has primarily been established through site specific collection and tabulation of empirical data (Lilly, 1986). In addition to this, some work has gone into relating the BI to rock fragmentation achievable with specified design and rock characteristics through the Cunningham (1983) fragmentation model and its rock factor component.

The geological variation of a rock mass along which final walls are excavated tends to occur in bands or zones with different properties. The importance of this fact is that the response to mining activity including rock breaking will vary across these zones as the rock properties vary. Successful wall control in such respective zones requires due engagement with geological and structural inputs in the rock breaking design processes.

The BQS methodology is a quick and easy tool to establish the blastability of a rock mass. It has been classified for applications in rock masses with joint spacing defined by the JPS bands of the BI. The approach taken was found to be potentially useful to the study at hand. Chatziangelou and Christaras (2013a) cited that the formulation of the BQS was led by the calculation of 90 000 different rock mass combinations as informed by the respective parameters of the BI. This implies that the method is inclusive of a large sample variety of rock mass property occurrences and their associated characteristics; and thus has sound scientific grounds for its application. The downfall of the BQS, as with other blastability indices, is that it focuses on providing its user with an absolute value of powder factor without elaborating on the design and energy distribution aspects.

The work of Bye (2006) and Little (2006) is relevant as both authors outline the significance of the incorporation of available rock mass data into various aspects of the design and optimisation processes in mining. In this research study, it will be attempted to progress towards the application of the available data in the actual design processes of rock breaking wall control.

The number of inputs that go into the achievement of the rock breaking are a testimony to the complexity of rock as a material and blasting as a process. The idea behind the study is to isolate and zone the rock mass properties that have controlling influences on blast damage and to capture them in an indexing tool or in indexed zones similar to that of the BQS. In each blast where a final highwall is concerned, the tool would be used to highlight zones with poor blastability, thus prompting querying of the wall control design and its appropriate adaptation in each zone in order to achieve the desired output.

In the context of the Phoenix operation, it is envisaged that the tool will afford the operation more informed application of wall control rock breaking designs using explosives. The primary measure of success will be the achievement of the pit designs' catchment berm width without catchment capacity being reduced by blast damage, frozen toes or crest damage.

## **CHAPTER 3: RESEARCH METHODOLOGY**

This chapter discusses the methodology adopted in conducting the study. The elements involved in this methodology are summarised under the following subheadings.

### **3.1 Introduction**

The study was conceived in response to the problem of crest loss coupled with frozen toes along the western highwall of the Phoenix pit. A potential solution to the problem thus had to look into the fundamental characteristics of the rock mass concerned and relate them to the effects of the rock breaking approach observed.

### **3.2 Literature Review**

At the onset of the study, a literature review was conducted gain insight into the various processes that take effect during a rock breaking exercise using explosives. The review then sought to establish the relationship between the various elements at play during rock breaking and the characteristics of the rock mass. Bias was taken towards seeking out the integration of rock mass classification inputs into final wall rock breaking with explosives in the bench blasting sense, and in the more specialised perimeter blasting techniques used in the industry.

### **3.3 Data Collection**

Data from the site was collected during the years 2014 and 2015. The bulk of the data utilised was historic data sourced from the Geotechnical department of the mine. Further data was collected through a series of audits, with the relevant parts drawn upon for furtherance of the study. The data comprised of borehole logs, lab test results, field measurements and observations, photographic data, as well as computer aided sections and plans.

### **3.4 Results and Analysis of Results**

The data collected was analysed through a series of calculations based on rock mass classification methodology. The first step of this process was the analysis of the potential influence of the joint planes traversing the western highwall of the pit, and identification of joint sets with orientations that have the greatest potential to exacerbate the problem of crest loss and wall damage. Having confirmed the potential effect of these joint sets, the following step was to separate the geotechnical data into various zones as informed by the rock mass classification elements of the RMR, Lilly's (1986) BI and joint plane spacing. The calculated outputs were then grouped according to the four main rock types forming the rock mass of the western highwall of the pit.

The perimeter blast designs (production and final wall) presently applied across the western highwall were analysed and assessed for their adequacy relative to the response observed in the rock. Practices and oversights with the potential to contribute to the wall damage and crest loss problem of the mine were highlighted.

The underlining premise was that ideal designs biased towards the end of wall control (in particular achievement of the pit design berm width presently precluded by crest loss) need to be inclusive of all the aspects that can adversely contribute to the problem experienced. As such correlations were established between the rock mass classification elements composing the RMR, BI and the joint spacing. These relationships were expressed in the form of rock type specific Design Input Tool (DIT). Intrinsically informed by rock mass classification inputs from the rock mass in question, the DIT was aligned with the Geological Strength Index (GSI). The ease of collection of data from a mining face allows the GSI to serve as an effective key input parameter to the various outputs that can be determined from the DIT.

A design was executed by applying the DIT procedure from the input DIT data to the resultant output design parameters for a perimeter trim blast and pre-split design. Summary analysis and comments on the designs were then given.

### **3.5 Conclusion**

A discussion on the findings leading up to the establishment of the DIT then followed with emphasis of how it will assist in mitigating the problem of crest loss that the mine has been experiencing. It was concluded that data that is collected periodically at the mine can be used to establish meaningful relationships between rock mass characteristics and effects of designs using rock mass classification as a medium. By so doing, designs developed for perimeter rock breaking would inherently account for elements of rock mass competence, jointing and its associated spacing and orientation, explosive energy. It would also account for considerations to which the developments of this study can be extended, such as fragmentation, slope stability and support.



## **CHAPTER 4: RESULTS AND ANALYSIS OF RESULTS**

The results and analysis of the results are presented in this section. Elements discussed include field audit findings from the existing operation, rock mass data, a multivariable BI for the site, the design input tool and the implications of its application thereof.

### **4.1 Description and Audit of drilling and blasting at Phoenix Mine**

In order to gain insight into possible factors contributing to the development of the problem observed, audits were conducted on the drilling and blasting operations. The audits spanned the process from blast planning to the implementation phases; however the sections summarised hereunder are those that deal with the subject of wall control. The design parameters employed in the blasting carried out at Phoenix will be reviewed. Aspects discussed include bench blasting, due to its influence on the outcome of the perimeter wall, and post-splitting. All bench blasting was done using Bulk Mining Explosives' (BME) HEF 206 bulk blend and pre-splitting is carried out using 50mm x 580mm Megamite cartridges (also from BME).

#### **4.1.1 Blast Planning**

Blast planning at Tati is conducted using BME's BlastMap 2 software. Once completed, the design is transcribed onto the relevant block polygon and submitted to the survey department for hole staking.

It was noted that inadequate attention is paid to the orientation and alignment of blast patterns relative to the shape and constraints of the respective blocks being blasted. This is manifested in two ways. In the first instance the patterns are not correctly aligned so as to allow the optimization of design parameters such as burden and in-fill holes where necessary (illustrated in Figure 4.1).

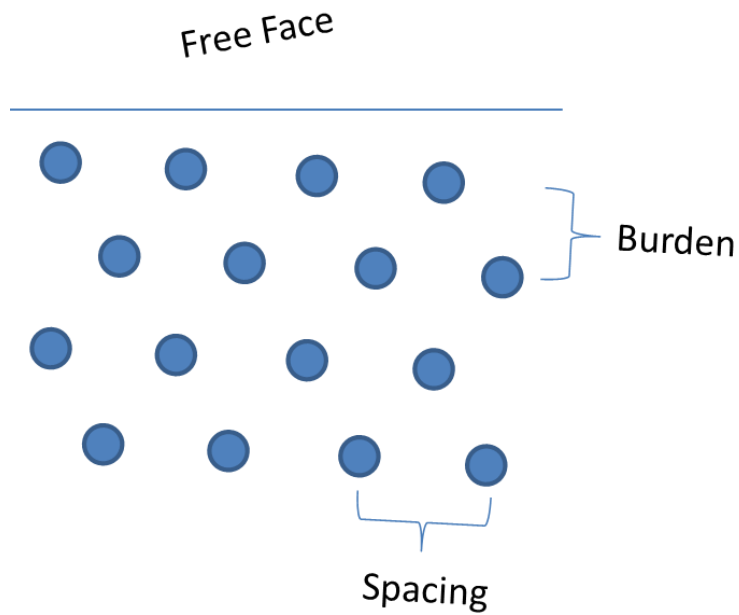


**Figure 4.1: Schematic of misaligned pattern**

The second instance comes about due to an incorrect firing direction relative to the designed pattern layout (Figure 4.2). The outcome of the oversight described above is the reversal of burden and spacing, which results in overburdening of holes, and amongst other effects, highwall damage caused by holes firing along the intended final perimeter.

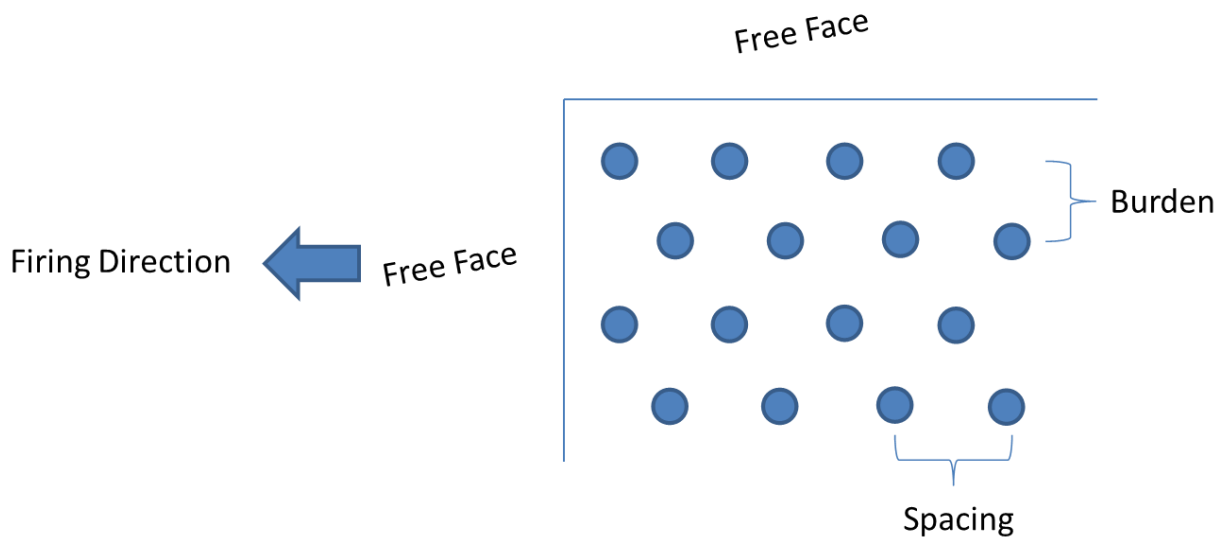


**Figure 4.2: Reversal of burden and spacing; spacing is larger than designed burden**

#### 4.1.2 Bench Blasting

The blast design parameters employed in the blasting of the blocks that are not adjacent to the final wall are as shown in Table 4.1. Figure 4.3 is a section of the typical layout of a blast design as detailed in the Table 4.1. The dotted ellipses model the estimated range of damage that each column of explosives will bring about in the surrounding rock during detonation (Holmberg and Persson, 2000).

**Table 4.1: Phoenix Mine bench blasting parameters**

Design Parameters	
Hole Diameter (mm)	171
Burden (m)	4.5
Spacing (m)	4.8
Burden : Spacing	1.07
Bench Height (m)	10
Hole Depth (m)	11
Sub-drill (m)	1
Stemming Length (m)	3
Column Length (m)	8
Pattern	Staggered
Design Technical Powder Factor (kg/m <sup>3</sup> )	0.94
Energy Factor (kg/m <sup>3</sup> )	0.9
Average Explosive Density (g/cc)	1.27

As shown in Figure 4.3, boundary holes for non-trim benches are typically placed along the intended limits of a block. The outcome of such an approach is extensive backbreak in the new highwall. As suggested by the damage contour of the nearest hole to the highwall, such damage can extend for a distance in excess of 3m, resulting in an unsafe highwall and unplanned rock volume increases through overbreak.

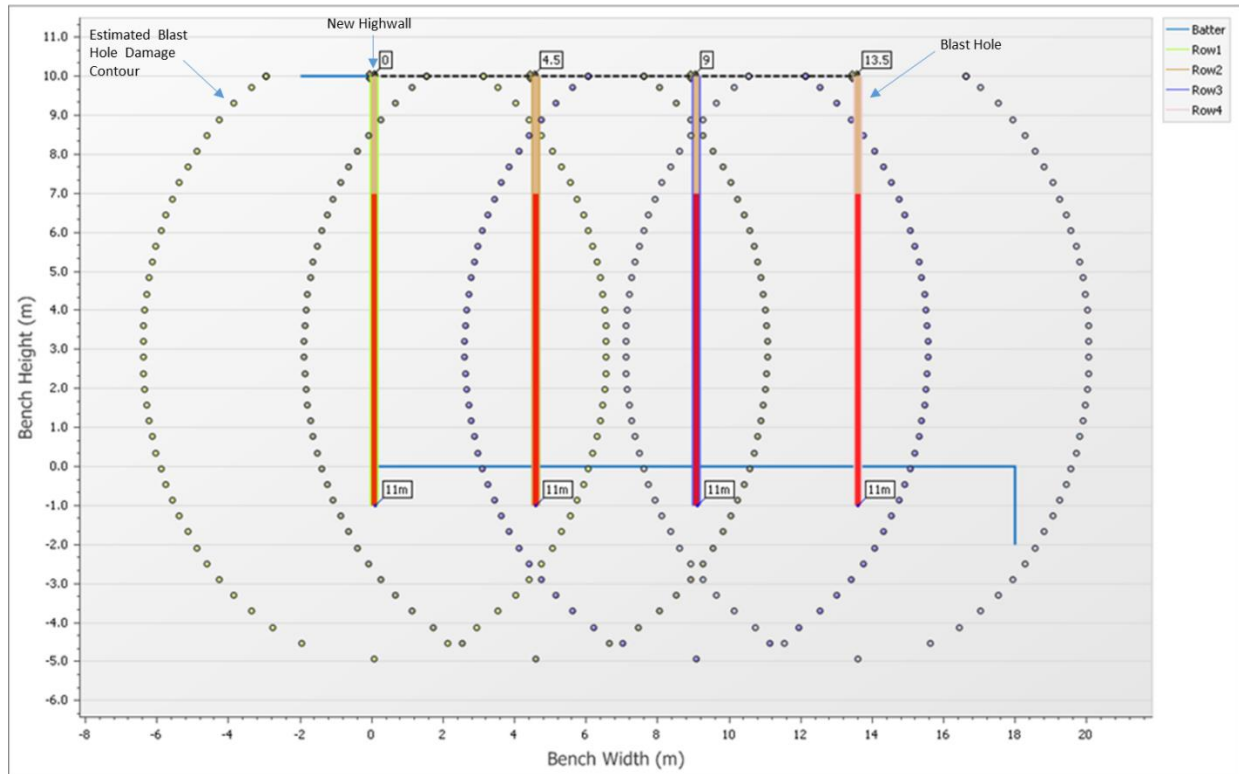


**Figure 4.3: Transverse section through a typical bench**

When blasting is carried out on benches adjacent to the final western highwall, two lines of buffer rows are added to the bench blast design; their drilling was inconsistent. The parameters of the production holes remain the same as those discussed above. The parameters for the buffer holes included for purposes of controlling wall damage are tabulated in Table 4.2. Inspection of Figure 4.4 highlights the fact that the area of influence of the energy of the holes extends considerably beyond the limits of the intended block.

**Table 4.2: Buffer row parameters**

<b>Buffer Row Parameters</b>	
Hole Diameter (mm)	171
Hole Depth (m)	11
Buffer 1 Burden (m)	2.5
Buffer 2 Burden (m)	4
Buffer 1 Spacing (m)	2.5
Buffer 2 Spacing (m)	4
Hole Angle	90°
Stand-off from Pre-split (m)	1.5
Stemming	Not stemmed
Subdrill (m)	1
Buffer 1 Column Length (m)	3.2
Buffer 2 Column Length (m)	4.8
Buffer 1 Technical Powder Factor (kg/m <sup>3</sup> )	1.03
Buffer 2 Technical Powder Factor (kg/m <sup>3</sup> )	0.69

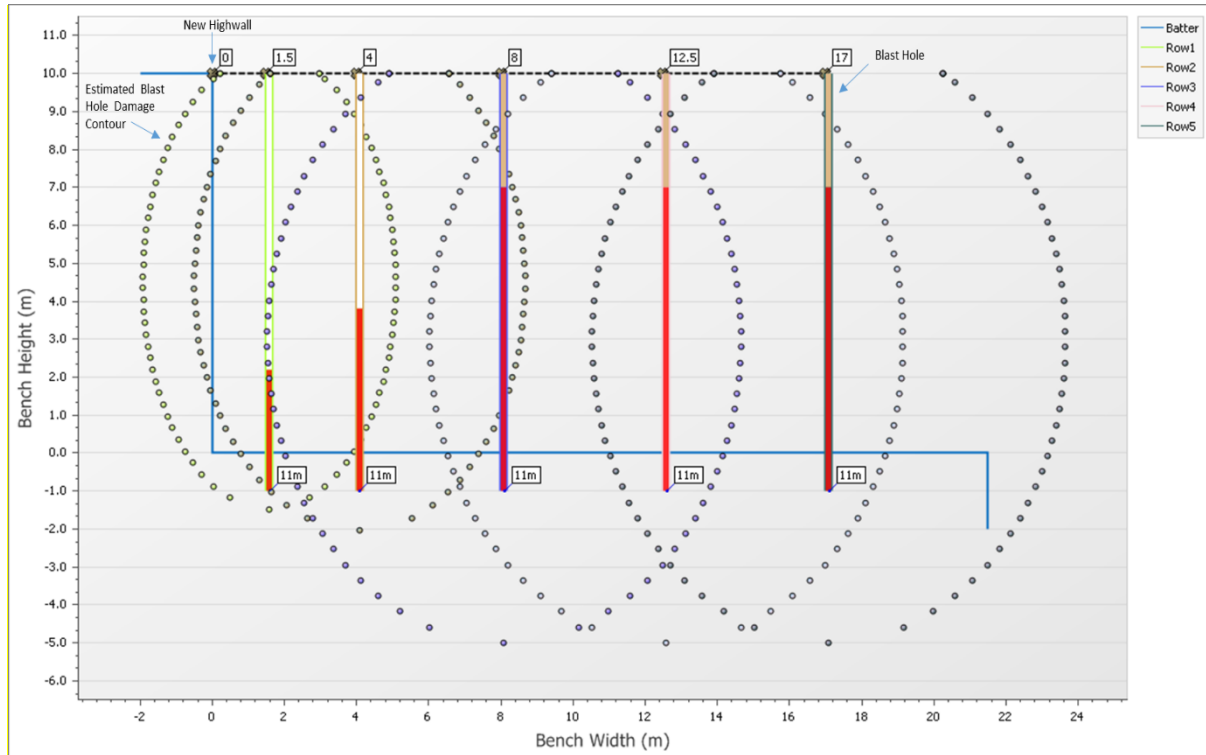


**Figure 4.4: Transverse section through bench adjacent to the final wall**

### 4.1.3 Perimeter Blasting

Post-splitting is done according to the design specifications in Table 4.3. Figure 4.5 is a graph showing the expected performance of the current design in terms of the adequacy of the charge used in relation to the rock strength –modelled using WallPro (BME, 2016) – a perimeter blast design software. The rock type considered is the Meta-Gabbro. The green vertical dotted line in Figure 4.5 marks the distance to which an adjacent hole should induce a splitting effect. The blue line estimates the decreasing borehole pressure (as distance from the centre of the hole increases) with a peak value at the centre of the pre-split hole. The red horizontal line denotes the tensile strength of the rock.

**Table 4.3: Post-split design parameters**

Design Parameters	
Hole Diameter (mm)	127
Hole Depth (m)	10
Splitting Factor ( $\text{kg/m}^2$ )	0.77
Hole Spacing (m)	1.2
Hole Angle	$90^\circ$
Borehole Pressure (MPa)	105.2

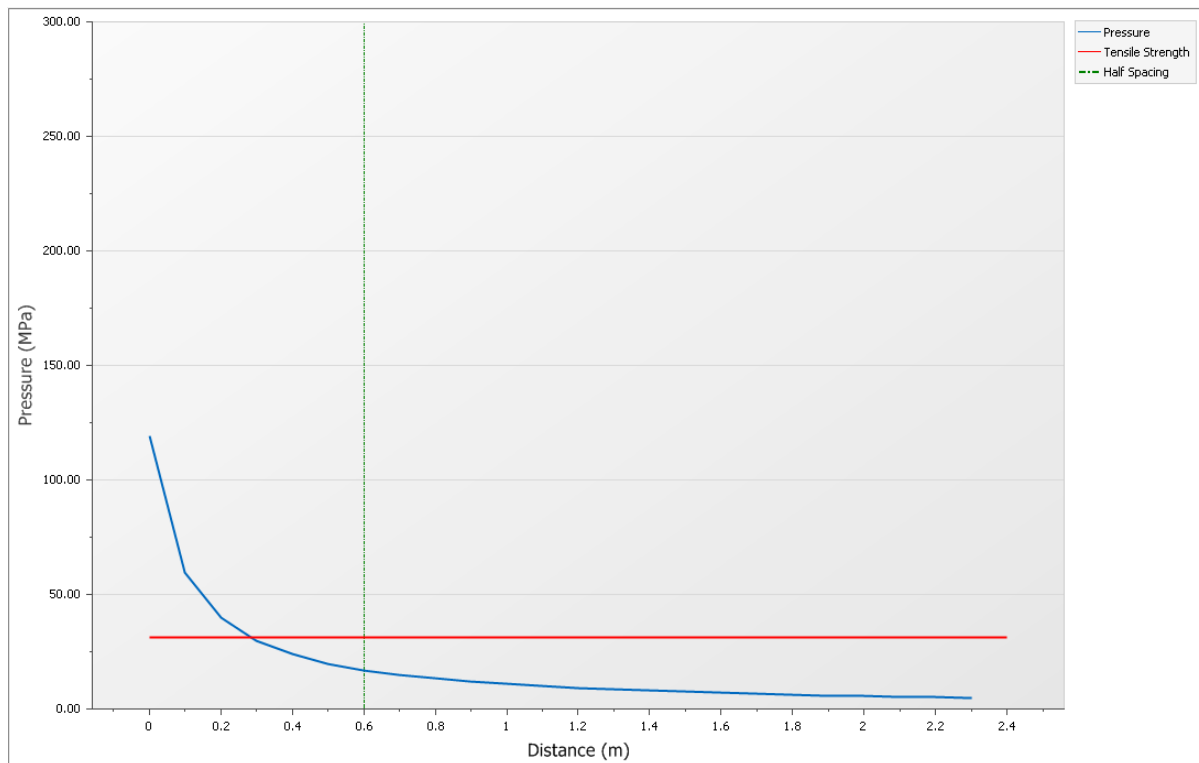


**Figure 4.5: Post-split design (Meta-Gabbro)**

Post-split holes are primed with 50mm x 580mm Megamite cartridges and detonating cord. A total of 7 cartridges (coupled into three pairs of two and a single cartridge towards the hole collar) are suspended a one metre from the hole collar.

In order for a splitting exercise to be successful, the borehole pressure at the medial point between adjacent holes should be equal to or greater than the tensile strength of the rock concerned.

Furthermore, energy that exceeds the compressive strength of the rock will cause counter-productive crushing damage to the wall; particularly at the hole collar where confinement is reduced.

Where insufficient information is available, blast designs should be tailored for the hardest rock encountered, particularly where shots traverse different rock types. Furthermore it is worth noting that split performance can be deteriorated by the presence of water in the pre-split holes.

In spite of the technical rock mass considerations that affect the performance of wall control, a few practical application inconsistencies were noted which have a significant effect on the effectiveness of wall control, regardless of design adequacy. It is suspected that the pairing up of cartridges, instead of having a linear evenly distributed charge, results in the last cartridge being positioned high up in the hole. The reduced borehole pressure at the bottom of the holes could contribute to the hanging up of rock against the highwall that is often observed towards the toe of perimeter highwalls (Figure 4.6). The presence of water in the holes below the suspended charge would contribute to this, as the water tends to reflect away the detonation energy at its surface. An additional cause of such hang-ups is holes that are drilled too short.





**Figure 4.6: Rock hung-up against highwall**

#### **4.1.4 Timing Design**

The timing design consisted of 350ms downhole delays, 25ms in inter-row delays and 42ms intra-row delays. Burden movement was thus orientated perpendicular to the free face. Figure 4.7 is a schematic of the timing design mentioned, and the resultant timing contours are shown in Figure 4.8. This design increases the potential for highwall damage. The near perpendicular orientation of the timing contours in Figure 4.8 relative to the highwall implies that the back row of holes will have a tight breaking or relief angle ( $90^\circ$  or less) resulting in highwall damage aggravation.

**Table 4.4: Initiation accessories**

Initiation System Component	Specification
Booster	400g Viper
Detonator Type	Prima Det Trunkline
Down-hole Delay	350ms
Surface Delay	25ms (Inter-row)
	42ms (Intra-row)
Capped Fuse	6min delay

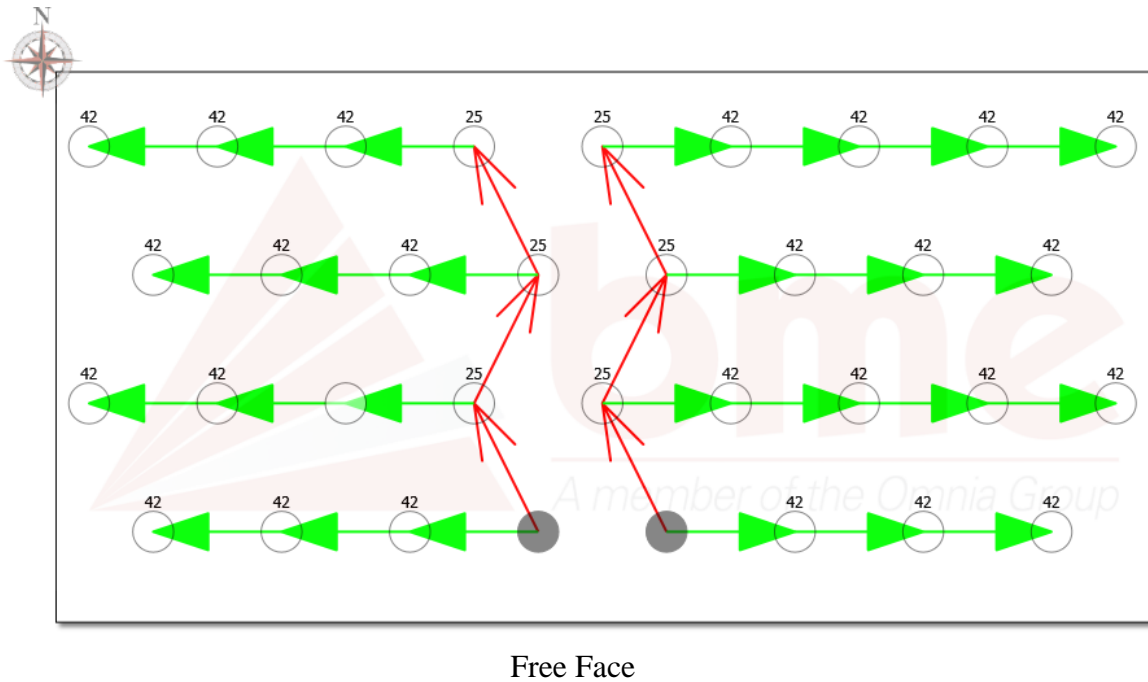


**Figure 4.7: Typical timing design schematic**

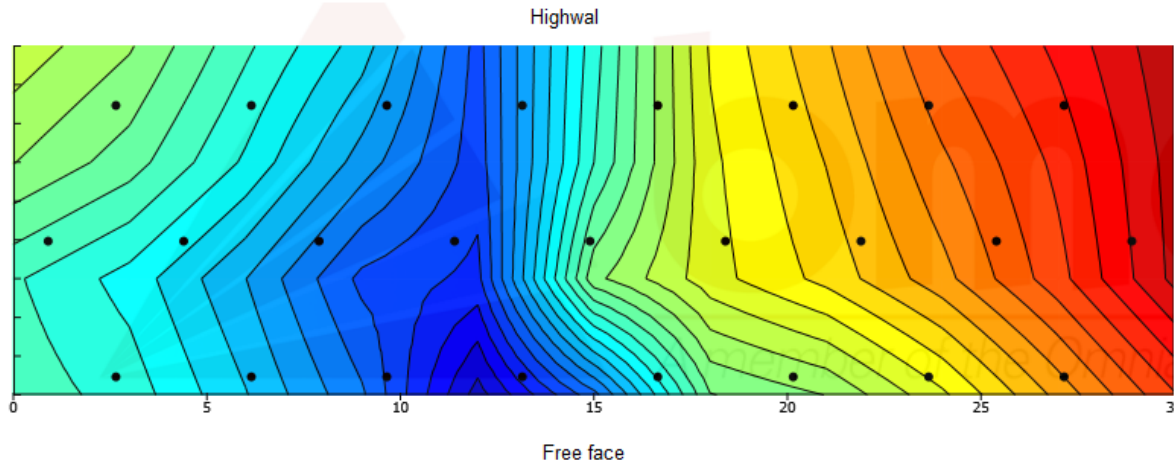


**Figure 4.8: Timing contours for previous design**

The timing design was changed on the waste blasts to 25ms intra-row and 42ms inter row. In addition to this, incremental delays of 67ms, 84ms were introduced on the back rows in final wall blasting in order to reduce the potential for high wall damage. The result of this was a notable reduction in back break where the timing change was implemented. The timing contours in Figure 4.9 reveal that the relief angle along the highwall allows sufficient breaking room thereby directing shock energy away from the wall rock. The diggability of the resulting muck also improved considerably as a result of improved burden relief and rock displacement.

It must be noted that typical inter-row timing lies in the range of 3 to 6ms/m of burden while intra row timing values range between 10ms/m and 30ms/m of burden (Prout, 2014). This implies that the 25ms and 42ms intra-row and inter-row timings employed on the mine are out of specification (by empirical standards). The change made was limited to the delays available at the mine. The empirical figures serve as a means of estimation in the absence of data. It should, therefore, be noted that the minimum rock response time ( $T_{min}$ ), for that particular rock mass, would have to be determined in order to establish the most suitable timing.

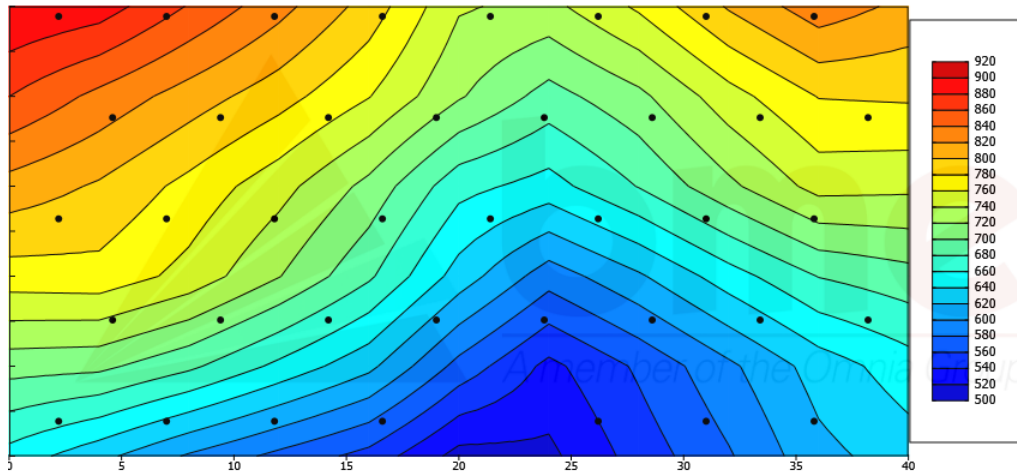


**Figure 4.9: Timing contours for change implemented**

## **4.2 Rock Mass Data**

Various types of rock mass data collected were sourced and used to gain a clearer understanding of the geological factors at play on the blast outcomes and high wall state observed. These include stereographic plots of joint set data, wall orientation data, mechanical data from lab tested core samples as well as rock mass classification data.

### **4.2.1 Stereographic Data**

A structural mapping exercise was previously conducted on the rock mass forming the pit and the outcome of the exercise is shown in Figure 4.10 (a stereonet plot of 241 pole data points collected from the Phoenix pit). Although the data presented in the stereonet was collected at a mining level preceding that of the current study, it remains relevant due to the fact that the formation of geological discontinuities occurs at depth within a rock mass; furthermore, the formation of the rock mass predates the formation of the discontinuities. The data was collected in three separate batches in different parts of the pit as shown by the distinctive data markers.

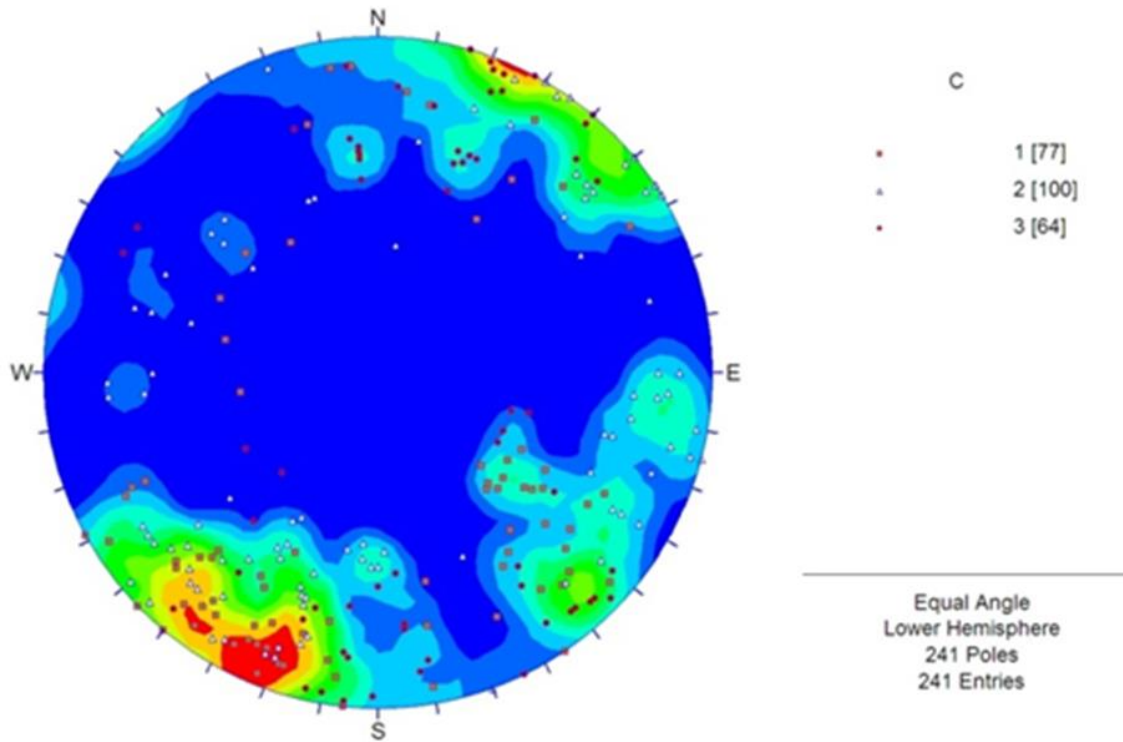


**Figure 4.10: Weighted joint data stereonet (Bosman, 2008)**

A further step was taken by plotting the planes of the weighted data biased towards low spread pole data points (ie. focusing on data points that reflected clusters of poles). The resultant number of data points considered was refined to 82 poles. These were subsequently aggregated into clusters from which the joint set planes were plotted. The planes representing the aggregate orientation of the joint sets were plotted together with the orientation of the western highwall (WHW) as shown in Figure 4.11 – plotted using Stereonet 9 (2016) software. The plane data is colour coded and presented in Table 4.5. The ranking denotes the author’s opinion on the hierarchy of influence of the various joints with 5 representing greatest influence.

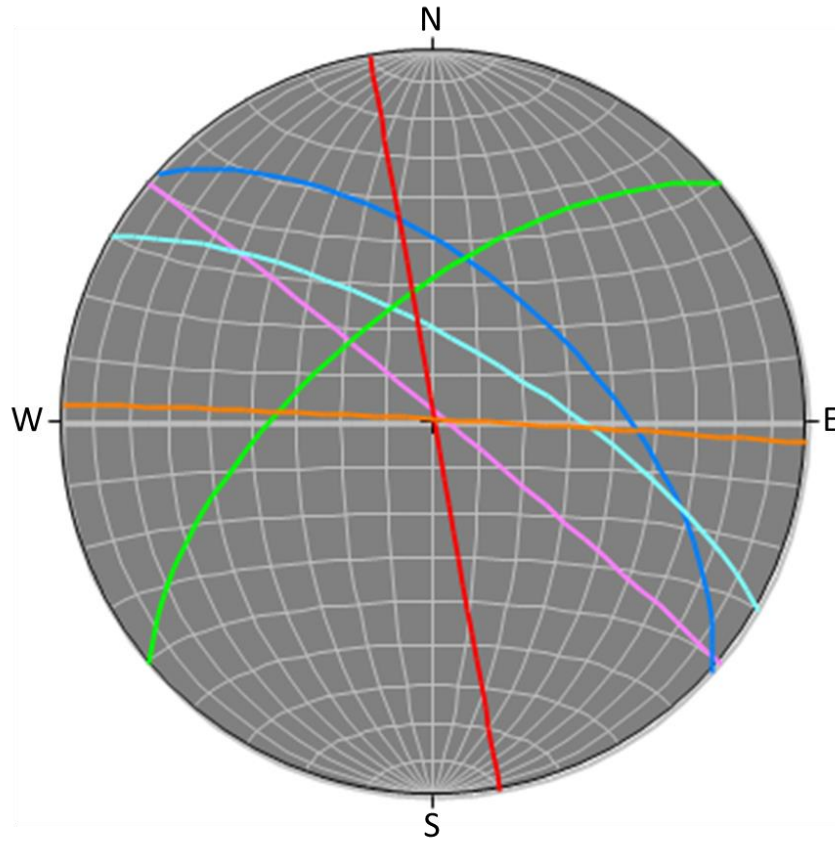


**Figure 4.11: Stereonet of joint set plane orientations and the western highwall**

**Table 4.5: Stereonet data**

Colour	Plane Orientation	Strike/Dip	Angle to WHW	Impact Ranking
	WHW	350/90	-	-
	J1	273/89	77	1
	J2	230/64	60	2
	J3	300/72	50	3
	J4	312/57	38	5
	J5	310/88	40	4



The purpose of the stereonet exercise was to establish the relative orientations of the joint sets to the western highwall. This would highlight the potential contribution of the various joint sets to the problem at hand.

It was established that three joint sets (J3, J4 and J5) out of the five have an orientation that is within 60 degrees of the orientation of the highwall. According to the findings of Worsey et al (1981) and the NHI (1991), such joint sets have the greatest potential to adversely affect the achievability of the planned final wall blasts and the stability of the resultant wall. Figure 4.12 was plotted using the Visiblegeology (Cockett, 2016), online application. It is 3-D representation of the planes representing the three joint sets that have an orientation that is within 60 degrees of the western highwall. The red plane represents the western highwall while the turquoise, blue and purple planes represent joint sets J3, J4 and J5 respectively.

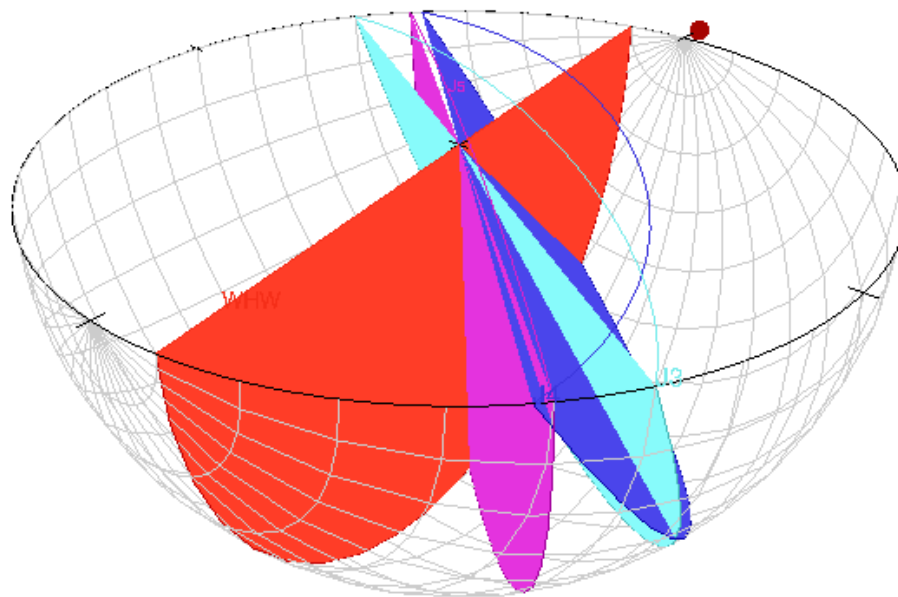


**Figure 4.12: 3-D projection of J3 to J5 and the western highwall**

In a study by Lewandowski et al (1996), it was concluded that the negative impact of jointing orientation on the achievement of the final wall design is manifested by attenuation of the perimeter blasting stress wave at the joint plane. Their findings highlighted the fact that the perimeter blast stress waves were most attenuated when the angle between the joint plane and face

under consideration was in the range of 15 to 45 degrees; with maximum attenuation observed at 45 degrees. With this in mind, a closer look at Table 4.5 reveals that J4 and J5 are five and seven degrees respectively from this angle of maximum stress wave attenuation. This makes them dominant contributors to the wall control difficulties experienced at Phoenix and confirms the presence of underlying root causes to the problem at hand.

It is suspected that joint set J4 contributes the most to the observed failure of bench crests. This is due to the fact that it not only has the closest to parallel orientation relative to the highwall, but it also has an angle and direction of dip (dipping diagonally into the pit) that make it easier for sections of wall crest to fail when excited by various mechanisms during primary and perimeter blasts (see Figure 2.12). Set J3 could also bring about a similar effect although to lesser extent as it is more steeply dipping.

#### **4.2.2 Mechanical Properties**

The mechanical properties of the four rock types found at Phoenix are presented in Table 4.6 Core samples were tested for each of the rock types.



**Table 4.6: Phoenix mine core sample data (TNMC, 2012)**

Parameter	Statistical Criteria	Rock Type			
		Dolerite	Meta - Gabbro	Pegmatite/ Aplite	Tonalite
UCS (MPa)	No of Samples	3	3	3	3
	Minimum	113,2	274,8	114,9	200,6
	Maximum	162	351,1	234,8	249,4
	Average	137,6	312,95	174,85	225
	Std Dev	24,4	38,15	59,95	24,4
Density (kg/cu m)	No of Samples	3	3	3	3
	Minimum	2930	2770	2620	2740
	Maximum	2940	2800	2630	2750
	Average	2935	2785	2625	2745
	Std Dev	5	15	5	5
E (tangential @ 50% max strength) (GPa)	No of Samples	3	3	3	3
	Minimum	58,5	75,4	61,5	69
	Maximum	74,4	77,6	64,7	71,4
	Average	66,45	76,5	63,1	70,2
	Std Dev	7,95	1,1	1,6	1,2
Poisson's ratio	No of Samples	3	3	3	3
	Minimum	0,216	0,231	0,13	0,202
	Maximum	0,25	0,256	0,206	0,258
	Average	0,233	0,2435	0,168	0,23
	Std Dev	0,017	0,0125	0,038	0,028
Base friction angle (°)	No of Samples	2	2	2	2
	Minimum	34,8	30,8	32,7	31,7
	Maximum	35,6	31,7	34	32
	Average	35,2	31,25	33,35	31,85
	Std Dev	0,4	0,45	0,65	0,15

Meta-Gabbro, which is the most common of the rock types present at Phoenix, has a UCS (Uniaxial Compressive Strength) that significantly surpasses those of the other rock types present; with a maximum strength of 351 MPa compared to the second hardest rock, Tonalite, with a maximum UCS of 251 MPa. The Dolerite and Pegmatite have maximum UCS values of 162MPa and 235MPa respectively. The broad difference in UCS values means that the rock response to blanket blast design inputs, of both primary and perimeter nature, will vary significantly. The challenge

that then arises is that calibrating the blast towards the hardest rock (as discussed in Section 4.1.3 ) raises the potential to cause damage to perimeter sections where lower compressive strength rocks are encountered. It is considered that the tensile strengths of the rock types in question are in the order of one tenth of their UCS.

The Poisson's ratio of a rock is the relationship between lateral and longitudinal deformation of a rock sample under stress. In the rock breaking context, it indicates the disposition of rock to crack propagation during pre-splitting. This is of particular interest to this study as the rock types in Table 4.6 were found to have significantly low Poisson's ratio values ranging between 0.13 and 0.258. The significance is that rocks with low Poisson's ratios are more responsive to wall control blasting to efforts such as pre-splitting (Williams et al, 2009).

The Young's moduli tabulated indicate that the rocks at Phoenix have a comparatively high ability to withstand elastic deformation due to applied stress. This speaks directly to the inversely proportional relationship between Young's modulus and the heave energy required from the explosive used (Roy, 2005). Stiffer rock tends to result in a higher equalisation energy from the early stages of the detonation process, thus leaving a sufficient energy complement to facilitate the heaving process. With this said, an explosive with higher brisance and therefore a higher equalisation energy (such as an emulsion) would be more ideal than 60:40, the blend utilised at Phoenix. Furthermore, such an explosive would be of particular benefit to the conservation of the final wall as less high-pressure, crack penetrating gas energy is produced during the detonation process. Exploitation and mobilization of weakness zones by gas pressure would thus be reduced significantly.

### **4.3 Field data**

Data was classified into sets from the four primary rock types found at Phoenix, and tabulated as shown in APPENDIX B – FIELD DATA. With the input of the geological model, it became apparent that the main rock mass into which the western highwall is excavated comprises of Meta-Gabbro with occurrences, to a lesser degree, of Dolerite, Pegmatite and Tonalite. The Dolerite occurs as bands of intrusions into the Meta-Gabbro, while the other two rock types are sparsely featured. The distribution of the data considered in this study is thus dominated by Meta-Gabbro data points as shown in Figure 4.13.

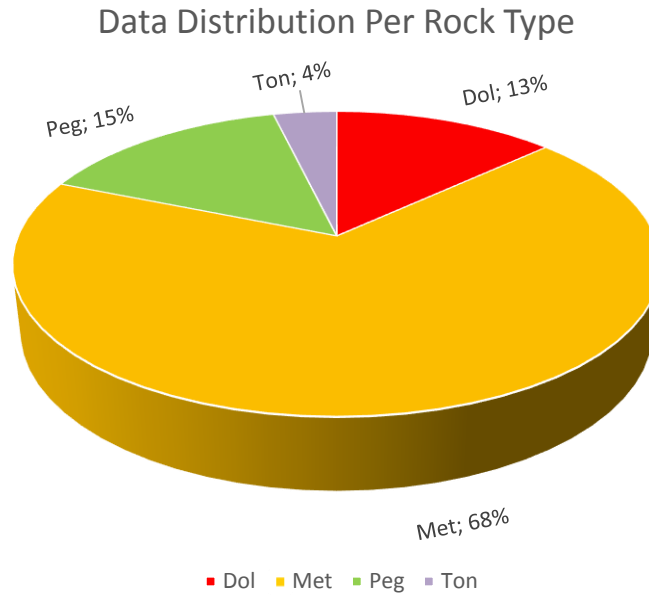


**Figure 4.13: Data distribution per rock type**

#### **4.3.1 Method of Data Collection**

Each of the data sets in the afore mentioned tables comprises of measurements taken from runs of core extracted from bore holes drilled into the rock mass, and at varying depths ranging from: 50 to 519m for Dolerite, 4 to 379m for Meta-Gabbro, 60 to 279m for Pegmatite and 131 to 260m for Tonalite. The number of joints encountered within those lengths of core, as well as their orientation relative to the core axis were recorded. The mean number joints per metre ( $J/m$  where  $J/m \approx J_v$ ) were then calculated, as well as the estimated in-situ block sizes ( $X_i$  in  $m^3$ ). The joint spacing was estimated as a function of the in-situ block sizes calculated.

#### **4.3.2 Joint Spacing**

The distribution of joint spacing in the collective sample is shown in Figure 4.14. This graph indicates that most joints encountered have a spacing between 1 and 100mm; and joints with spacing between 300mm and 400mm are also expected to be encountered frequently in the Phoenix rock mass. The observations made concerning joint spacing, according to the sample data, requires attention to be paid to inputs to wall control blast designs, as most of the joint spacing data falls below the design post-split spacing applied to the western highwall. It is probable that this is one of the core causes promoting the failure to achieve the desired wall control results.

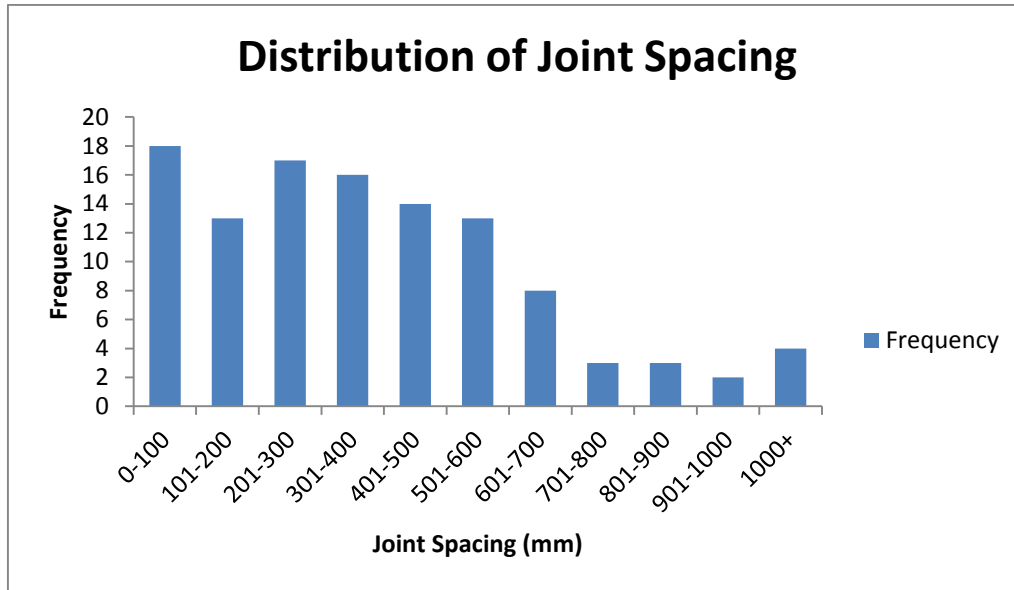


**Figure 4.14: Joint spacing data distribution**

### 4.3.3 Rock Mass Rating

Using joint spacing values tabulated in APPENDIX B – FIELD DATA and the graph in Figure 4.15 (Bieniawski, 1979), the RQD % (Rock Quality Designation) values were determined using the joint spacing for each data point. This method was found to be more sensitive to small (millimetre order) variances in joint spacing compared to the application of the following equation (Stacey, 2015) on the data:

$$RQD = 115 - 3.3 J_v$$

This approach was selected as the preferred method for the estimation of RQD for this study in order to narrow the precision of the estimates for each data set. The values of RQD % achieved using the described method are presented in Appendix C – RQD Data. The respective average RQD % values were calculated as 84% for Dolerite, 92% for Meta-Gabbro, 87% for Pegmatite and 98% for Tonalite. Based on the data considered, the rock mass quality is classified as “Good” in accordance with Deere et al (1967).

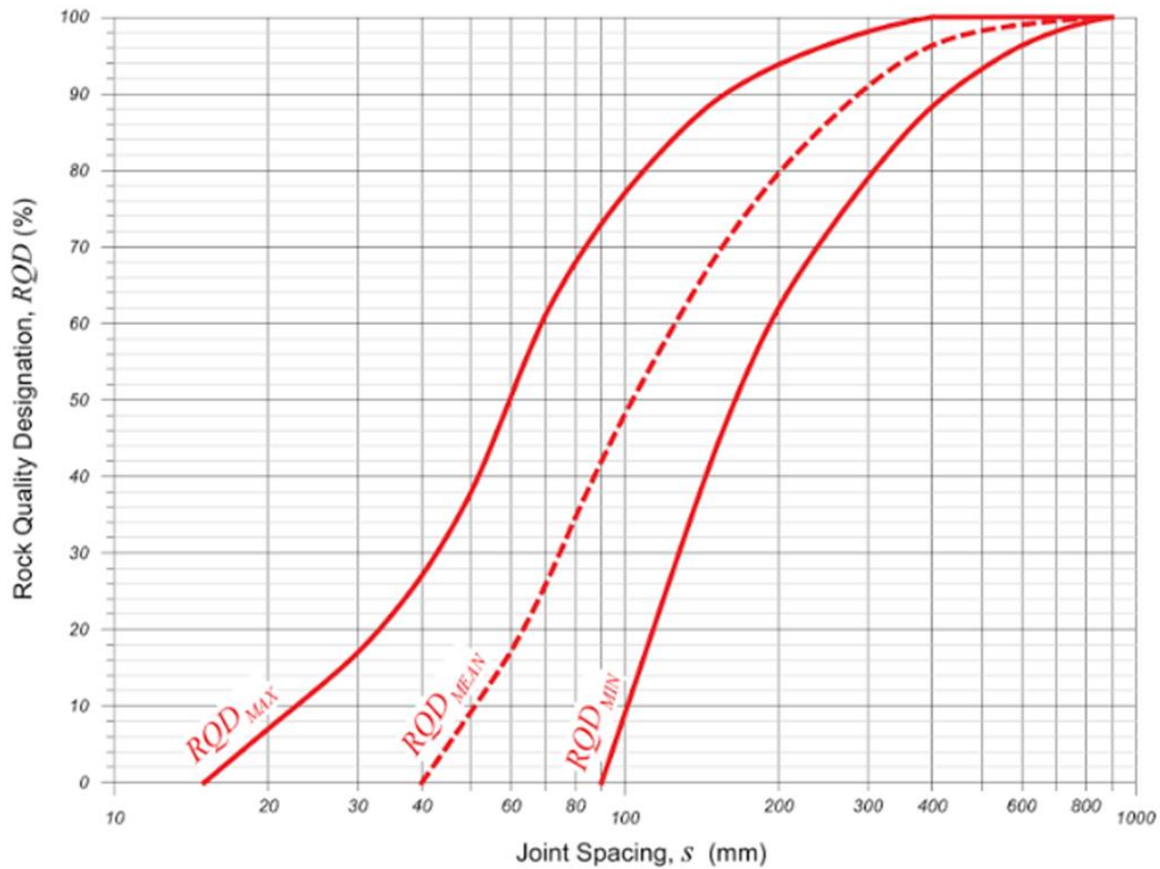


**Figure 4.15: RQD % as a function of joint spacing (Bieniawski, 1979)**

Ratings of the RMR as derived from Table 2.2 are presented in Appendix E – RMR Calculation Data. The UCS ratings (A1) used in the calculation of the RMR were based on the lab test data of Table 4.6. Average UCS values were utilised to derive the ratings in each case as lab test readings are typically biased due to the practice in which the best core samples are selected and sent to the labs for testing (Karzulovic and Read, 2009). The average values are more representative of the overall rock mass strength.

RQD ratings (A2) were derived using RQD % values established through the graphical method above. Various ratings for spacing of discontinuities (A3) were selected and based on the corresponding joint spacing data. A standard rating (A4) for the condition of discontinuities (25) was selected based on the overall impression across the rock mass and the fact that the main rock in the Phoenix was established to be a metamorphosed Gabbro with tight set discontinuities.

Through the site observations made during the study, it was concluded that the groundwater, particularly in the wall in question, was not present. As such, a dry condition classification was taken with a rating (A5) of 15 applied.

It was the opinion of the author that a rating (B) of -25 was appropriate for the adjustment relating to the orientation of discontinuities. This conclusion was based on the observation that the loss of crests of berms planned for the western highwall appeared to be influenced considerably by the orientation of discontinuities; particularly those that are near parallel with the strike of the highwall (Figure 4.12).

The respective ratings were summed into the RMR values using the following expression:

$$RMR = A1 + A2 + A3 + A4 + A5 + B$$

The average RMR values calculated for the Dolerite, Meta-Gabbro, Pegmatite and Tonalite rock types were 55, 60, 57 and 64 respectively.

#### **4.3.4 Geological Strength Index**

The GSI values shown in Appendix E – RMR Calculation Data reflect a range of values of 10 GSI units. The mean value of each respective range is related to the RMR<sub>89</sub> (Rock Mass Rating version of 1989) through the expression:

$$GSI = RMR_{89} - 5$$

The nature of the GSI is such that a single value of GSI applicable to a rock mass cannot be allocated. Instead a range of values is noted in collection of data from a rock face and related to mean RMR value or corresponding range of RMR values.

#### **4.3.5 Blastability Index (BI)**

Several approaches are taken to the establishment of the RMD (Rock Mass Description) for a given rock mass. In order to capture the influence of the varying discontinuity spacings on the RMD, the approach chosen was that given by the equation:

$$RMD = 10 + 10X_i$$

Where  $X_i$  is the in-situ block size in metres. Average ratings of RMD for Dolerite, Meta-Gabbro, Pegmatite and Tonalite were calculated at 14, 14, 13 and 16 respectively.

Rating values for joint plane spacing (JPS) were derived from the joint spacing data. Instead of using the broad rating categories defined by Lilly (1986) for the JPS [(eg rating of 20 for intermediately spaced joints (0.1m to 1m)], ratings were weighted to reflect values representative of the joint spacing of a data point within a rating category. This was achieved by taking the full rating of the lower category and adding a spacing weighted rating from the higher category to it.

The rating for joint plane orientation (JPO) was arrived with consideration of the collective effect of the joints in Figure 4.12. This rating was applied across the calculation of the BI as discontinuity orientations were assumed to be consistent across the rock mass.

Using the equation in Section 2.7.1 and the average densities in Table 4.6, the Specific Gravity Influence (SGI) ratings of for the respective rock data sets were calculated as follows:

$$SGI = 25 \times Density - 50$$

The rock hardness factor (H) ratings were calculated using the following empirical equation from the work of Lilly in Rorke (2003):

$$H = \frac{UCS + 23.7}{47.6}$$

The five rating components of the BI were summed to arrive at a BI value for each data point using the equation:

$$BI = 0.5 (RMD + JPS + JPO + SGI + H)$$

Average values of BI calculated for Dolerite, Meta-Gabbro, Pegmatite and Tonalite were 37, 38, 33 and 38 respectively. BI values in the range of 20 to 40 are considered to be indicative if relatively easy blasting (Chatziangelou and Christaras, 2013b). The input ratings as well as the resulting BI calculated for each of the rock types are presented in Appendix D - BI Calculation Data. This implies that with all the factors above taken into consideration, the desired rock breaking outcomes should be achievable to a significant degree if designs applied were optimally aligned with the rock mass characteristics highlighted.

#### 4.3.6 Slope Mass Rating (SMR)

The SMR (Slope Mass Rating) presented in Hudson (2013) is an extension of the RMR developed by Romana in 1985. It was applied to the study data in order to establish the stability of the rock mass forming the benches. The SMR brought focus to the potential for failures of blocks of rock caused by the interaction of joint plane strikes and dips relative to the strike and dip of the western highwall. It further incorporated the influence of blasting on the excitation of blocks and wedges formed by the interacting planes. The SMR is derived using the following equation:

$$SMR = RMR + (F_1 \times F_2 \times F_3) + F_4$$

Where  $F_1$ ,  $F_2$ ,  $F_3$  and  $F_4$  are derived from Table 4.7. Inputs for the SMR evaluation were sourced from Table 4.5. The calculation data for each of the four rock types is shown in Appendix F – SMR Calculation Data. The average RMR value was used for the SMR calculation in each case.

**Table 4.7: SMR metrics (Hudson, 2013)**

Case		Very favorable	Favorable	Fair	Unfavorable	Very unfavorable
P	$ \alpha_j - \alpha_s $	$> 30^\circ$	30-20°	20-10°	10-5°	5°
T	$ (\alpha_j - \alpha_s) - 180^\circ $					
P/T	$F_1$	0.15	0.40	0.70	0.85	1.00
P	$ \beta_j $	$< 20^\circ$	20-30°	30-35°	35-45°	45°
P	$F_2$	0.15	0.40	0.70	0.85	1.00
T	$F_2$	1	1	1	1	1
P	$\beta_j - \beta_s$	$> 10^\circ$	10-0°	0°	0° to 10°	$< -10^\circ$
T	$\beta_j - \beta_s$	$< 110^\circ$	110-120°	$> 120^\circ$	-	-
P/T	$F_3$	0	-6	-25	-50	-60
Method		Natural Slope	Presplitting	Smooth blasting	Blasting or mechanical	Deficient blasting
$F_4$		+ 15	+ 10	+ 8	0	- 8

P, plane failure; T, toppling failure;  $\alpha_j$ , joint dip direction;  $\alpha_s$ , slope dip direction;  $\beta_j$ , joint dip;  $\beta_s$ , slope dip



The SMR values were found to be within a range of 50 to 60; classified as Class 3 according to Table 4.8. The author is of the opinion that these figures could have been more conservative as the application of smooth wall blasting (in the form of post-splitting) was not consistent nor correctly executed at the mine in question.

**Table 4.8: SMR Classes (Hudson, 2013)**

Class	SMR	Description	Stability	Failures	Support
I	81-100	Very good	Completely stable	None	None
II	61-80	Good	Stable	Some blocks	Occasional
III	41-60	Normal	Partially stable	Some joints or many wedges	Systematic
IV	21-40	Bad	Unstable	Planar or big wedges	Important/corrective
V	0-20	Very bad	Completely unstable	Big planar or soil-like	Reexcavation

The inference drawn from the SMR classification was that the interaction of the identified joint planes and the plane of the highwall may cause localised failures on benches (as in bottom schematic in Figure 2.12). It is suspected that this is the main contributor to the crest failure problem that is experienced at Phoenix. J3, J4 and J5 approach an orientation of dipping into the pit such that crest rock that occurs along isolating weakness planes could fail during blasting. To confirm this suspicion, the data of the three joints was entered into J-Block (2003) software to create a visual interpretation of the block that would be formed along the crest of a western highwall bench due to the joint interaction. The resulting block is shown in Figure 4.16.

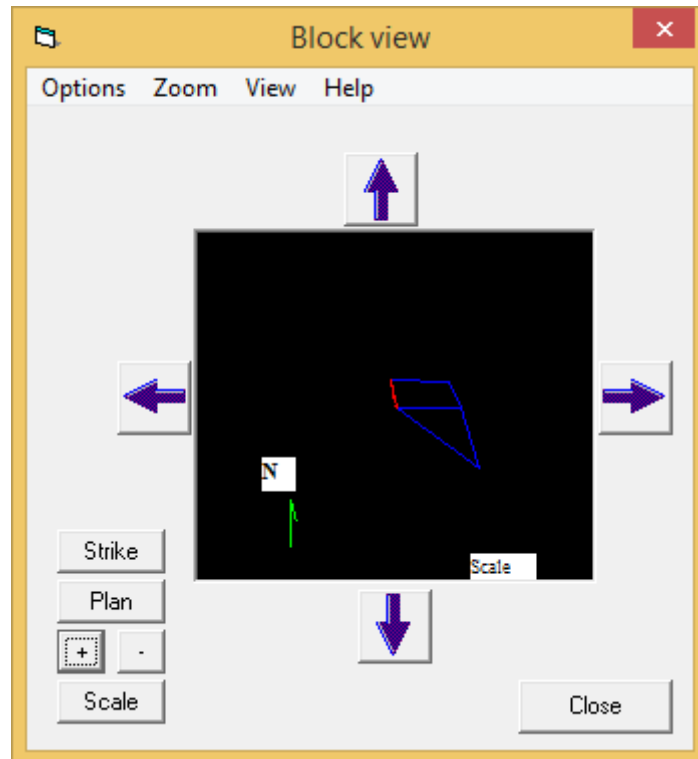


**Figure 4.16: J-Block view of J3, J4 and J5**

The juxtaposed pictures in Figure 4.17 support the suspicion above in that the block produced by J-Block is consistent with the profile of the crest that is persistently lost along the western highwall. The red line in both pictures denotes a common direction along the damaged crest. It is worth noting that the photo taken in the field was of a section along the western highwall where the post-spilt performed relatively well, yet crest loss prevailed.



**Figure 4.17: Crest block loss indicated by J-Block**

Practising post-splitting is not a good approach as blast energy impacts the wall beyond the post-split line (before the post-split line fires) thus making efforts to protect the wall using a post-split ineffective. An ideal solution would be the reduction of the bench slope angle to one that is less than the dip of the joint planes. As this would affect a multitude of other aspects of the operation including its profitability, the practicable alternative is to manage wall control design inputs diligently using actual rock mass information (and not blasting “rules of thumb”) in efforts to impart minimal disturbance to the rock forming the final western highwall.

#### **4.4 Design Input Tool (DIT)**

Drawing from parts of the generic approach of the BQS, the material presented in Section 4.2 and Section 4.3 was brought together into the development of an empirical design input tool by plotting all the data analysed into a series of charts. The tool comprises of the graphical representation of the design inputs for the four rock types forming the rock mass in this study (Figure 4.18 to Figure 4.21).

The zoning of the inputs, as classified according to the rock type and rock characteristics, allows for the concurrent consideration of various elements that influence the degree of achievement of rock breaking plans and designs, as and when the different rock types are encountered. The primary vertical axis represents Lilly’s Blastability Index, while the secondary vertical axis represents the joint spacing (JPS). The values on the horizontal axis are RMR values.

Goodness of fit ( $R^2$ ) values obtained for the plotted data ranged between 0.8 and 0.91. This suggests that the trendlines plotted in the various graphs estimate the behaviour of the data well. In practical terms, the DIT graphs can be used to estimate design inputs concerned with reasonable confidence (with due consideration of the data sample size).

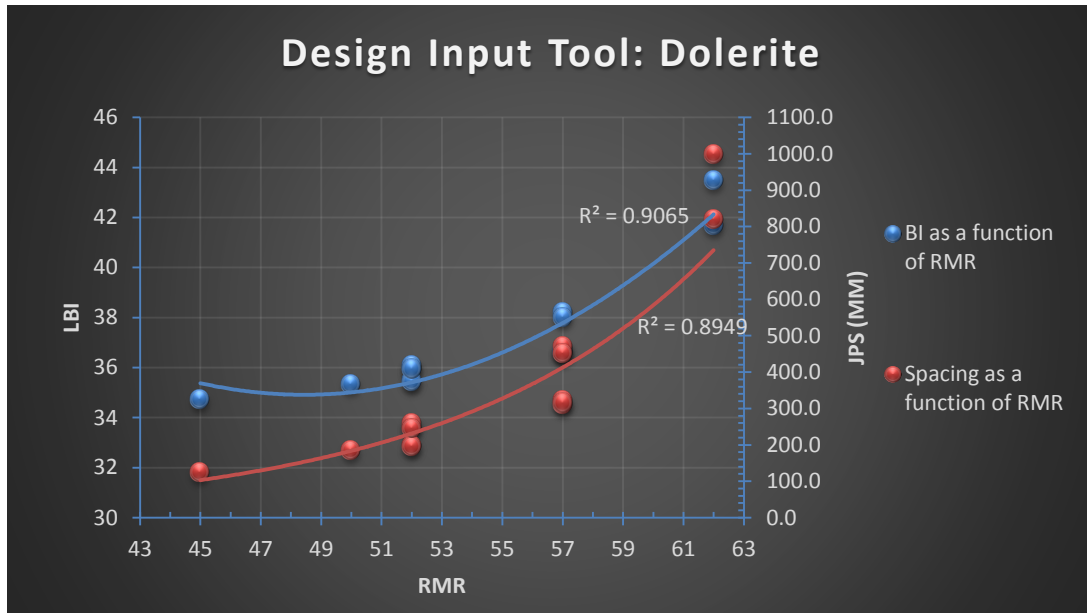


**Figure 4.18: Design Input Tool for Dolerite**

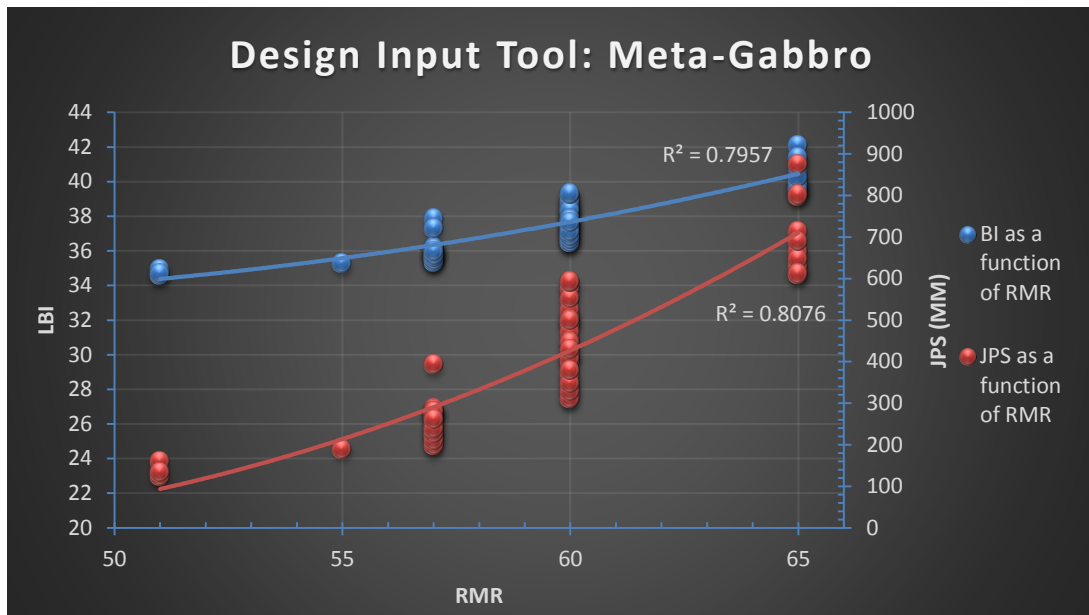


**Figure 4.19: Design Input Tool for Meta-Gabbro**

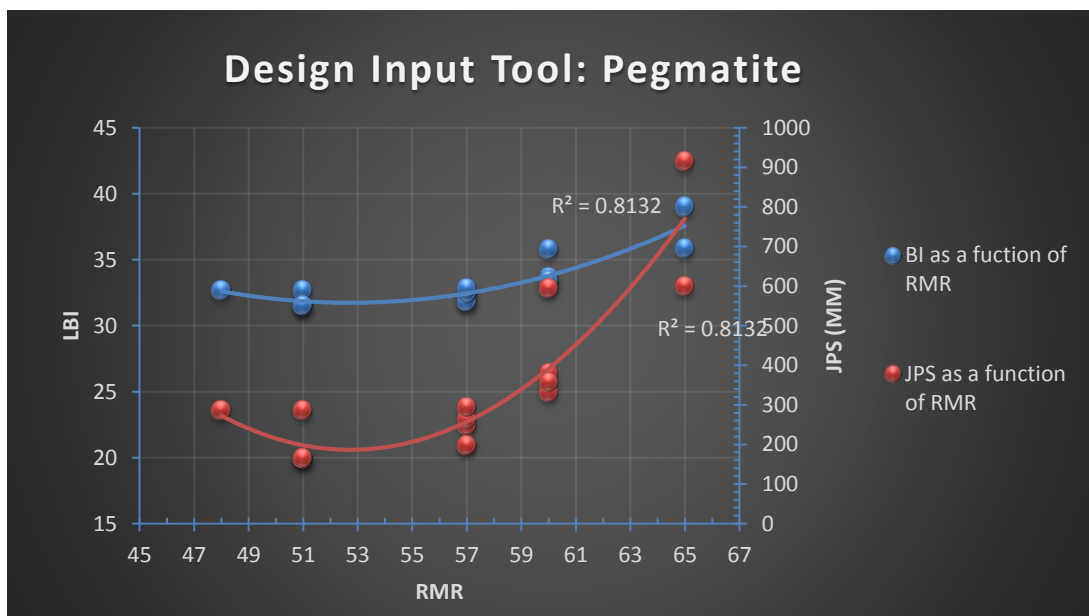


**Figure 4.20: Design Input Tool for Pegmatite**

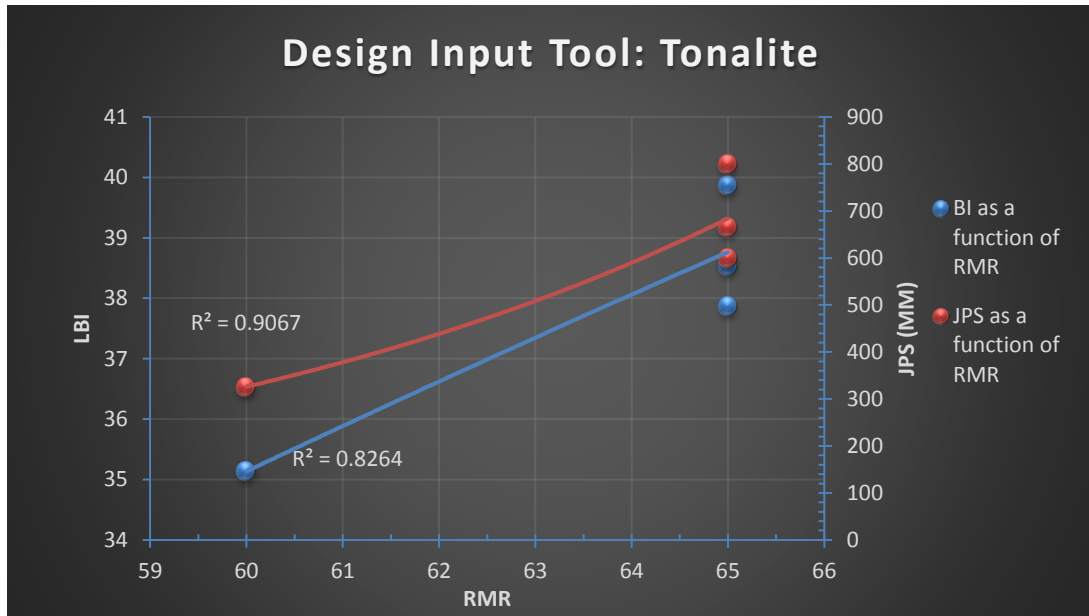


**Figure 4.21: Design Input Tool for Tonalite**

The General Design Input tool (GDIT) is a collation of the data in the preceding graphs. In an ideal setting where rock type boundaries are clearly defined using geological models and transcribed into physical demarcation in the pit, the graphs are the first choice in design input derivation. In cases where such information is not readily available, an all-inclusive GDIT will find its use as an aggregate representation of the state of the rock mass. This input tool is shown in Figure 4.22. As it combines distinct properties from different rock types, the goodness of fit of the graphs estimating the trends of the data is considerably lower than those observed in the respective independent DITs (0.55 – for the RMR:BI data and 0.75 for the RMR:JPS data). This is expected as it is indicative of the non-uniform distribution of various properties in a rock mass.

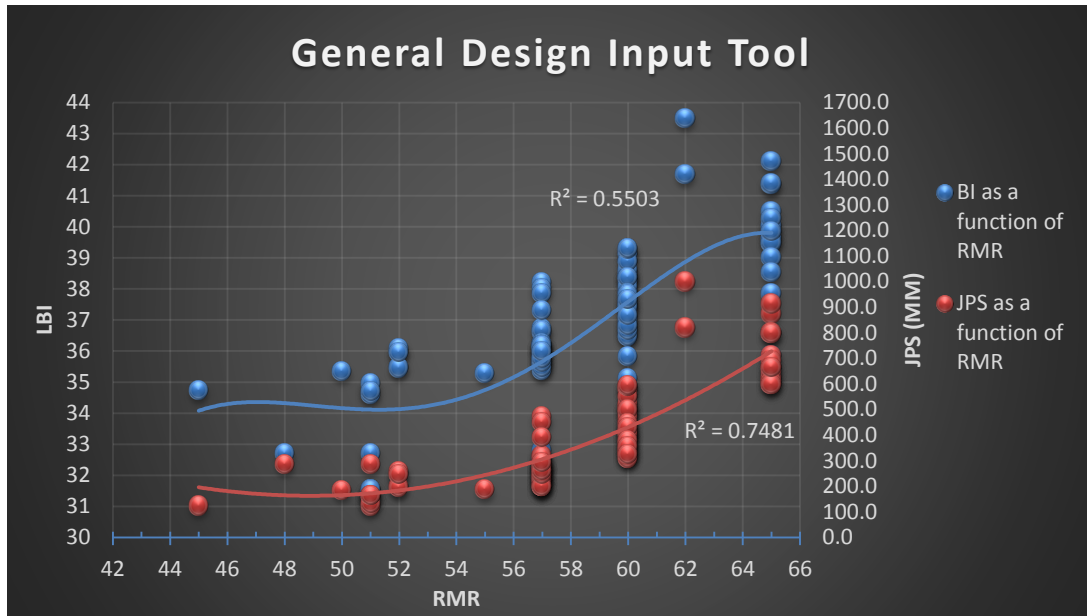


**Figure 4.22: General Design Input Tool**

#### 4.5 Application of the DIT

The process of the application of the DIT is shown schematically in Figure 4.23. The sequence of its application is as follows:

1. GSI data is collected on the concerned mining face by a competent technical person. The subjectivity of the data collected will influence the downstream application of the tool as this is the key input fed into the tool.
2. The mean value of the GSI range estimated is then established, and the associated RMR value is calculated using the equation in Section 4.3.4 .
3. If the rock type in which the prospective mining activity is known through consultation with the geological model, the relevant DIT for that rock type can be applied. When it is known that more than one of the rock types traverse the ground that will be mined (as well as the contacts of the rock types in question), then the respective independent DITs can be utilised. Where this information is not available for the section of rock mass, or it is not practicable to apply specific input due to limited availability of information, the GDIT can be applied.

4. In the case of specialised wall control blasting such as pre-splitting, the estimated RMR can then be used to extrapolate the joint spacing for the concerned rock type on the DIT. With a known joint spacing, an informed decision can be made on the maximum hole spacing interval that does not exceed three joints per unit spacing (as per Section 2.6 ). An appropriate splitting factor can then be calculated using the UCS information in Table 4.6 and the relevant properties of the explosives available. Through monitoring of the outcome of results of designs applied, the HFC (Half Cast Factor – ratio of half barrel length to drill hole length) achieved can be measured plotted back into the DIT as a function of the RMR.
5. Where rock breaking is concerned with primary, buffer or trim blast designs that are adjacent to the highwall, the estimated RMR can be used to extrapolate the BI value from the DIT. The BI value is in turn linked to the appropriate design powder factor as described by Lilly (1986). With a known powder factor, the geometric bench blast designs can be calculated, making appropriate changes for the sensitivity due to proximity of the highwall. Measured outcomes of the designs based on the DIT can then be fed back into the DIT to continuously improve precision.

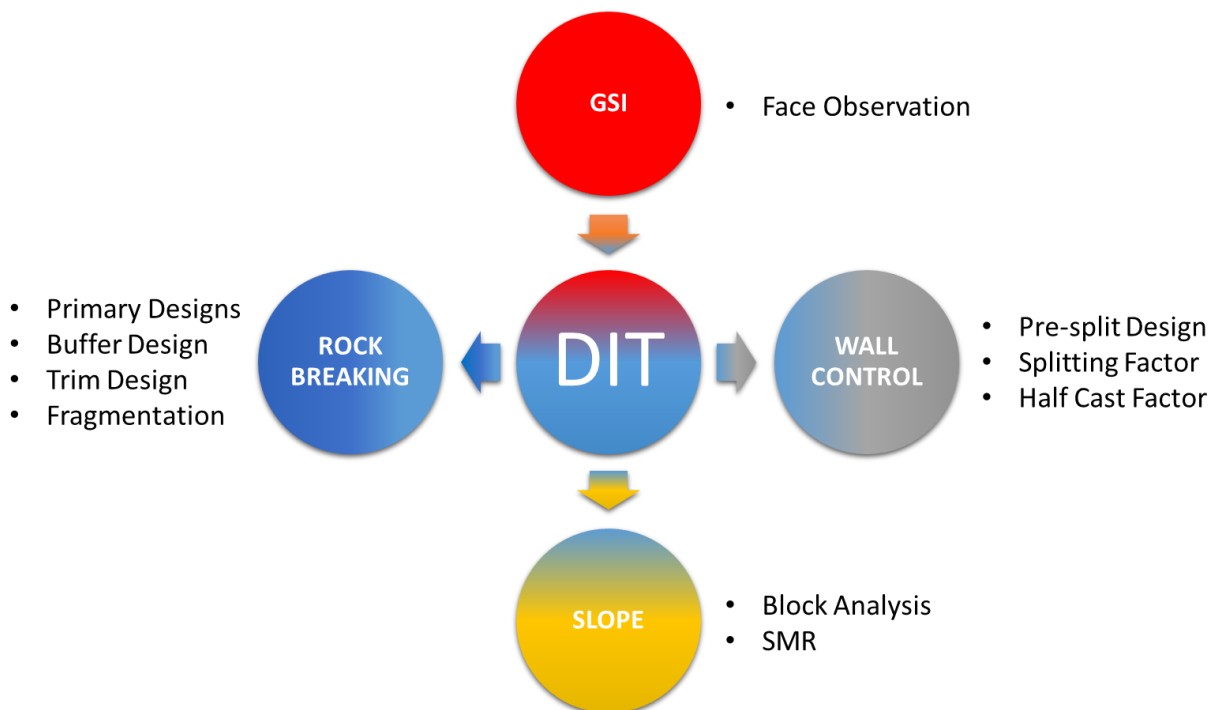


**Figure 4.23: Information flow for Design Input Tool**



#### 4.6 RMC and BI Informed Blast Design – A Case Study of DIT Application

To demonstrate the application of RMC towards wall control as coordinated by the DIT, the following case study is presented.

1. Rock Type: Known to be predominantly Meta-Gabbro for western highwall section of concern.
2. GIS description: very blocky, partially disturbed rock mass, with fair and moderately weathered surfaces.
3. GIS Range: 45 – 55. Mean GIS: 50.

$$RMR = GIS + 5 = 50 + 5 = 55$$

4. DIT

At an RMR of 55, the joint spacing expected is approximately 220mm and the BI rating is approximately 36.

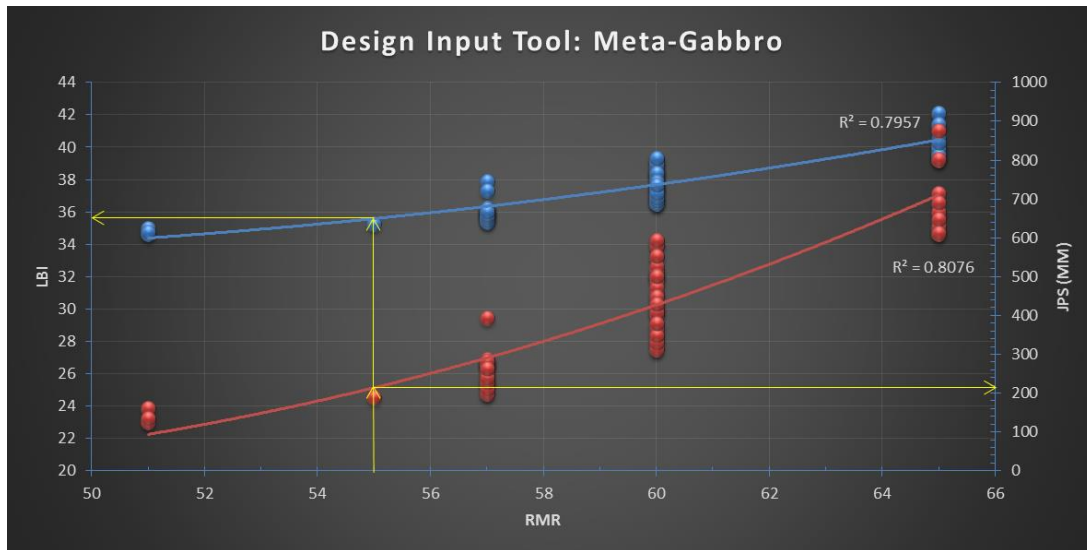


**Figure 4.24: DIT application on Meta-Gabbro**

Using WallPro, the wall control design parameters in Table 4.9 were established. When developing designs without software access, a borehole pressure and hole spacing can be calculated using the equations:

$$P_b = \frac{1.2555\rho V^2 (\sqrt{C} \frac{D_e}{D_h})^{2.4}}{1000}$$

$$S = \frac{D_h(P_b + T)}{T \times 1000}$$

Where,  $\rho$  is the explosive density,  $V$  is the explosive velocity of detonation,  $C$  is the percentage of explosive in a hole as a fraction = (Length of explosive)/(Length of hole),  $D_e$  is the diameter of explosive,  $D_h$  is the diameter of the hole,  $S$  is the hole spacing and  $T$  is the tensile strength of the rock. The hole diameter was pre-determined as 127mm, as this is the smallest blasthole drill at the mine. If set to 800mm, the hole spacing selected would ensure that not more than three joints are spanned by any two adjacent blast holes. This would increase the effectiveness of the pre-split in forming the split plane along the new highwall. It is also worth noting that the design borehole pressure in this case is greater than the respective rocks' tensile strength (estimated as a tenth of the UCS), but remains lower than its UCS (Figure 4.25). Crushing damage and weakening of the new highwall would thus be avoided. Emphasis is placed on the need for the pre-split to be drilled, charged and fired ahead of the trim and primary blasts.

**Table 4.9: RMC informed Pre-split design using DIT inputs**

Design Parameters	
Hole Diameter (mm)	127
Hole Depth (m)	10
Splitting Factor ( $\text{kg/m}^2$ )	1.5
Hole Spacing (mm)	800
Uncharged Collar Length (m)	2.5
Hole Angle	$90^\circ$
Cartridges per hole	9
Borehole Pressure (MPa)	163

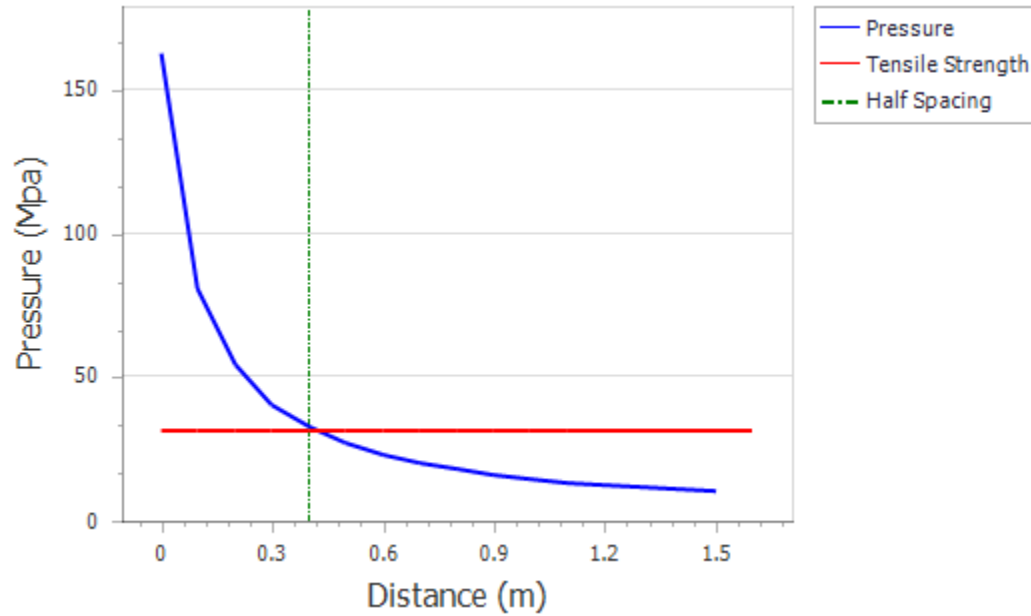


**Figure 4.25: Pre-split design**

- Using the Relative Weight Strength of the bulk explosives used (HEF 206 from BME) at Phoenix, data from the empirical graph from Lilly (1986) was adapted to plot the relationship between the BI and the powder factor as shown in Figure 4.26. The powder factor derived from the graph is approximately  $0.95\text{kg/m}^3$ . According to the author's experience at the mine, this powder factor was well within the range at which blasts were

found to perform well in terms of the fragmentation achieved and the muck diggability. This is therefore a well matched powder factor for the rock type. As more site data linking the BI derived from the DIT with the powder factor that produced satisfactory results is collected, the graph can be updated to increase the representation of site specific inputs, thereby improving its precision.

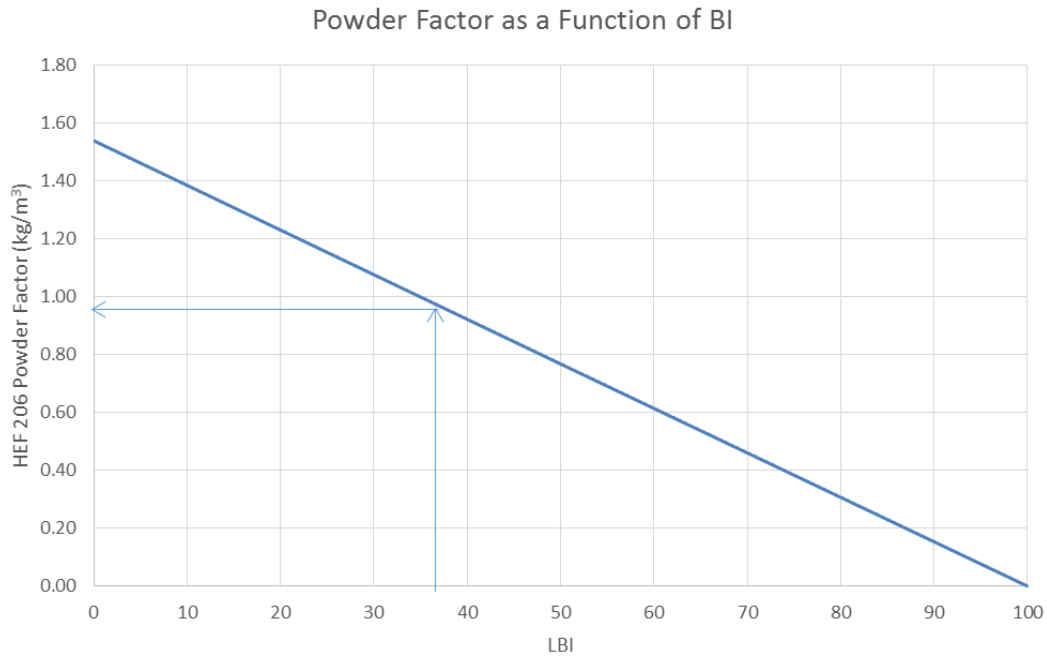


**Figure 4.26: Powder factor extrapolation**

With a known powder factor, other parameters of the design can then be calculated using the equation:

$$\text{Powder Factor} = \frac{\text{Kg per hole}}{\text{Burden} \times \text{Spacing} \times \text{Bengh height}}$$

Spacing ranges between 1 and 1.5 times the burden. The ideal value is typically set at 1.15 for optimum distribution of energy. The burden and spacing consistent with a powder factor of one

were calculated as 3.2m and 3.7m respectively. Figure 4.27 is a section through a trim blast design developed using the DIT process and WallPro (BME, 2016) software.

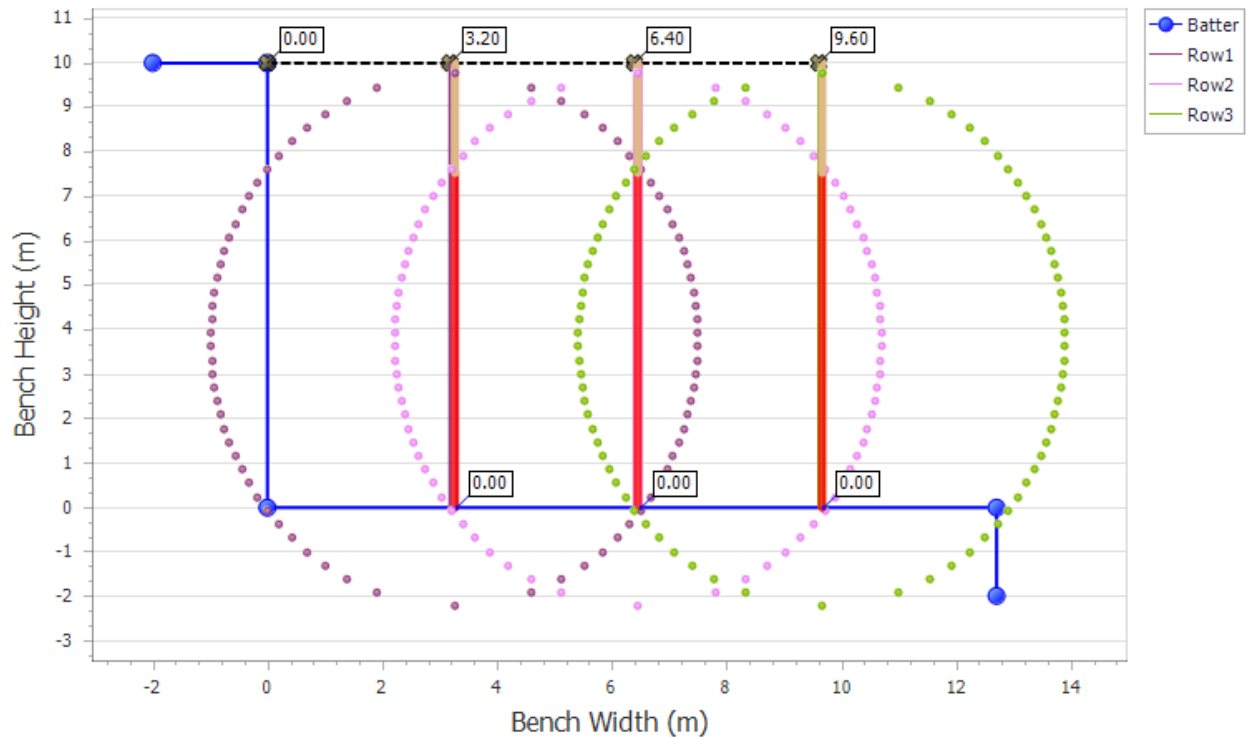


**Figure 4.27: Trim Design**

### Case study Conclusion

The over-riding element in this case is the fact that, because the design inputs were arrived at using actual rock mass inputs, conservative case sensitive designs can be developed systematically. This can be achieved without overdesigning wall control blasts or designing blasts that impart damage to the resultant highwall.

Emphasis is placed on causing as little disturbance as possible to the highwall with due cognisance that the pre-split discussed in Point 4 would be fired prior to the application of the trim. The pre-split hole spacing defined by the DIT improves the precision of estimation of subsequent design parameters such as the applicable splitting factor, energy distribution and borehole pressure.

By drilling smaller diameter holes on trim blasts, energy distribution would be improved within the trim block while reducing the energy directed towards the highwall per delay. This is shown by the zone of influence of the hole closest to the highwall in Figure 4.3 and Figure 4.4 when compared with Figure 4.27.

#### **4.7 Discussion of Results and Analysis**

The audits conducted at the mine brought several operation inconsistencies to the fore that were suspected to contribute to the problem experienced by the mine. The author is, however, of the opinion that the core of the problem lies in the understanding and application of the rock mass fundamentals. Operational discipline in the execution of drilling and blasting plans is important, but it is preceded by the application of informed inputs at the design stage.

Analysis of the rock mass jointing data highlighted findings similar to those observed in related work Worsey et al (1981) and the NHI (1991). The orientation and inclination of J3, J4 and J5 were found to be consistent with the difficulties in the achievement of wall control efforts in the studies cited. This drew focus to the evaluation of their contribution to the problem at Phoenix mine.

The applicability of the approach proposed in this study is possible and practical. It outlines the dynamic incorporation of information that is often available on most operations (and is readily collectable from the mining face), but remains unused. It promotes the elimination of information silos between the various departments (Geology, Geotech, Planning, Drill and Blast etc) and the use of this information to formulate scientifically driven wall control designs (and if desired, primary rock breaking designs as well), that are not limited to the confines of incorrectly applied blasting conventions. This has the potential effect of re-circulating value add to the various stakeholders along the mine's value chain.

The zoning of the mechanical and field data into the respective rock types in the rock mass forming the high wall of concern, allowed for the influence of the various rock mass classification inputs to be observed in detail. This was done to allow for case specific application of design inputs that are centred on the stability factors of the RMR, and extended to the empirically related indices of explosives application and rock mass discontinuity defined geometric designs.

It became apparent through this study that the approach to perimeter blasting in place did not take into account the rock mass constraints that brought about the behaviour that was observed. The information required to gain an understanding of what was unfolding was in fact available, and was collected routinely. The skills required to collect the information objectively were also available. Funnelling the information into a design input tool eliminates the guess work in the perimeter blast design process, and excludes the need to apply a blanket approach to all blasts in varying rock mass conditions.

At Phoenix, this approach will bring into focus the cause and effect relationship between the applied systems, and the response of the rock mass to those systems. It brings into context what has been observed over the years in terms of the failure to achieve designed berm widths due to perpetual crest failure, and proposes a means of controlling this failure, through an engineered solution based on key rock mass characteristics.

## **CHAPTER 5: CONCLUSIONS AND RECOMMENDATIONS**

The conclusions drawn from the study are discussed in this Chapter. Recommendations derived from the study are also provided.

### **5.1 Conclusions**

The study found its significance in the use of rock mass classification methods for the reduction of the typical dependence on inadequately informed rules of thumb applied in the perimeter wall rock blast design process. The conventional application of parametric ratios in the development of designs neglects to account for fundamental rock mass factors that affect the achievability of final wall designs. In the case of Phoenix mine, the key design aspects referred to were the berm width (reduced by the loss of final wall crests) and the wall rock competence (aggravated by frozen rock against the batter).

Exploiting the commonalities between the BI and the rock mass classification methods allowed for the establishment of empirical relationships linking the blastability of a rock mass, which is commonly concerned with breaking it into desired fragments with the use of appropriate explosive energy, to factors concerned with rock mass stability. Designs established through the correlation of these concepts thus remain inclusive of elements play a pivotal role in the control of blast damage.

The separation of data according to geological zones highlighted the variation of the properties of the rock mass in each zone. The varying response to the blasting activity observed along the western highwall was therefore justified as the design inputs were not tailored to suit rock mass behaviour in each zone. The need for geological and structural inputs in the rock breaking design processes for successful wall control in the respective domains was demonstrated.

The zoning of data was achieved according to the types of rock forming the western highwall. Within each of the rock type zones, rock mass classification characteristics were assigned and used to carry out a series of calculations feeding into the BI, Rock Mass Rating and the Slope Mass Rating. Lack of consideration of primary rock mass characteristics was identified as the source of the development and execution of designs that led to highwall damage and perpetual loss of designed berm crests. One highlighting facet of this realisation was the fact that more than 90% of



the data points reflected a joint spacing that was significantly less than the spacing of the blanket perimeter blast design utilised.

The applicability of the approach proposed as a solution to the problem identified in this study is possible and practical. It outlines the dynamic incorporation of information that is commonly available, but is not used effectively; if at all, for reporting purposes after the fact. It encourages the elimination of information silos between stakeholders along the mine value chain, and facilitates the use of information in the formulation of scientifically driven wall control and primary blast designs along the highwall.

Taking the problem experienced by the mine into consideration, and the practices and omissions suspected to be at the centre of the cause of the problem, the author is of the opinion that the implementation of the DIT, in its rock type specific or general rock mass form, will enforce due consideration of the overlooked factors such as the joint frequency, joint orientation and the link between the profile of the blocks formed by the interaction between various joint sets and the western highwall.

The implementation of the Design Input Tool requires no capital expenditure as rock mass classification data is collected from the exposed mining faces and supplemented with exploration and lab test data. Designs developed with inputs from the tool will be conservative and biased towards preservation of the western highwall. The Design Input Tool is a simple yet powerful tool that consolidates knowledge about the rock mass, and relates it to the stability factored inputs that are otherwise overlooked in favour of a blanket rock breaking approach. Granted, the tool may suggest a hole spacing that would not be practically achievable due to operational and economic constraints. An informed decision can be made, however, by the competent persons involved, weighing economic factors against the acceptable outcome of the alternative design executed. By reducing the human factor in the design process, the adoption of the Design Input Tool approach will play a significant role in the ability to proactively manage crest loss and highwall damage along the western highwall.

## 5.2 Recommendations

The following are recommendations derived from the study:

1. It is recommended that the measurements of Half Cast Factor are incorporated into the Design Input Tool, as and when they become available, and correlated with the input parameters utilised. The Half Cast Factor is given by the length of half barrels measured on the new highwall after the blast expressed as percentage of the initial length of the blast holes. The Half Cast Factor would serve as the primary measure of success for the pre-split designs developed. The goal would be to eventually use the accumulated data over numerous blasts to forecast the potential performance that can be expected of the design. The benefit would be the enhanced ability to adjust plans prior to their execution, based on empirical observations made following previous blasts.
2. The Geotechnical department should assume the responsibility of actively managing the Design Input Tool database in order to continuously increase the data points it contains, and similarly its accuracy in estimating outputs. In facilitation of this, data concerning rock mass classification inputs should be collected by competent persons who have a functional understanding of the limitations and subjectivity of rock mass classification methods.
3. As the coordinator of mining activity, the planning framework at the mine should be extended to include the effective exchange of observed Design Input Tool outputs with the Geotechnical department as data is collected and assimilated from each successive mining face. This will ensure that the rock breaking design processes that follow the delineation of mining blocks will be coupled with instructions on the rock mass behaviour or properties expected, as well as suggestions on spatial blast design parameters. It should be noted that the Design Input Tool approach does not completely eliminate the use of blasting rules of thumb. It is intended to assist the competent person by objectively including primary factors that must form the foundation of the design process.

It is further recommended that further work is done in putting the approach presented in this study to the test in different rock mass environments. This will assist in assessing its merit as an alternative to the conventional application of blasting rules of thumb as primary inputs of the design process. Such conventions create a blind spot in relation to understanding the rock mass characteristics that bring about particular responses to rock breaking activity.

## REFERENCES

- Allmendinger, R., 2016. Stereonet 9. *Richard Allmendinger Department of Earth and Atmospheric Sciences, Cornell University*. New York, USA. [12 July 2016]
- Bosman, J. 2008. Slope Stability Assessment – Tati Nickel Mining Company. Consulting Rock Engineer Report. *Open House Management Solutions*. South Africa. pp. 1-56.
- Bieniawski, Z., 1979. The Geomechanics Classification in Rock Engineering Classifications. *Proceeding of the 4<sup>th</sup> Congress of the International Society of Rock Mechanics*. Montreux, Rotterdam. pp. 41-48.
- Bieniawski, Z., 1989, Engineering Rock Mass Classifications: A Complete Manual for Engineers and Geologists in Mining, Civil, and Petroleum Engineering. *Wiley*. New York. pp. 51-68.
- Bulk Mining Explosives (BME), 2016. Wall Pro. *BME*. Johannesburg, South Africa [16 September 2016]
- Bye, A., 2006. The Strategic and Tactical Value a 3D Geotechnical Model for Mining Optimisation. Anglo Platinum, Sandsloot Open Pit. *South African Institute of Mining and Metallurgy*, vol. 106, no.2, February. pp. 97-104.
- Chatziangelou, M. and Christaras, B., 2013a. Rock Mass Blastability Dependence on Rock Mass Quality. *Bulletin of the Geological Society of Greece, Proceedings of the 13th International Congress*, vol. 47, September. pp. 1-12.
- Chatziangelou, M. and Christaras, B., 2013b. Blastability Index on Poor Quality Rock Mass. *International Journal of Civil Engineering*, vol. 2, no. 5, November. pp. 9-16.
- Chatziangelou, M. and Christaras, B., 2015. A Geological Classification of Rock mass Quality for Intermediate Spaced Formations. *International Journal of Engineering and Innovative Technology*, vol. 4, no.9, March, pp. 52-61.
- Chiappetta, F. 1991. Pre-Splitting And Controlled Blasting Techniques, *Proceedings of the Blast Technical Instrumentation and Explosives Application Seminar*, San Diego, USA. pp. 171-186.
- Cockett, R., 2016. Visiblegeology. *Rowan Cockett*, [Online], Available: <http://app.visiblegeology.com/stereonetApp.html> [12 July 2016].

- Cunningham, C., 1983. The Kuz-Ram model for prediction of fragmentation from blasting, *First International Symposium on Rock Fragmentation By Blasting*, Lulea, Sweden. pp. 439-454.
- Cruise, J., 2011. Rock Breaking – A Science, Not An Art. *Southern African Institute of Mining and Metallurgy*. Namibia. pp. 25-40.
- Deere, D., Hendron, A., Patton, F., and Cording, E., 1967. Design Of Surface And Near Surface Construction In Rock, 8th U.S. Symposium On Rock Mechanics: Failure And Breakage Of Rock: New York, Society Of Mining Engineers, *American Institute Of Mining, Metallurgical, And Petroleum Engineers*. pp. 237-302.
- De Graaf, W., 2011. Specialised Blasting Techniques. *Southern African Institute of Mining and Metallurgy*. Namibia. pp. 1-23.
- Dey, K. and Sen, P., 2003. Concept of Blastability – An Update. *The Indian Mining and Engineering Journal*, vol. 42, no. 8-9, September, pp. 24-31.
- Google Earth, 2016. Location of Tati Nickel Mine.
- Google, 2016. Graph of Two Super Imposed Waves, [Online], Available: <https://figures.boundless-cdn.com/17169/large/figure-17-10-02a.jpeg> [20 July 2016]
- Hoek, E., 1995. Strength of Rock and Rock Masses. *35<sup>th</sup> U.S Symposium on Rock Mechanics. International Society for Rock Mechanics*, vol 2, no 2. Lake Tahoe. pp 4-15.
- Hoek, E., Marinos, V., and Marinos, P. 2005. The Geological Strength Index: application and limitations. *Bulletin of Engineering Geology and the Environment*, vol, 64, no. 1, pp. 55-65.
- Holmberg, R., and Persson, P., 2000. The Swedish Approach to Contour Blasting. *International Society of Explosives Engineers*. Stockholm, Sweden. pp. 1-14
- Hornsby, P. and Jermy, C. 2011. Phoenix Pit Rockfall Mitigation Project. *Golder Associates Africa*. Midrand, South Africa. pp. 1-7.
- Hudson, J. 2013. Comprehensive Rock Engineering. Principles, Practice and Projects. *Imperial College of Science, Technology and Medicine*. London, United Kindom, vol. 3, pp. 4-13.
- Imperial Chemical Industries (ICI) Explosives, n.d. Safe and Efficient Blasting in Open Cut Mines. *ICI Explosives*. pp. 111-121.
- International Society of Explosives Engineers (ISEE). 2011. ISEE Blasters Handbook, 17<sup>th</sup> Edition. *ISEE*, Cleaveland, Ohio. pp. 341-345

- Karzulovic, A., and Read, J., 2009. Chapter 5: Rock Mass Model. Guidelines for Open Pit Slope Design. *CSIRO Publishing*. Australia. pp. 83-85.
- Kekana, R. 2015. Tati Site Visit Report. *Bulk Mining Explosives*. Johannesburg, South Africa. pp. 1-10.
- Lewandowski, T., Luan Mai, V., and Danell, R., 1996. Influence of Discontinuities on Presplitting Effectiveness in *Proceedings of the Fifth International Symposium on Rock Fragmentation by Blasting*. Montreal, Canada. pp. 217-225.
- Lilly, P. 1986. An Empirical Method of Assessing Rock mass Blastability. *The AusIMMIEAust Newman Combined Group, Large Open Pit Mining Conference*. Australia. pp. 89–92.
- Little, M., 2006. The Benefit to Open Pit Rock Slope Design of Geotechnical Databases. *Southern African Institute of Mining and Metallurgy, International Symposium on Stability of Rock Slopes in Open Pit Mining and Civil Engineering*. pp. 97-116
- Morolong, K. 2014. Personal Correspondence. Tati Nickel Mine, Francistown, Botswana
- National Highway Institute (NHI), 1991. Rock Blasting and Overbreak Control. Course 13211. *U.S. Department of Transport*. USA. pp. 176-182.
- Prout, B., 2014. MINN0140: Blast Design for Surface Mines. *University of the Witwatersrand, Johannesburg: Department of Mining Engineering*. South Africa. pp 30-32.
- Rorke, A. 2003. BME Training Module: Pre-Splitting. *Bulk Mining Explosives*. Johannesburg. South Africa. pp. 1-24.
- Roy, P. 2005. Rock Blasting, Effects and Operations. *Central Mining Research Institute*. Dhanbad, India. pp. 24-27.
- Segaetsho, G. 2014. Tati Nickel Mining Company Baseline Drilling and Blasting Audit. Explosives Engineering for Surface and Underground Mines. *University of the Witwatersrand, Johannesburg, South Africa*. pp. 7-36.
- Scoble, M, Lizotte, Y and Paventi, M, 1996. Rock mass Damage From Blasting: Characterization and Impact. Workshop on Measurement of Blast Fragmentation. Montreal, Canada. pp. 225-235.
- Singh, P., 2003. The Influence of Rock mass Quality in Controlled Blasting. *12<sup>th</sup> International Symposium on Mine Planning and Equipment Selection*. Kalgoorlie, Australia. pp. 219-222.

Stacey, T. 2015. MINN7036: Rock Mass Classification in Rock Engineering. *University of the Witwatersrand: Department of Mining Engineering*. Johannesburg, South Africa. pp. 1-32.

Tati Nickel Mining Company (TNMC), 2012. Summary of Rock Strength Data. *TNMC*. Botswana.

University of the Witwatersrand, 2003., JBlock Academic, *University of the Witwatersrand*, Johannesburg, South Africa. [14 August 2016]

Williams, P., Floyd, J., Chitombo, G., and Maton, T. 2009. Chapter 11: Design Implementation. Guidelines for Open Pit Slope Design. *CSIRO Publishing*. Australia. pp. 265-313

Workman, J., and Calder, P, 1993. Considerations in Pre-split Blasting for Mines and Quarries, *Proceedings of the 19<sup>th</sup> International Conference on Explosives and Blasting Technique, Society of Explosives Engineers*. pp. 357-370.

Worsey, P., Farmer, I. and Matheson, G., 1981. The mechanics of presplitting in discontinuous rock, in *Proceedings of the 22nd US Rock Mechanics Symposium*. Missouri, USA. pp 205-210

## APPENDIX A – BQS CHART

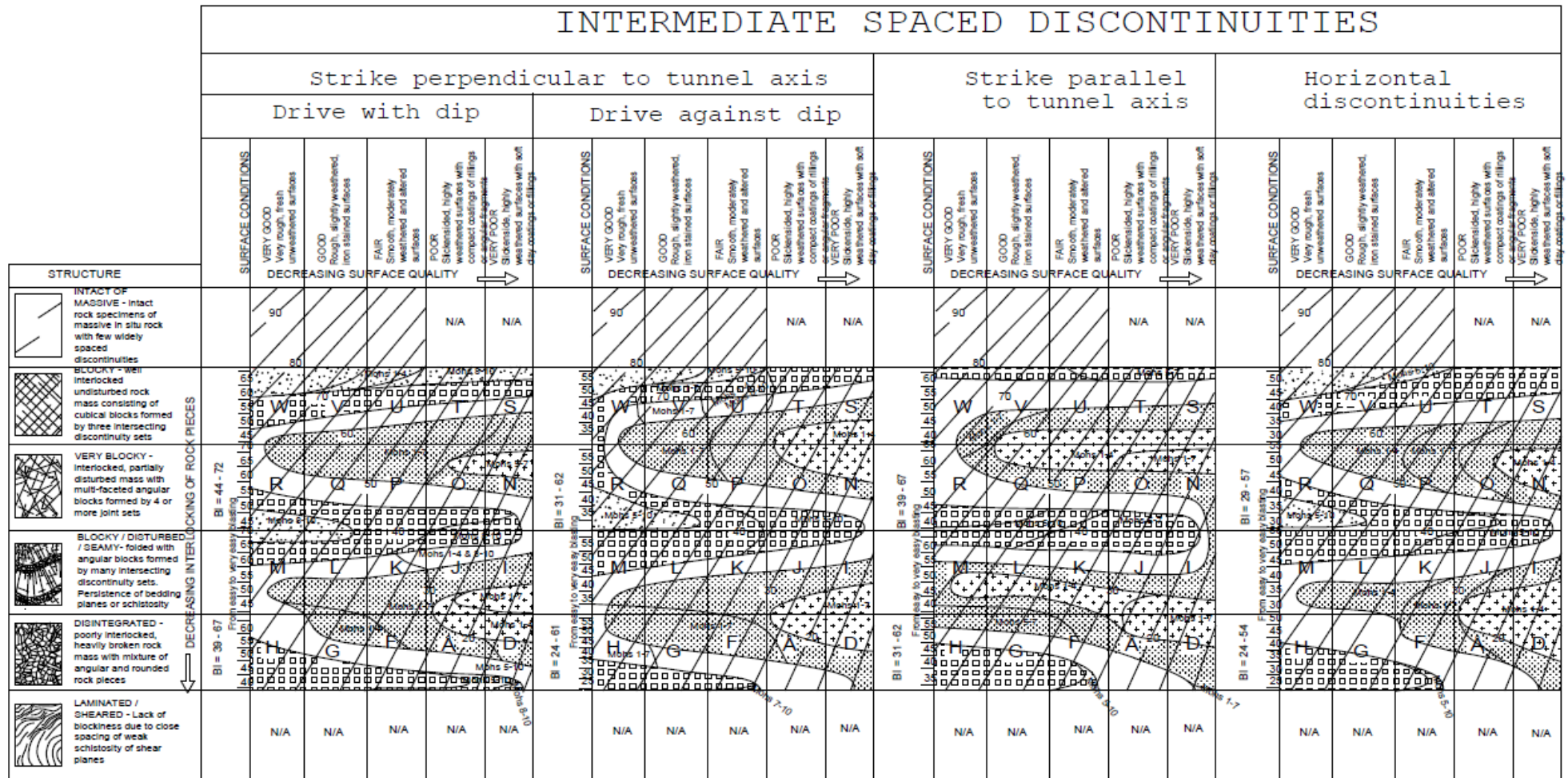


Figure A.1: BQS System Chart (Chatziangelou and Christaras, 2015)

## APPENDIX B – FIELD DATA

**Table B.1: Dolerite field data**

Hole_id	Rock_type	From	To	Length(m)	0-30	31-60	61-90	Total	J/m	Xi(m)	Spacing (mm)
PS137	dol	264	265	1.00	1	0	3	4	4	0.25	250.0
PS141	dol	130	131	1.00	2	6	0	8	8	0.13	125.0
PS156	dol	101	102	1.00	0	5	0	5	5	0.20	200.0
PS137	dol	310	313	3.00	3	0	0	3	1	1.00	1000.0
PS137	dol	393	398	5.00	5	0	11	16	3	0.31	312.5
PS158	dol	244	250	5.50	6	11	0	17	3	0.32	323.5
PS159	dol	180	188	7.60	8	14	2	24	3	0.32	316.7
PS141	dol	412	423	11.00	1	5	50	56	5	0.20	196.4
PS155	dol	100	113	13.00	5	40	25	70	5	0.19	185.7
PS157	dol	214	231	17.00	1	25	10	36	2	0.47	472.2
PS137	dol	289	310	21.00	21	0	60	81	4	0.26	259.3
PS158	dol	252	275	23.10	35	13	3	51	2	0.45	452.9
PS137	dol	50	81	31.00	31	0	95	126	4	0.25	246.0
PS137	dol	405	519	114.00	114	0	25	139	1	0.82	820.1



**Table B.2: Meta-Gabbro field data**

Hole_id	Rock_type	From	To	Length(m)	0-30	31-60	61-90	Total	J/m	Xi(m)	Spacing (mm)
PS155	mg	129.0	130.0	1.0	0	5	0	5	5	0.20	200
PS141	mg	80.0	81.5	1.5	0	6	0	6	4	0.25	250
PS141	mg	154.0	156.0	2.0	0	7	2	9	5	0.22	222
PS157	mg	180.0	182.0	2.0	1	5	0	6	3	0.33	333
PS141	mg	65.0	67.3	2.3	0	4	4	8	3	0.29	288
PS155	mg	257.6	260.0	2.4	0	15	0	15	6	0.16	160
PS141	mg	57.1	60.0	2.9	0	8	5	13	4	0.22	223
PS137	mg	22.0	25.0	3.0	3	1	20	24	8	0.13	125
PS137	mg	44.0	47.0	3.0	3	2	10	15	5	0.20	200
PS141	mg	291.0	294.0	3.0	3	3	5	11	4	0.27	273
PS158	mg	168.0	171.0	3.0	4	2	0	6	2	0.50	500
PS158	mg	183.0	186.0	3.0	3	4	0	7	2	0.43	429
PS137	mg	40.0	44.0	4.0	4	2	15	21	5	0.19	190
PS137	mg	218.0	222.0	4.0	4	0	15	19	5	0.21	211
PS137	mg	242.0	246.0	4.0	4	0	13	17	4	0.24	235
PS157	mg	135.0	139.0	4.0	0	4	2	6	2	0.67	667
PS141	mg	41.9	46.4	4.5	4	7	6	17	4	0.26	265
PS157	mg	130.0	135.0	5.0	6	6	4	16	3	0.31	313
PS157	mg	175.0	180.0	5.0	2	20	15	37	7	0.14	135
PS158	mg	186.0	191.0	5.0	7	3	0	10	2	0.50	500
PS141	mg	6.1	11.8	5.7	1	10	0	11	2	0.52	518
PS137	mg	192.0	198.0	6.0	6	0	10	16	3	0.38	375
PS141	mg	124.0	130.0	6.0	4	15	2	21	4	0.29	286
PS158	mg	90.0	96.0	6.0	6	2	1	9	2	0.67	667
PS141	mg	13.5	19.7	6.2	6	12	0	18	3	0.34	344
PS137	mg	4.0	10.6	6.6	6.6	5	7	19	3	0.35	355
PS157	mg	140.0	147.0	7.0	4	10	5	19	3	0.37	368
PS141	mg	34.6	41.9	7.3	4	20	2	26	4	0.28	281
PS137	mg	10.6	18.0	7.4	7.4	2	17	26	4	0.28	280
PS137	mg	198.0	206.0	8.0	8	1	20	29	4	0.28	276
PS156	mg	190.0	198.0	8.0	0	20	15	35	4	0.23	229
PS141	mg	71.0	80.0	9.0	3	16	3	22	2	0.41	409
PS141	mg	115.0	124.0	9.0	8	18	6	32	4	0.28	281
PS137	mg	30.0	40.0	10.0	10	0	15	25	3	0.40	400
PS137	mg	81.0	91.0	10.0	10	0	31	41	4	0.24	244
PS137	mg	279.0	289.0	10.0	10	0	6	16	2	0.63	625
PS141	mg	230.0	240.0	10.0	1	15	8	24	2	0.42	417
PS158	mg	99.0	109.0	10.0	15	9	0	24	2	0.42	417
PS141	mg	156.0	166.6	10.6	2	15	9	26	2	0.41	408
PS141	mg	46.4	57.1	10.7	2	26	10	38	4	0.28	282
PS155	mg	113.0	124.0	11.0	2	10	7	19	2	0.58	579
PS158	mg	172.0	183.0	11.0	13	8	3	24	2	0.46	458
PS137	mg	265.0	277.0	12.0	12	3	35	50	4	0.24	240
PS158	mg	194.4	206.5	12.2	14	7	0	21	2	0.58	579
PS141	mg	320.0	333.0	13.0	1	25	7	33	3	0.39	394
PS141	mg	301.0	316.0	15.0	3	15	3	21	1	0.71	714
PS159	mg	165.0	180.0	15.0	24	21	3	48	3	0.31	313
PS141	mg	131.0	146.5	15.5	5	27	15	47	3	0.33	330
PS137	mg	248.0	264.0	16.0	16	0	45	61	4	0.26	262
PS156	mg	253.0	269.0	16.0	6	25	15	46	3	0.35	348
PS157	mg	284.0	300.0	16.0	4	10	15	29	2	0.55	552
PS157	mg	149.0	166.0	17.0	7	15	5	27	2	0.63	630
PS158	mg	114.0	131.5	17.5	10	8	2	20	1	0.88	875
PS141	mg	246.0	265.0	19.0	0	17	20	37	2	0.51	514
PS141	mg	360.0	379.0	19.0	0	30	9	39	2	0.49	487
PS141	mg	265.0	285.0	20.0	3	12	10	25	1	0.80	800
PS157	mg	108.0	128.0	20.0	3	20	15	38	2	0.53	526
PS141	mg	81.5	102.0	20.5	6	40	8	54	3	0.38	380
PS157	mg	260.0	282.0	22.0	6	25	5	36	2	0.61	611
PS159	mg	90.0	112.6	22.6	18	22	5	45	2	0.50	502
PS141	mg	334.0	358.0	24.0	0	27	10	37	2	0.65	649
PS155	mg	138.0	164.0	26.0	5	30	20	55	2	0.47	473
PS155	mg	201.0	227.0	26.0	2	20	25	47	2	0.55	553
PS155	mg	229.0	256.0	27.0	2	40	12	54	2	0.50	500
PS158	mg	136.5	167.0	30.5	21	13	4	38	1	0.80	803
PS137	mg	161.0	192.0	31.0	31	3	35	69	2	0.45	449
PS155	mg	167.0	199.0	32.0	6	28	20	54	2	0.59	593
PS160	mg	161.0	195.0	34.0	35	38	3	76	2	0.45	447
PS159	mg	130.0	165.0	35.0	37	17	5	59	2	0.59	593
PS160	mg	224.0	276.0	52.0	53	28	4	85	2	0.61	612
PS141	mg	168.5	230.0	61.5	5	54	30	89	1	0.69	691
PS137	mg	92.0	156.0	64.0	64	5	80	149	2	0.43	430

**Table B.3: Pegmatite field data**

Hole_id	Rock_type	From	To	Length(m)	0-30	31-60	61-90	Total	J/m	Xi(m)	Spacing (mm)
PS159	peg	127.5	128.0	0.5	1	2	0	3	6	0.2	167
PS155	peg	256.0	257.0	1.0	0	6	0	6	6	0.2	167
PS141	peg	166.6	168.5	1.9	2	2	1	5	3	0.4	380
PS137	peg	277.0	279.0	2.0	2	0	5	7	4	0.3	286
PS155	peg	227.0	229.0	2.0	0	6	4	10	5	0.2	200
PS157	peg	128.0	130.0	2.0	0	10	0	10	5	0.2	200
PS158	peg	249.5	251.5	2.0	6	2	0	8	4	0.3	250
PS159	peg	128.0	130.0	2.0	3	8	1	12	6	0.2	167
PS155	peg	135.0	138.0	3.0	1	3	1	5	2	0.6	600
PS141	peg	67.3	71.0	3.7	3	9	2	14	4	0.3	264
PS141	peg	60.0	65.0	5.0	0	7	10	17	3	0.3	294
PS155	peg	124.0	129.0	5.0	0	5	10	15	3	0.3	333
PS158	peg	131.5	136.5	5.0	10	4	0	14	3	0.4	357
PS137	peg	234.0	242.0	8.0	8	0	20	28	4	0.3	286
PS159	peg	112.6	127.5	14.9	16	9	0	25	2	0.6	596
PS158	peg	206.5	244.0	37.5	27	14	0	41	1	0.9	915

**Table B.4: Tonalite field data**

Hole_id	Rock_type	From	To	Length (m)	0-30	31-60	61-90	Total	J/m	Xi(m)	Spacing (mm)
PS157	ton	252	260	8	0	10	0	10	1	0.8	800
PS157	ton	166	175	9	0	12	3	15	2	0.6	600
PS156	ton	243	253	10	0	5	10	15	2	0.7	667
PS156	ton	131	176	45	8	70	60	138	3	0.3	326

## APPENDIX C – RQD DATA

Table C.1: RQD percentage values

RQD Percentage Values			
Dolerite	Meta-Gabbro	Pegmatite	Tonalite
86	80	72	100
57	85	72	99
80	82	95	99
100	93	66	93
91	89	80	
92	68	80	
91	82	85	
80	56	72	
79	80	99	
97	89	87	
86	98	89	
97	96	93	
85	76	94	
98	81	1	
	83	99	
	99	100	
	87		
	91		
	63		
	98		
	99		
	95		
	88		
	99		
	93		
	95		
	96		
	88		
	88		
	87		
	82		
	96		
	88		
	96		
	82		
	99		
	97		
	97		
	96		
	88		
	98		
	97		
	85		
	99		
	86		
	100		
	92		
	93		
	87		
	92		
	98		
	99		
	100		
	98		
	98		
	100		
	98		
	95		
	99		
	98		
	99		
	97		
	99		
	98		
	100		
	97		
	99		
	97		
	99		
	99		
	99		
	96		

## APPENDIX D - BI CALCULATION DATA

**Table D.1: Dolerite BI Data**

RMD	JPS	JPO	SGI	H	BI
12.5	12.5	20.00	23.50	3.50	36
11.3	11.3	20.00	23.50	3.50	35
12.0	12.0	20.00	23.50	3.50	36
20.0	20.0	20.00	23.50	3.50	44
13.1	13.1	20.00	23.50	3.50	37
13.2	13.2	20.00	23.50	3.50	37
13.2	13.2	20.00	23.50	3.50	37
12.0	12.0	20.00	23.50	3.50	35
11.9	11.9	20.00	23.50	3.50	35
14.7	14.7	20.00	23.50	3.50	38
12.6	12.6	20.00	23.50	3.50	36
14.5	14.5	20.00	23.50	3.50	38
12.5	12.5	20.00	23.50	3.50	36
18.2	18.2	20.00	23.50	3.50	42

**Table D.2: Meta-Gabbro BI Data**

RMD	JPS	JPO	SGI	H	BI
12	12	25	20	7	38
13	13	20	20	7	36
12	12	20	20	7	36
13	13	20	20	7	37
13	13	20	20	7	36
12	12	20	20	7	35
12	12	20	20	7	36
11	11	20	20	7	35
12	12	20	20	7	35
13	13	20	20	7	36
15	15	20	20	7	38
14	14	20	20	7	38
12	12	20	20	7	35
12	12	20	20	7	35
12	12	20	20	7	36
17	17	20	20	7	40
13	13	20	20	7	36
13	13	20	20	7	37
11	11	20	20	7	35
15	15	20	20	7	38
15	15	20	20	7	39
14	14	20	20	7	37
13	13	20	20	7	36
17	17	20	20	7	40
13	13	20	20	7	37
14	14	20	20	7	37
14	14	20	20	7	37
13	13	20	20	7	36
13	13	20	20	7	36
13	13	20	20	7	36
12	12	20	20	7	36
14	14	20	20	7	37
13	13	20	20	7	36
14	14	20	20	7	37
12	12	20	20	7	36
16	16	20	20	7	40
14	14	20	20	7	38
14	14	20	20	7	38
14	14	20	20	7	37
13	13	20	20	7	36
16	16	20	20	7	39
15	15	20	20	7	38
12	12	20	20	7	36
16	16	20	20	7	39
14	14	20	20	7	37
17	17	20	20	7	41
13	13	20	20	7	37
13	13	20	20	7	37
13	13	20	20	7	36
13	13	20	20	7	37
16	16	20	20	7	39
16	16	20	20	7	40
19	19	20	20	7	42
15	15	20	20	7	39
15	15	20	20	7	38
18	18	20	20	7	41
15	15	20	20	7	39
14	14	20	20	7	37
16	16	20	20	7	39
15	15	20	20	7	38
16	16	20	20	7	40
15	15	20	20	7	38
16	16	20	20	7	39
15	15	20	20	7	38
18	18	20	20	7	41
14	14	20	20	7	38
16	16	20	20	7	39
14	14	20	20	7	38
16	16	20	20	7	39
16	16	20	20	7	39
17	17	20	20	7	40
14	14	20	20	7	38

**Table D.3: Pegmatite BI Data**

RMD	JPS	JPO	SGI	H	BI
12	12	20	16	4	32
12	12	20	16	4	32
14	14	20	16	4	34
13	13	20	16	4	33
12	12	20	16	4	32
12	12	20	16	4	32
13	13	20	16	4	32
12	12	20	16	4	32
16	16	20	16	4	36
13	13	20	16	4	33
13	13	20	16	4	33
13	13	20	16	4	33
14	14	20	16	4	33
13	13	20	16	4	33
16	16	20	16	4	36
19	19	20	16	4	39

**Table D.4: Tonalite BI Data**

RMD	JPS	JPO	SGI	H	BI
18	18	20	19	5	40
16	16	20	19	5	38
17	17	20	19	5	39
13	13	20	19	5	35

## APPENDIX E – RMR CALCULATION DATA

**Table E.1: Dolerite RMR Data**

UCS	RQD	Spacing	Condition	Water	Orientation		RMR	GSI
12	15	10	25	15	-25	✓	52	42-52
12	10	8	25	15	-25	✓	45	35-45
12	15	10	25	15	-25	✓	52	42-52
12	20	15	25	15	-25	✓	62	52-62
12	20	10	25	15	-25	✓	57	47-57
12	20	10	25	15	-25	✓	57	47-57
12	20	10	25	15	-25	✓	57	47-57
12	15	10	25	15	-25	✓	52	42-52
12	15	8	25	15	-25	✓	50	40-50
12	20	10	25	15	-25	✓	57	47-57
12	15	10	25	15	-25	✓	52	42-52
12	20	10	25	15	-25	✓	57	47-57
12	15	10	25	15	-25	✓	52	42-52
12	20	15	25	15	-25	✓	62	52-62

**Table E.2: Meta-Gabbro RMR Data**

UCS	RQD	Spacing	Condition	Water	Orientation	RMR	GSI
15	17	10	25	15	-25	57	47-57
15	17	10	25	15	-25	57	47-57
15	17	10	25	15	-25	57	47-57
15	20	10	25	15	-25	60	50-60
15	17	10	25	15	-25	57	47-57
15	13	8	25	15	-25	51	41-51
15	17	10	25	15	-25	57	47-57
15	13	8	25	15	-25	51	41-51
15	17	10	25	15	-25	57	47-57
15	17	10	25	15	-25	57	47-57
15	20	10	25	15	-25	60	50-60
15	20	10	25	15	-25	60	50-60
15	17	8	25	15	-25	55	45-55
15	17	10	25	15	-25	57	47-57
15	17	10	25	15	-25	57	47-57
15	20	15	25	15	-25	65	55-65
15	17	10	25	15	-25	57	47-57
15	20	10	25	15	-25	60	50-60
15	13	8	25	15	-25	51	41-51
15	20	10	25	15	-25	60	50-60
15	20	10	25	15	-25	60	50-60
15	20	10	25	15	-25	60	50-60
15	17	10	25	15	-25	57	47-57
15	20	15	25	15	-25	65	55-65
15	20	10	25	15	-25	60	50-60
15	20	10	25	15	-25	60	50-60
15	17	10	25	15	-25	57	47-57
15	17	10	25	15	-25	57	47-57
15	17	10	25	15	-25	57	47-57
15	20	10	25	15	-25	60	50-60
15	17	10	25	15	-25	57	47-57
15	20	10	25	15	-25	60	50-60
15	17	10	25	15	-25	57	47-57
15	20	15	25	15	-25	65	55-65
15	20	10	25	15	-25	60	50-60
15	20	10	25	15	-25	60	50-60
15	17	10	25	15	-25	57	47-57
15	20	10	25	15	-25	60	50-60
15	17	10	25	15	-25	57	47-57
15	20	10	25	15	-25	60	50-60
15	20	15	25	15	-25	65	55-65
15	20	10	25	15	-25	60	50-60
15	20	10	25	15	-25	60	50-60
15	20	10	25	15	-25	60	50-60
15	17	10	25	15	-25	57	47-57
15	20	10	25	15	-25	60	50-60
15	20	10	25	15	-25	60	50-60
15	20	15	25	15	-25	65	55-65
15	20	15	25	15	-25	65	55-65
15	20	10	25	15	-25	60	50-60
15	20	10	25	15	-25	60	50-60
15	20	15	25	15	-25	65	55-65
15	20	10	25	15	-25	60	50-60
15	20	10	25	15	-25	60	50-60
15	20	10	25	15	-25	60	50-60
15	20	15	25	15	-25	65	55-65
15	20	10	25	15	-25	60	50-60
15	20	10	25	15	-25	60	50-60
15	20	10	25	15	-25	60	50-60
15	20	15	25	15	-25	65	55-65
15	20	15	25	15	-25	65	55-65
15	20	10	25	15	-25	60	50-60



**Table E.3: Pegmatite RMR Data**

UCS	RQD	Spacing	Condition	Water	Orientation	RMR	GSI
15	13	8	25	15	-25	51	41-51
15	13	8	25	15	-25	51	41-51
15	20	10	25	15	-25	60	50-60
15	13	8	25	15	-25	51	41-51
15	17	10	25	15	-25	57	47-57
15	17	10	25	15	-25	57	47-57
15	17	10	25	15	-25	57	47-57
15	13	8	25	15	-25	51	41-51
15	20	15	25	15	-25	65	55-65
15	17	10	25	15	-25	57	47-57
15	17	10	25	15	-25	57	47-57
15	20	10	25	15	-25	60	50-60
15	20	10	25	15	-25	60	50-60
15	3	5	25	15	-25	38	28-38
15	20	10	25	15	-25	60	50-60
15	20	15	25	15	-25	65	55-65

**Table E.4: Tonalite RMR Data**

UCS	RQD	Spacing	Condition	Water	Orientation	RMR	GSI
15	20	15	25	15	-25	65	55-65
15	20	15	25	15	-25	65	55-65
15	20	15	25	15	-25	65	55-65
15	20	10	25	15	-25	60	50-60

## APPENDIX F – SMR CALCULATION DATA

**Table F.1: Dolerite SMR data**

Dolerite												
Plane	Strike	Dip	RMR <sub>Ave</sub>	aj-as	F1	Bj	F2	Bj-Bs	F3	Exc Method	F4	SMR
WHW	350	90	-	-	-	-	-	-	-	-	-	-
J3	300	72	55	50	0.15	18	1	-18	-60	S/B	4	50
J4	312	57	55	38	0.15	33	1	-33	-60	S/B	4	50
J5	310	88	55	40	0.15	2	1	-2	-50	S/B	4	51

**Table F.2: Meta-Gabbro SMR data**

Meta-Gabbro												
Plane	Strike	Dip	RMR <sub>Ave</sub>	aj-as	F1	Bj	F2	Bj-Bs	F3	Exc Method	F4	SMR
WHW	350	90	-	-	-	-	-	-	-	-	-	-
J3	300	72	60	50	0.15	18	1	-18	-60	S/B	4	55
J4	312	57	60	38	0.15	33	1	-33	-60	S/B	4	55
J5	310	88	60	40	0.15	2	1	-2	-50	S/B	4	56

**Table F.3: Pegmatite SMR data**

Pegmatite												
Plane	Strike	Dip	RMR <sub>Ave</sub>	aj-as	F1	Bj	F2	Bj-Bs	F3	Exc Method	F4	SMR
WHW	350	90	-	-	-	-	-	-	-	-	-	-
J3	300	72	57	50	0.15	18	1	-18	-60	S/B	4	52
J4	312	57	57	38	0.15	33	1	-33	-60	S/B	4	52
J5	310	88	57	40	0.15	2	1	-2	-50	S/B	4	53

**Table F.4: Tonalite SMR data**

Tonalite												
Plane	Strike	Dip	RMR <sub>Ave</sub>	aj-as	F1	Bj	F2	Bj-Bs	F3	Exc Method	F4	SMR
WHW	350	90	-	-	-	-	-	-	-	-	-	-
J3	300	72	64	50	0.15	18	1	-18	-60	S/B	4	59
J4	312	57	64	38	0.15	33	1	-33	-60	S/B	4	59
J5	310	88	64	40	0.15	2	1	-2	-50	S/B	4	60